POLYCYCLIC AROMATIC HYDROCARBONS:

SPECTROFLUOROMETRIC QUENCHING AND SOLUBILITY
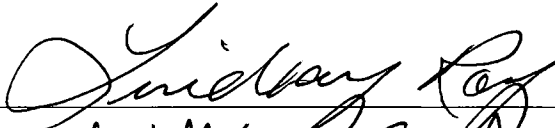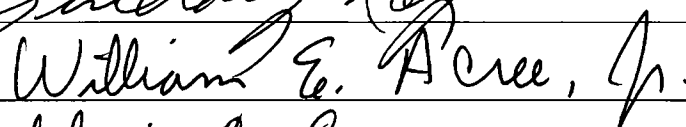
BEHAVIOR

HONORS THESIS

Presented to the University of North Texas

Honors Program in Partial Fulfillment of

the Requirements for University Honors

By

Lindsay Elizabeth Roy

May 1999

Approved by:

(signature)	Lindsay Roy
(signature)	Faculty Advisor
(signature)	Honors Director

Acknowledgements

First and foremost, I would like to extend my gratitude to Dr. William E. Acree, Jr. I am grateful to him for providing his valuable time and for all of his efforts in helping me fulfil my goals. Secondly, I would like to say thank you to all of the undergraduate students and graduate students I have worked with along the way. Without their support, I would have never been able to write this thesis.

Lastly, I would like to thank Dr. Gloria Cox for providing me the opportunity to write this thesis. Without all of her support throughout the years, I would not have succeeded this far in my academic career.

TABLE OF CONTENTS

LIST OF TABLES

LIST OF FIGURES

Chapter 1

Introduction

Polycyclic Aromatic Hydrocarbons in Soil

Contamination of soil by Polycyclic Aromatic Hydrocarbons (PAHs) is of considerable importance because of their carcinogenic and mutagenic potential. PAHs are non-polar hydrophobic organic compounds characterized by two or more fused benzene rings in various arrangements. Although these compounds occur ubiquitously, the primary source to the environment is anthropogenic activity, particularly through the incomplete combustion of high molecular weight hydrocarbon species and through the process of pyrolysis.[1] Pyrolysis, exposure of organic substances to substantially high temperatures, has been occurring since antiquity and results in the formation of minute quantities of PAHs.[2]

PAHs now enter the environment from new sources and in greater quantities than they did in human and geologic past. The environmental status of PAHs is of particular concern because although PAHs are naturally occurring compounds and essentially present at low concentrations in the environment, high concentrations of PAHs are found near high-temperature industrial sites such as petroleum refining, coke production, wood preservation and synthetic oil and gas production.[3] As a result, PAHs can be highly sorbed to soil matrices and hinder a rapid biodegradation of the hydrophobic contaminants, thus accumulating in organic fatty material and infecting the food chain.[4,5]

Landfarming is a waste remediation method in which contaminated soil is kept free of vegetation, fertilizer elements such as N and P are added frequently, and the soil is

routinely tilled. This management strategy is used with soils contaminated with

petroleum hydrocarbons to promote atmospheric losses of volatile compounds and

enhance microbial degradation of contaminants. Dissipation initially proceeds at a rapid

rate but slows to a steady state over time for nonvolatile, recalcitrant compounds.[6]

Though PAHs are considered recalcitrant, losses do occur over time through

processes including leaching, photodegradation, volatilization, and chemical oxidation.[7]

However, the ultimate fate of the PAHs in soils is controlled almost exclusively by

surface adsorption.[6] PAHs with three or more rings tend to be very strongly adsorbed to

the soil. Strong adsorption coupled with very low water solubility make leaching an

insignificant pathway of loss. Volatility also is an unlikely mechanism of dissipation for

PAHs with three or more rings because of very low vapor pressures and strong retention

by soil solids.

Microbial degradation is believed to be the most important process for removal of

PAHs from contaminated soils.[8] Biodegradation in soil is a fairly complex process which

involves diffusion of contaminants in the porous soil matrix, adsorption of the soil

surface, biodegradation in the biofilms existing on the soil particle surface and in the

large pores, as well as in the bound and free water phases, after desorption from the soil

surface.[9] Several environmental factors are known to influence the capacity of

indigenous microbial populations to degrade PAHs.[3] The interactions among

environmental factors such as temperature, pH, soil gas oxygen concentrations,

oxidation-reduction potential and the presence of other substrates often control the

feasibility of biodegradation.[10-12]

During recent years, a number of bacteria and fungi that degrade PAHs have been isolated.[13,14] Examples include *Pseudomonas, Mycobacterium, Flavobacterium, Acinetobacter, Arthrobacter, Bacillus*, and *Nocardia* being the most active species.[6] The prokaryotic pathway of degradation of PAHs involves a dioxygenase enzyme and incorporates both atoms of molecular oxygen into the substrate. The metabolites from this pathway are dioxetanes, *cis*-dihydrodiols, and quinones. In contrast, degradation by eukaryotic fungi incorporates only one atom of oxygen into the ring structure and can produce carcinogenic epoxides. Therefore, under soil conditions that favor fungal activity, early PAH metabolic products could increase the mutagenicity and carcinogenicity of the parent PAHs. As degradation proceeds, the majority of the fungal transformations detoxify the PAH compounds.[6]

Polycyclic aromatic compounds incorporate numerous subclasses of compounds. Examples include PAH6 benzenoids and their derivatives, fluoranthenoids and fluorenoids and their derivatives, polycyclic aromatic nitrogen, oxygen, and sulfur heterocycles and their derivatives, acenaphthalene and acephenanthrylene derivatives, cyclopenta polycyclic aromatic hydrocarbons and derivatives, etc.

The concern regarding PAHs as environmental pollutants and toxic substances has prompted researchers to develop analytical methods specific for different compounds.[15] Later in this chapter, I will discuss the limitations of these methods and the advantage of using predictive expressions and fluorescence quenching. The purpose of this thesis is to investigate two analytical methods, ultraviolet/visible and fluorescence spectroscopy. UV/Vis allows investigators to study the behavior of polycyclic aromatic hydrocarbons in binary solvents systems and determine and/or develop predictive

mathematical expressions for describing that behavior in the solvent media. Selective

fluorescence quenching using nitromethane and surfactant quenching in mixed micellar

surfactant systems allows a means to detect, identify, and separate PAHs in

environmental samples.

Ultraviolet/Visible and Fluorescence Spectroscopy

Experimental approaches to identifying polycyclic aromatic hydrocarbons include

both ultraviolet/visible (UV/Vis) and fluorescence spectroscopy, gas chromatography,

and mass spectrometry. For the purpose of this thesis, we will only examine PAHs using

UV/Vis and fluorescence spectroscopy. Figure 1 is a pictorial view of a Jablonski or

partial energy level diagram for a photoluminescent molecule.

Absorption measurements based upon ultraviolet and visible radiation have

widespread application for the quantitative determination of a large variety of inorganic

and organic species. Quantitatively, it is expressed through the Beer-Lambert Law:

$$A = - \log T = \varepsilon bc \qquad\qquad 1.1$$

where A equals absorbance, T is the transmittance, ε is the molar absorptivity in

liter$*$mol$^{-1}*$cm^{-1}, b is the cell thickness in cm, and c is the concentration in mol$*$liter^{-1}.

The molar absorptivity is defined as the amount of radiation absorbed by one mole of

analyte per liter, which is determined through standard solutions containing known

concentrations of analyte. If the path length is held constant, the absorbance of the

species becomes directly proportional to the concentration.
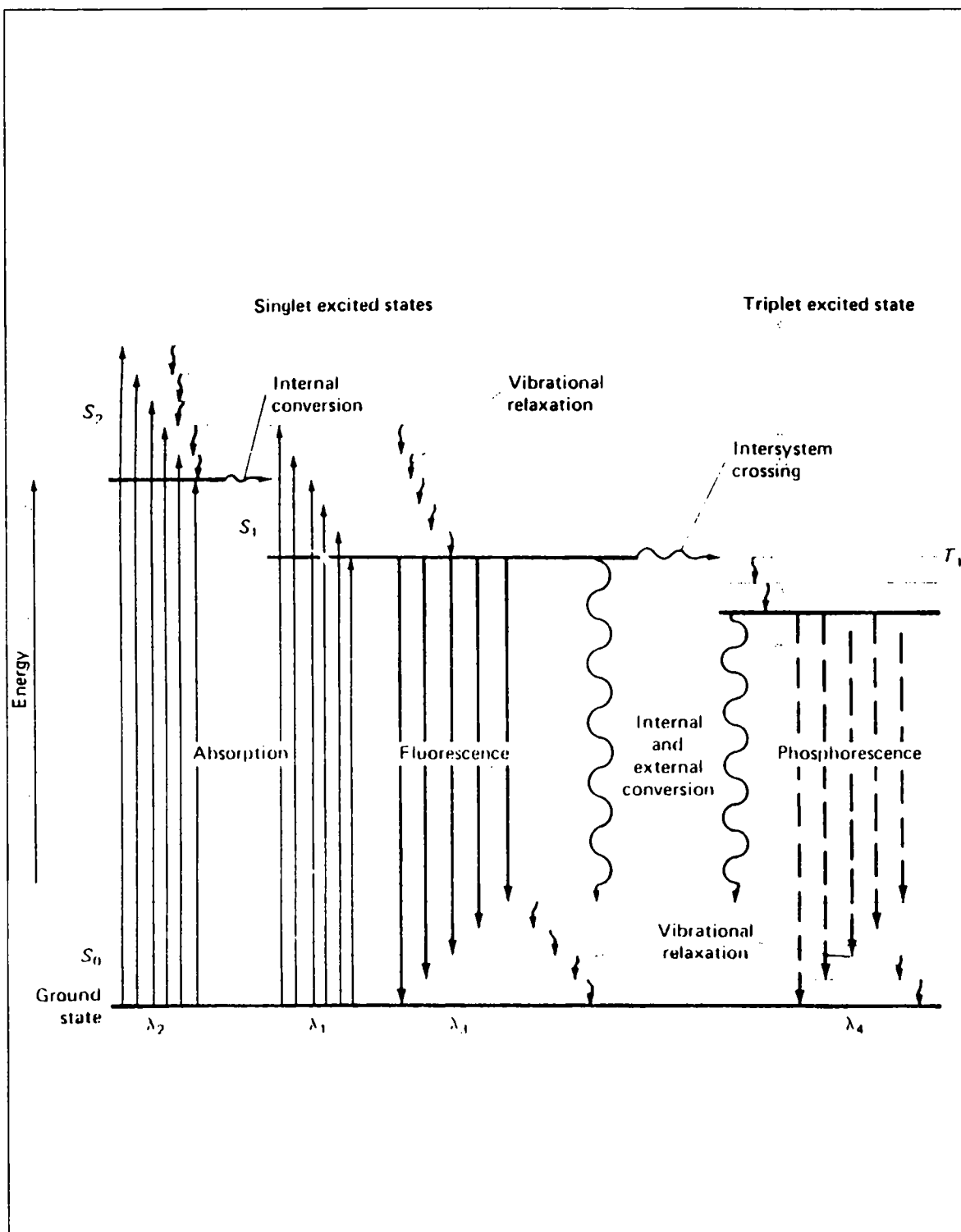
FIGURE 1: Jablonski diagram showing fates of photoexcited complex polyatomic molecules. S_0 represents ground state of singlet manifold of the molecule. S_1 and T_1 denote electronic singlet and electronic triplet excited states. Numerous vibration energy levels associated with electronic states are also depicted.

Limitations to the Beer-Lambert Law include describing the absorption behavior of a species containing high analyte concentrations and chemical changes associated with concentration changes. The former is known as a limiting law; the Beer-Lambert Law is successful in describing absorption behavior of dilute concentrations (< 0.01M). The latter deviation arises when an analyte dissociates, associates, or reacts with a solvent to produce a product having a different absorption spectrum from the analyte.

Another deviation can also result from changes in the concentration of the solution. Since the molar absorptivity, ε, is dependent upon the refractive index of the medium, concentration changes cause significant alteration in the refractive index of the solution, thus deviations from the Beer-Lambert Law are observed. A correction factor for this effect can be made by substituting:

$$\varepsilon n/(n^2+2)^2 \hspace{4cm} 1.2$$

for ε in the Beer-Lambert Equation. However, this correction is never very large and is rarely significant at concentrations less than 0.01M.[16] Other causes of nonlinearity include:

- scattering of light due to particulates in the sample
- fluoresecence or phosphorescence of the sample
- shifts in chemical equilibria as a function of concentration
- non-monochromatic radiation, deviations can be minimized by using a relatively flat part of the absorption spectrum such as the maximum of an absorption band
- stray radiation

Fluorescence behavior of a molecule is dependent upon the structure of the molecule and the environment in which the spectrum is measured.[17] Analytically useful fluorescence is restricted to compounds having large conjugated systems. For example, a molecule with less strongly bound π-electrons can be promoted to π^*-anti-bonding orbitals by absorption of electromagnetic radiation of fairly low energy without extensive disruption of bonding.[18] Molecular fluorescence is the optical emission from molecules that have been excited to higher energy levels by absorption of electromagnetic radiation. The main advantage of fluorescence detection compared to absorption measurements is the greater sensitivity achievable because the fluorescence signal has (in principle) a zero background.[16] Analytical applications include quantitative measurements of molecules in solution and fluorescence detection in liquid chromatography. Referring to Figure 1, after a radiative excitation (absorption), the molecule undergoes a radiative de-excitation (luminescence) or radiationless deactivation. The latter process, described as an internal conversion, is the transition from S_2 to S_1 without a change in multiplicity. This process occurs on the scale of 10^{-11} to 10^{-14} seconds. From that point, internal conversion is preceded by vibrational relaxation where excess vibrational energy is lost due to collisions between solute and solvent. Intersystem crossing, described as the radiationless transition between states of different multiplicity (S_1 to T_1), constitutes the internal quenching of S_1 and competes with fluorescence. The radiative de-excitation incorporates the radiative transitions between states of the same multiplicity is called fluorescence and occur on the order of 10^{-6} to 10^{-9} seconds. For the purpose of this thesis, only fluorescence will be described in detail.

Light emission from atoms or molecules can be used to quantitate the amount of

the emitting substance in a sample. The power of fluorescence emission, F, is

proportional to the radiant power of the excitation beam that is absorbed by the system:

$$F = k \; \varphi \; (P_o - P) \tag{1.3}$$

where P_o is the power of the beam incident upon the solution, P is its power after

traversing a length b of the medium, k is a geometric instrumental factor characterizing

the collection efficiency of the optical system, φ is the quantum efficiency (photons

emitted/photons absorbed).

The relationship between fluorescence intensity and analyte concentration is;

$$F = k \; \varphi \; P_o(1 - 10^{[-\varepsilon bc]}) \tag{1.4}$$

where ε is the wavelength-dependent molar absorptivity coefficient, b is the path length,

and c is the analyte concentration (ε, b, and c are the same as used in the Beer-Lambert

law).

Expanding the above equation in a Maclaurin series and dropping higher terms

gives:

$$F = k \; \varphi \; P_o \; (2.303 \; \varepsilon bc) \tag{1.5}$$

This relationship is valid at low concentrations ($<10^{-5}$ M) and shows that fluorescence

intensity is linearly proportional to analyte concentration. Determining unknown

concentrations from the amount of fluorescence that a sample emits requires calibration

of a fluorimeter with a standard (to determine K and φ) or by using a working curve.[19]

When c becomes great enough so that the absorbance is larger than about 0.05, the higher

order terms in the Maclaurin series become important and linearity is lost.

Many of the limitations of the Beer-Lambert law also affect quantitative

fluorimetry. Fluorescence measurements are also susceptible to inner-filter effects. These

effects include self-quenching resulting from the collisions between excited molecules

and self-absorption when wavelength of emission overlaps an absorption peak. The

former can expect to increase with concentration because of greater probability of

collisions occurring. During the latter phenomenon, fluorescence is then decreased as the

emission traverses the solution and is reabsorbed by other fluorescent molecules. Both of

these effects are discussed in greater detail in chapter 3.

Development of Predictive Expressions

Based Upon Mobile Order Theory

Learning more about the solubility of compounds in hydrogen-bonding systems

aids researchers in many different fields. Solubility is an important consideration in drug

design, chemical separation, extraction of chemicals from soil samples, and the transport

of organic pollutants in water systems. A problem facing researchers in solution

thermodynamics has been the development of a systematic approach for predicting phase

equilibria in hydrogen-bonding systems containing multifunctional alcohols.

Thermodynamic models have been used to estimate the composition of the solvational surrounding a chromophoric molecule and to rationalize how the observed spectroscopic behavior changes with solvent polarity. Many of the solution models currently used to describe the thermodynamic properties apply only to binary monofunctional alcohol mixtures and assume that the hydrogen-bonded self-associated complexes are linear, infinite polymers. For the most part, predictive methods provide fairly reasonable estimates for noncomplexing systems which contain only nonspecific interactions. However, many of the published expressions start to fail as the solution nonideality increases.

Mobile Order theory provides an alternative approach to mathematically describing associated solutions. The basic theory considers the fraction of time during which the alcoholic -OH groups are either free or involved in hydrogen bonding. The theory assumes that all molecules change the identity of their neighboring molecules as those molecules move, but not necessarily in a random fashion. The perpetual change in the contacts between molecular groups includes those molecules that do not form hydrogen bonds. Bonded groups do not remain at rest; they move together until the hydrogen bond is broken.

To date, the predictive expressions derived from the basic ideas of Mobile Order theory have often been comparable to (and sometimes even superior than) equations based upon the more conventional Nearly Ideal Binary Solvent (NIBS), Extended NIBS, Wilson, UNIFAC, Log-Linear, Kretschmer-Wiebe and Mecke-Kempter models.[20]

As mentioned, Mobile Order theory assumes that the molecules are constantly moving in liquid and that the neighbor of a given atom in a molecule is constantly

changing identity. All molecules of a given kind dispose of the same volume, equal to the total volume V of the liquid divided by the number N_A molecules of the same kind, i.e. Dom A = V/N_A. The center of this domain perpetually moves. The highest mobile disorder is given whenever groups visit all parts of their domain without preference. In this model, hydrogen bonds are not permanent. Rather, the hydrogen-bonded partners are continually changing and the lifetime of any given bond is between 10^{-11} to 10^{-5} seconds.[20,21,22] As argued by Huyskens, Kapuku, and Colemonts-Vandevyvere, thermodynamic and spectroscopic entities are not necessarily equal.

The spectroscopic alcoholic (component C) monomer concentration, $\gamma_{:Ch}$, is equal to the product of the fractions of time that the hydroxylic proton and oxygen lone electron pairs are not involved in hydrogen-bond formation. These time fractions are equal (i.e., $\gamma_{:C} \approx \gamma_{:Ch}$) and $\gamma_{:Ch} \approx \gamma_{Ch}^{2}$.

Hydrogen bonding is negligible in the vapor phase, but not in the liquid phase where the alcohol molecules are in much closer proximity to each other. The thermodynamics of Mobile Order theory expresses the equilibrium conditions in terms of time fractions for the time schedule of a given molecule, and not in terms of concentrations for various entities in the ensemble. Thus in the case of alcohols, one considers the fraction of time the hydroxylic proton is not involved in hydrogen bonding. This equation is given by;

$$1/\gamma_{Ch} = 1 + K_{Alco}\, C_{Alco} \qquad\qquad 1.6$$

where C_{Alco} is the stoichiometric concentration of the alcohol and K_{Alco} is the hydrogen-bond stability constant. The time that a given hydroxylic proton follows the oxygen of a neighboring alcohol molecule is proportional to the probability that the free proton encounters such an insertion site in its walk through the liquid. If γ_{Ch} vanishes, then all alcohol molecules are involved in a single, infinite hydrogen-bonded chain.[20]

Mobile Order theory expresses the Gibbs free energy of mixing for a multicomponent solution as;

$$\Delta G^{mix} = \Delta G_{conf} + \Delta G_{chem} + \Delta G_{phys} \qquad 1.7$$

the sum of three separate contributions. The first term describes the configurational entropy based upon the Huyskens and Haulait-Pirson definition of solution ideality;

$$\Delta G_{conf} = 0.5\ RT\ \Sigma n_i\ \ln x_i + 0.5\ RT\ \Sigma\ n_i\ \ln \phi_i \qquad 1.8$$

whereas the latter two terms in eqn. 1.7 result from formation of hydrogen-bonded complexes and weak, nonspecific interactions in the liquid mixture. The configurational Gibbs energy is an arithmetic average of free energies from Raoult's law and the Flory-Huggins model.

The chemical contribution depends upon the functional groups present and the characteristics of the various molecules present in the liquid mixture. Alcohols have one hydrogen "donor" site and the lone electron pairs on the oxygen provide two "acceptor" sites. The maximum possible number of hydrogen bonds is determined by the number of

sites that are in minority. According to Mobile Order theory, the hydrogen-bonding

contribution is given by;

$$\Delta G_{chem} = n_A RT \ln((1 + K_A/V_A)/(1 + K_A \phi_A/V_A)) \qquad 1.9$$

where K_A refers to the stability (equilibrium) constant of the hydrogen bond.

Acree suggested a more generalized description of nonspecific interactions;

$$\Delta G_{phys} = (\Sigma \, n_i \Gamma_i)^{-1} \, \Sigma\Sigma n_i \Gamma_i n_j \Gamma_j \beta_{ij} \qquad 1.10$$

based upon the Nearly Ideal Binary Solvent (NIBS) mixing model. In this expression, Γ_i

is the weighting factor for component i and β_{ij} is a binary interaction parameter that is

independent of composition. The NIBS approach is more general in that β_{ij}-parameters

can be determined for the specific binary interactions under consideration, rather than

calculated from "average" δ_i'-values obtained by regressing solubility data.

The types of functional groups present on the solute and solvent molecules

determine the number of terms in the Mobile Order theory predictive expressions. In the

case of an inert crystalline solute dissolved in a self-associating solvent, Mobile Order

theory expresses the volume fraction saturation solubility, ln ϕ_A^{sat}, as;

$$\ln \phi_A^{sat} = \ln a_A^{solid} - 0.5 \, (1 - V_A/V_{solv})\phi_{solv} + 0.5 \ln [\phi_A^{sat} + \phi_{solv} (V_A/V_{solv})]$$

$$- \phi_{solv}^2 V_A(\delta_A{}' - \delta_{solv}{}')^2 (RT)^{-1} - r_{solv}(V_A/V_{solv})\phi_{solv} \qquad 1.11$$

where ϕ_{solv} is the volume fraction of the solvent, $r_{solv}(V_A/V_{solv})\phi_{solv}$ represents the

contributions resulting from hydrogen-bond formation between the solvent molecules. A

more exact value for monofunctional alcoholic solvents can be calculated from;

$$r_{solv} = (K_{solv}\phi_{solv}/V_{solv})/(1 + K_{solv}\phi_{solv}/V_{solv}) \qquad 1.13$$

with a numerical value of $K_{solv} = 5,000 \text{ cm}^3 \text{ mol}^{-1}$ assumed for all monofunctional

alcohols. Regressing spectroscopic and vapor pressure data determined this value.

If complexation does occur between the crystalline solute and solvent;

$$\ln \phi_A{}^{sat} = \ln a_A{}^{solid} - 0.5 (1 - V_A/V_{solv})\phi_{solv} + 0.5 \ln [\phi_A{}^{sat} + \phi_{solv} (V_A/V_{solv})]$$

$$- \phi_{solv}{}^2 V_A(\delta_A{}' - \delta_{solv}{}')^2 (RT)^{-1} + \ln[1 + \phi_{solv}(K_{Asolv}/V_{solv})] \qquad 1.14$$

then an additional term involving the solute-solvent equilibrium constant, K_{Asolv}, must be

introduced to describe the solubility enhancement that arises as a result of specific

interactions. The numerical value of $a_A{}^{solid}$ can be computed from;

$$\ln a_A{}^{solid} = -\Delta H_A{}^{fus} (T_{mp}-T)/(RTT_{mp}) \qquad 1.15$$

the molar enthalpy of fusion, $-\Delta H_A{}^{fus}$, at the normal melting point temperature, T_{mp}.

Mobile Order theory has been successfully extended to solid solutes dissolved in

binary alkane (B) + alcohol (C) mixtures.[23] The simplest predictive treatment expresses

the volume fraction solubility of the solute $\phi_A{}^{sat}$;

$$\ln \phi_A{}^{sat} = \phi_B{}^\circ \ln (\phi_A{}^{sat})_B + \phi_C{}^\circ \ln (\phi_A{}^{sat})_C - 0.5 [\ln x_B{}^\circ V_B + x_C{}^\circ V_C) - \phi_B{}^\circ \ln V_B - \phi_C{}^\circ \ln V_C]$$

$$+ (V_A K_B \phi_B{}^\circ / V_B{}^2)(1 + K_B / V_B)^{-1} - (V_A K_B \phi_B{}^{\circ 2} / V_B{}^2)(1 + \phi_B{}^\circ K_B / V_B)^{-1}$$

$$+ (V_A K_C \phi_C{}^\circ / V_C{}^2)(1 + K_C / V_C)^{-1} - (V_A K_C \phi_C{}^{\circ 2} / V_B{}^2)(1 + \phi_C{}^\circ K_C / V_C)^{-1}$$

$$+ V_A \phi_B{}^\circ \phi_C{}^\circ (\delta_B{}' - \delta_C{}')^2 (RT)^{-1} \qquad \qquad 1.16$$

in terms of the measured solubility data in both pure solvents, $(\phi_A{}^{sat})_B$ and $(\phi_A{}^{sat})_C$. $x_B{}^\circ$ is

the mole fraction composition of component B in the binary solvent mixture, calculated

as if the third component were not present. The K_C is the Mobile Order theory self-

associated constant describing the hydrogen-bond formation involving the

monofunctional alcohol C where the concentration is in molarity and $\phi_C{}^\circ$ is the ideal

volume fraction composition of component C in the binary solvent mixture.

This relatively simple mathematical expression describes how the solubility varies

with binary solvent composition. Like many of the expressions derived previously, this

equation is limited to solutes having a very low mole fraction solubility $(1 - \phi_A \approx 1)$ and

reduces to a correct mathematical description of solute solubility in both neat and pure

alcohol cosolvents. Also, the final derived expression does not requite a prior knowledge

of the solute's enthalpy of fusion and melting point temperature, which would be needed

to calculate the numerical value of $a_A{}^{solid}$ at the temperature corresponding to the

solubility measurements.

Having failed at earlier attempts to calculate a meaningful value of K_C from

measured solubility, Ruelle et al. explored the feasibility of using "average" values of K_C

= 5000 cm^3 mol^{-1}.[20] For many of the systems, this value of K_C, combined with the

modified solubility parameter description of nonspecific interactions, led to slightly better

predictions. By treating anthracene and pyrene as inert solute molecules, incapable of interacting specifically with the polar alcohol cosolvent, Acree and coworkers simplified Mobile Order theory so as to enable the solubilities to be predicted with a minimum number of "curve-fit" and/or "input" parameters.

The success of Mobile Order theory in describing the solubility in binary alkane + alcohol solvent mixtures led to the extension of the basic model to systems containing a second monofunctional alcoholic cosolvent and alcohol + alkoxyalcohol solvent mixtures. For the purpose of this thesis, we will concentrate on alkane + alkoxyalcohol solvent mixtures, alkane + alcohol solvent mixtures, and neat organic nonelectrolyte solvents.

McHale *et al.* applied Mobile Order theory to inert solutes dissolved in alcohol + alkoxyalcohol solvent mixtures.[24] Such mixtures are characterized not only by the presence of long H-bonded chains wherein hydrogen-bonding occurs through the hydroxyl group, but also by chains involving hydrogen-bonding through the ether linkage.

```
OH----OR'OH----OH----OH----OROH----OH----OH
 I     I      I    I    I       I    I
 R     R      R  R'OR   R'      R  ROR'
```
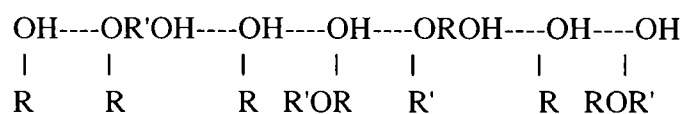
Both scenarios lead to extension of hydrogen-bonded chain, and it should be possible to treat the alkoxyalcohol as a "pseudo" monofunctional alcohol cosolvent.

From a hydrogen bonding point-of-view, the alkoxy oxygen atom provides in principle a second site for the fixation of the hydroxylic proton. It is expected that hydrogen bonding should occur largely through the hydroxylic OH groups because of its

much greater K_C stability constant. The fraction of time that the alcohol (B) and 2-

alkoxyethanol (C) molecules is not involved in hydrogen-bond formation are given by:

$$\gamma_{Bh} = 1/[1 + K_B\phi_B/V_B + (K_{BC} + K_{OBC})\phi_C/V_C] \qquad 1.17$$

$$\gamma_{Ch} = 1/[1 + K_{CB}\phi_B/V_B + (K_C + K_{OC})\phi_C/V_C] \qquad 1.18$$

Except for the two additional stability constants involving hydrogen bond formation

through the alkoxy oxygen atom (K_{OBC} and K_{OC}), both equations are identical to time-

fraction equations for binary alcohol + alcohol mixtures. For convenience, we will now

define two "pseudo" equilibrium/stability constants K_{BC}^* and K_C^* such that $K_{BC}^* = K_{BC} +$

K_{OBC} and $K_C^* = K_C + K_{OC}$. This set of conditions leads to the following expression for

the saturation solubility of a sparingly soluble solute;

$$\ln \phi_A^{sat} = \phi_B^\circ \ln (\phi_A^{sat})_B + \phi_C^\circ \ln (\phi_A^{sat})_C - 0.5 [\ln x_B^\circ V_B + x_C^\circ V_C) - \phi_B^\circ \ln V_B - \phi_C^\circ \ln V_C]$$

$$- (V_A/V_B) \phi_B^\circ [\phi_B^\circ (K_B/V_B) + \phi_C^\circ (K_{BC}^*/V_C)]/[1 + \phi_B^\circ (K_B/V_B) + \phi_C^\circ (K_{BC}^*/V_C)$$

$$+ (V_A K_B \phi_B^\circ /V_B^2)(1 + K_B/V_B)^{-1} - (V_A/V_C) \phi_C^\circ [\phi_B^\circ (K_{CB}/V_B) + \phi_C^\circ (K_C^*/V_C)]/[1 +$$

$$\phi_B^\circ (K_{CB}/V_B) + \phi_C^\circ (K_C^*/V_C) + (V_A K_C^* \phi_C^\circ /V_C^2)(1 + K_C^*/V_C)^{-1} + V_A\phi_B^\circ \phi_C^\circ (\delta_B' -$$

$$\delta_C')^2 (RT)^{-1} \qquad 1.19$$

dissolved in a binary alcohol + alkoxyethanol solvent mixture. The final derived

expression is mathematically identical to the expression for a binary alcohol cosolvent

solution with the difference being that the actual numerical values assumed for K_{BC}^* and K_C^* may not necessarily be equal $K_C = K_{BC} = 5,000 \ cm^3 \ mol^{-1}$.

Up to that time, all previous studies had assumed identical numerical values of $K_{alco} = 5,000 \ cm^3 \ mol^{-1}$ for the stability constant(s) for all monofunctional alcohols. Stability constants for hydrogen bond formation involving alcohols and ethers, however, are much weaker. Here, calculated values range between $K_{OC} = 100 \ cm^3 \ mol^{-1}$ and $K_{OC} = 300 \ cm^3 \ mol^{-1}$. Given the relative magnitudes of the two stability constants, combined with the fact that the alkoxy hydroxylic OH and ether O atom molar concentrations are equal, it is expected that hydrogen bond formation should occur largely through the OH group. Close proximity of the OH and O functional group may further encourage proton fixation at the OH "acceptor" site. Assuming numerical values of $K_C = 5,000 \ cm^3 \ mol^{-1}$, $K_{OC} = 100 \ cm^3 \ mol^{-1}$, and $V_C = 100 \ cm^3 \ mol^{-1}$, the authors calculated that a typical alkoxyalcohol would be engaged in hydrogen bonding approximately 98 % of the time.

Part of the purpose of this thesis is to extend mobile order theory to alkane + alkoxyalcohols. Also, earlier studies of alkane + alcohol used a limited number of solubility data. Another part of this research looks at pyrene solubilities in alkane + alcohol solvent mixtures to further test the applications and limitations of predictive expressions derived from mobile order theory. Finally, I report anthracene and *trans*-stilbene solubilities in a number of organic solvents. These results, combined with previous solubility data, further test the predictive expressions derived from mobile order theory.

Quenching of Fluorescence Emission

This research is a continuation of past work to develop a better experimental methodology for the analysis of mixtures of polycyclic aromatic hydrocarbons. Current methods often use HPLC with fluorescence detection. However, there are several problems with the current method. Often, many mixtures contain several PAHs and is therefore hard to isolate one PAH. Also, baseline resolution is not always easily achievable. Finally, while several PAHs may absorb at the same excitation wavelength, not all will emit at the wavelengths monitored by the detector. Solutes often co-elute; resulting in overlapping peaks which makes quantification more difficult. While HPLC separations are very useful, they are also very time consuming whenever a large number of isomeric compounds are present.

To approach this problem, we need to make the fluorescence detector respond to only a single class of PAHs. Fluorescence affords the most selectivity in that the excitation and emission wavelengths can vary independently. Also, fluorescence quenching agents can be used to selectively eliminate signals of entire classes of PAHs. This will further simplify the observed emission spectra and eliminate undesired chemical interferences having only slightly different molecular structures.

To classify PAHs used in this thesis, PAHs are classified as alternant polycyclic aromatic hydrocarbons if every alternant carbon atom in the aromatic ring system can be starred i.e. all six-membered rings. Nonalternant PAHs, on the other hand, would have at least one pair of adjacent starred (or unstarred) carbon atoms. For example, an alternant methylene-bridged cyclopenta PAH initially appears to be a nonalternant PAH. However, starring and unstarring takes place only in the aromatic portion. Since the

bridgeheads have two hydrogen bonds and do not contain a double bond, they are not included in the aromatic portion of the ring.

Quenching of the intensity of fluorescence emission may be due to the deactivation of the excited states responsible for fluorescence emission by an interaction of either the ground state or the excited state of the fluorescing species with other species in solution. The fluorescence quenching process may occur through different mechanisms and induced by many quenchers. For the purpose of this thesis, we will only examine static and dynamic quenching in detail.

Earlier studies of the impurity quenching of fluorescence in fluid solutions as a function of solvent viscosity identifies three quenching processes;

1. Viscosity-independent process, referred to as static quenching;

2. Diffusion controlled process, referred to as dynamic quenching;

3. A combination of both static and dynamic quenching.[25]

When the quenching involves a collisional encounter between $^1PAH^*$ and Q, a reasonable distinction can be made between static and dynamic quenching. Static quenching is attributed by a complex formation, present in the ground state, which competes with ^1PAH for the incident excitation, and which yields an excited complex (and thus quenching) directly by absorption.

$$^1PAH + Quencher \rightleftarrows {}^1PAH\text{-}Quencher \qquad\qquad 1.20$$

The equilibria can be described by an association of binding constant:

$$K_{PAH-Q} = [PAH-Quencher]/[PAH][Quencher] \qquad 1.21$$

If the quencher and complex do not fluoresce, the fluorescence signal is directly proportional to the free PAH. A mass balance on the total molar concentration of the PAH fluorophore:

$$[PAH] = [PAH]_{free} + [PAH-Quencher] \qquad 1.22$$

The measured fluorescence emission intensity in terms of the associating bonding constant is;

$$F_0 = F\{1 + K_{PAH-Q}[Quencher]\} \qquad 1.23$$

where F_0 is the initial fluorescence intensity equal to [PAH] and F is observed fluorescence emission intensity at any time (equal to $[PAH]_{free}$).[26]

Dynamic quenching, on the other hand, occurs in the excited state and causes a decrease in fluorescence emission through collision deactivation involving the excited fluorophore. The nonradiative decay mechanism for returning the fluorophore back to its original ground state is

$$^1PAH^* + Quencher \xrightarrow{k_Q} {}^1PAH + Quencher \qquad 1.24$$

where k_Q refers to the second-order rate constant for quenching.

In the absence and presence of quenching agents, the change in the molar

concentration of the excited fluorophore species with time is given by;

$$d[PAH^*]/dt = k_{abs}[PAH] - k_{fluor}[PAH^*] - k_{IC}[PAH^*] - k_{ISC}[PAH^*]$$ 1.25

$$d[PAH^*]/dt = k_{abs}[PAH] - k_{fluor}[PAH^*] - k_{IC}[PAH^*]$$
$$- k_{ISC}[PAH^*] - k_q[Quencher][PAH^*]$$ 1.26

where k_{abs}, k_{fluor}, k_{IC}, and k_{ISC} refer to the rate constants for absorbance, fluorescence,

internal conversion, and inter-system crossing, respectively. Under steady state

conditions;

$$d[PAH^*]/dt = 0$$ 1.27

and equations 1.22 and 1.23 are solved for the molar concentration of the excited

fluorophore;

$$[PAH^*] = k_{abs}[PAH]/(k_{fluor} + k_{IC} + k_{ISC})$$ 1.28

$$[PAH^*] = k_{abs}[PAH]/(k_{fluor} + k_{IC} + k_{ISC} + k_Q[Quencher])$$ 1.29

which is directly proportional to the emission signal, F, since the fluorescence process

begins with absorption of excitation radiation. Through mathematical manipulation, a

relatively simple expression is derived for relating the measured fluorescence emission to the quencher concentrations;

$$[PAH^*] = k_{abs}[PAH](k_{fluor} + k_{IC} + k_{ISC})^{-1}$$

$$X \{1 + k_Q[Quencher]/(k_{fluor} + k_{IC} + k_{ISC})\}^{-1} \qquad 1.30$$

$$F_0 / F - 1 = k_Q[Quencher] X (k_{fluor} + k_{IC} + k_{ISC})^{-1} \qquad 1.31$$

$$F_0 / F - 1 = k_Q[Quencher] \qquad 1.32$$

where F_0 refers to the measured fluorescence intensity in the absence of quenching agents.

The numerical value for k_Q is determined by preparing a series of standard solutions having known quencher concentrations, in the same fashion as one determines the molar absorptivity coefficient in the Beer-Lambert law, except one is monitoring fluorescence emission as opposed to absorbance of the solution. In the above treatment, we assume that the stoichiometric concentration of the fluorophore is constant for all the solutions, and that the quenching process results from collisions between the excited fluorophore and quenching agents.

The third possible mechanism is a combination of both static and dynamic quenching. Examining both the static quenching equation (1.20) and the dynamic quenching equation (1.24), the two reactions taking place are the formation of the ground state complex;

$$^1PAH + Quencher \rightleftharpoons {}^1PAH\text{-}Quencher \qquad\qquad 1.20$$

and the collisional deactivation of the vibrational relaxed excited state fluorophore:

$$^1PAH^* + Quencher \xrightarrow{k_Q} {}^1PAH + Quencher \qquad\qquad 1.24$$

The equilibrium of the complex formation by static quenching can be described by equation 1.18 and the steady-state conditions for dynamic quenching can be described by equation 1.26. Keeping in mind the fluorescence emission intensity is directly proportional to the excited state $[PAH^*]$, substitution of equation 1.21 into equation 1.26 arrives at the general result which is a more complex model.

$$F = k_{fluor} \, k_{abs}[PAH]_{total}\{(1 + k_Q[Quencher])$$

$$X \, (k_Q[Quencher] + k_{fluor} + k_{IC} + k_{ISC})\}^{-1} \qquad\qquad 1.33$$

Quenching behavioral differences between alternant and nonalternant PAHs upon addition of an electron/charge acceptor quenching agent can be rationalized in terms of processes originating from the virbrationally relaxed first electronic excited singlet state via a dynamic quenching mechanism. Deactivation from the $^1PAH^*$ state is governed by the competition between radiative and nonradiative processes. Rate constants for fluorescence decay, k_{fluor}, for PAH fluorophores are generally insensitive to molecular environment. Efficiencies of nonradiative processes depend to a large extent upon

external perturbations resulting form interactions involving PAH solutes with solvent/quenching molecules. Excited state electron/charge transfer is commonly supposed to be a general mechanism of fluorescence quenching in the absence of energy transfer and heavy-atom effects.

Zander, Breymann, and co-workers attributed nitromethane's selectivity towards alternant PAHs to an electron/charge transfer reaction whereby intermolecularly an electron (or charge) was transferred from the excited PAH fluorophore to nitromethane, which served as the electron/charge acceptor.[27] Quantum mechanical computations show the highest occupied molecular orbital (HOMO) and the lowest unoccupied molecular orbital (LUMO) energies of nonalternant PAHs to be lowered against those of alternant PAHs of equal HOMO-LUMO energy separation. For the electron transfer reaction;

$$^1PAH^* + {}^1Quencher \rightarrow {}^2PAH^{\delta+/-} + {}^2Quencher^{\delta+/-} \qquad 1.34$$
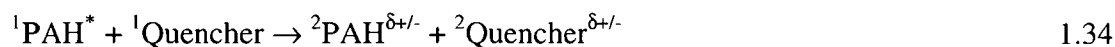
the change in free energy is expected to be more negative in the case of alternant PAHs. Figure 2 depicts the molecular orbital diagram indicating the conditions for electron/charge transfer between an electron donor alternant PAH and an electron acceptor quenching agent. The quencher's LUMO and nonalternant's LUMO are placed at energies so as to discourage electron/charge transfer. Slow electron/charge transfer reactions are not expected to affect fluorescence intensities, since the photon is emitted long before electron/charge transfer from the PAH* donor to the quencher acceptor can occur.

ELECTRON
TRANSFER

??

(LUMO) PAH*

(LUMO) PAH*

QUENCHER*

(LUMO) PAH*

$E_{REDUCTION}$

(HOMO) PAH

$E_{OXIDATION}$

(HOMO) PAH

QUENCHER

NONALTERNANT PAH
(ELECTRON DONOR)

QUENCHER
(ELECTRON ACCEPTOR)

ALTERNANT PAH
(ELECTRON DONOR)
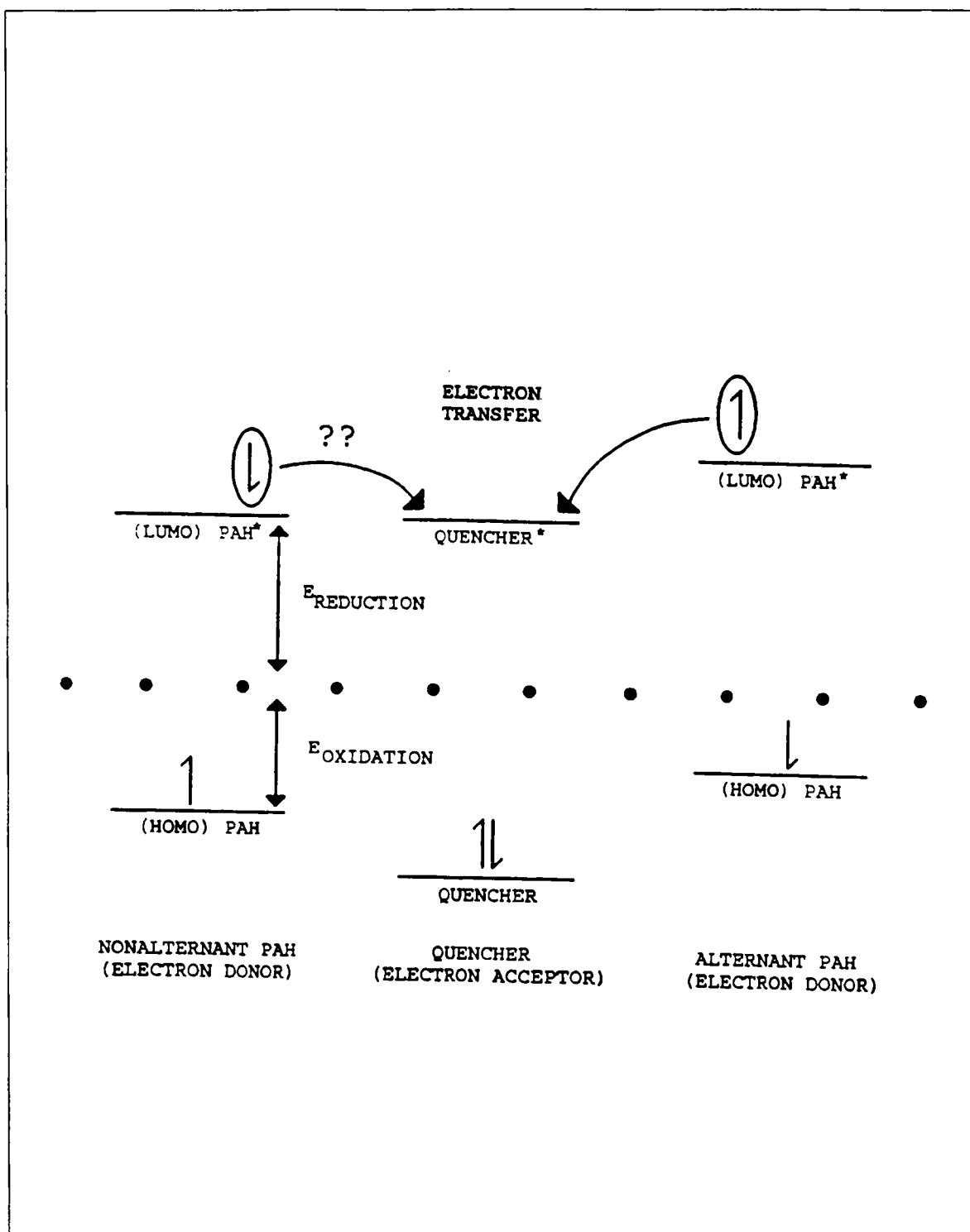
FIGURE 2: Simplified molecular orbital diagram indicating favorable conditions for electron transfer between electron donor alternant polycyclic aromatic hydrocarbon and an electron acceptor quenching agent. The dotted line represents the potential of a reference electrode.

Quenching of the fluorescence emission of PAHs by nitromethane is now well documented and involves an electron/charge transfer mechanism. The electron transfer mechanism postulated above requires favorable reaction kinetics and thermodynamic conditions. From a strictly thermodynamic point of view, it is conceivable that the extent of quenching could be altered. By changing the electronic nature of the surrounding solvent media, the charge (or partial charge) that is temporarily formed on the polycyclic aromatic hydrocarbon could be to either stabilize or destabilize with the addition of functional groups to the molecule. Electron donating groups should stabilize a positive charge, while electron-withdrawing groups should destabilize the same. Previous studies show that for the most part, strongly deactivating, electron-withdrawing groups effectively hinder the electron/charge transfer process. The electron-donating substituents expedite the electron transfer process, however one would expect these results given that electron/charge transfer does occur for all alternant parent compounds. Also, several derivatives of nonalternant parent compounds have been studied. For the most part, their quenching behavior is identical to that of the parent compound. Using nitromethane or any other selective quenching agent for identification and separation purposes requires that the experimentally determined spectra be free of chemical and instrumental discrepancies that might reduce emission intensities. Primary and secondary inner-filtering is a major problem associated with obtaining correct fluorescence data, assuming that the sample is optically dilute at all analytical wavelengths. With nitromethane, it absorbs significant quantities of radiation in the spectral region (300-350 nm) used to excite the PAHs. There is a need to measure the absorbance of the solution at the excitation wavelength when using nitromethane as a

selective quenching agent in HPLC. Thus, a search for a selective quenching agent with minimal inner-filtering corrections is called for. Later, I will discuss research with a new group of selective quenching agents that act with the same mechanistic pathways of nitromethane, alkylpyridinium cations.

Molecularly Organized Assemblies

In 1913, it was postulated that fatty acid salts in aqueous dilute solution

spontaneously from dynamic aggregates, now called micelles.[28] Later it was found that

natural and synthetic amphipathic molecules such as surfactants and detergents also form

micelles in aqueous solution.[29] A surfactant or detergent is characterized by having a

molecular structure incorporating a long hydrocarbon chain attached to ionic or polar

head groups. The polar head group of the molecule is intrinsically soluble in water; the

fatty acid tails are hydrophobic.

Spontaneous organization of surfactants to form spherical or ellipsoidal micelles

in water creates dynamic aggregates that provide the solutions with some unique

properties depending on amphiphile structure and solution composition (see Figure 3).
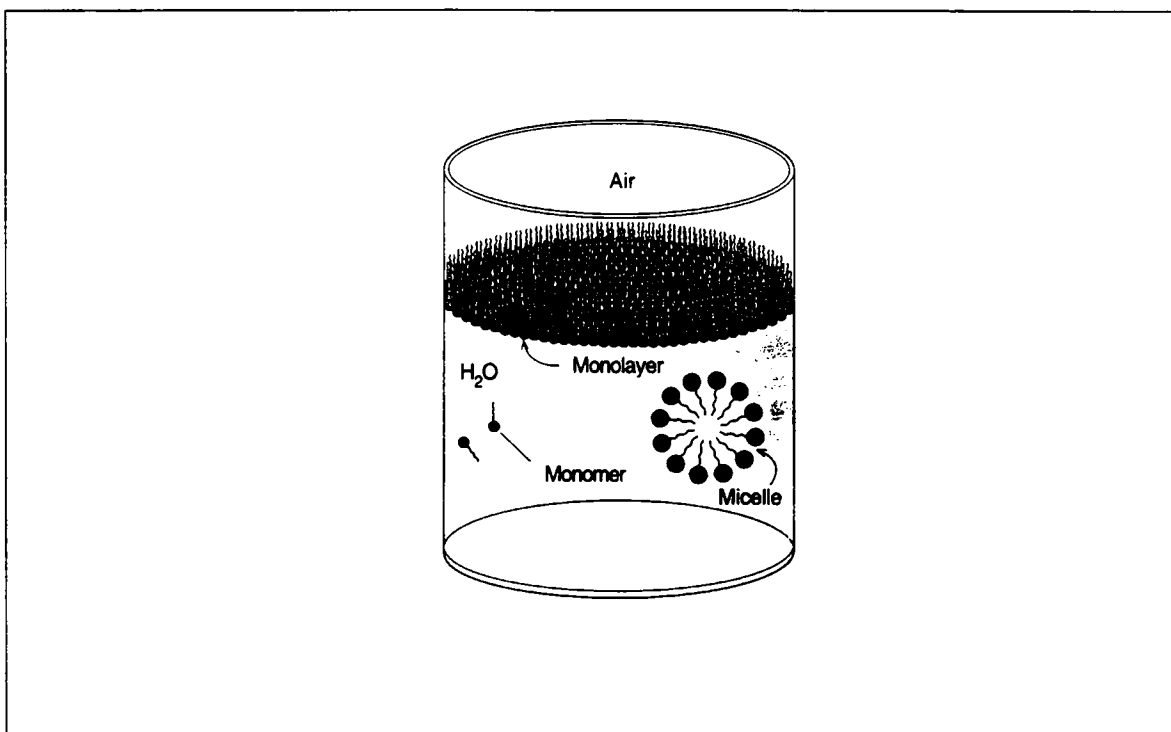
FIGURE 3: Structures formed by detergents in aqueous solutions.
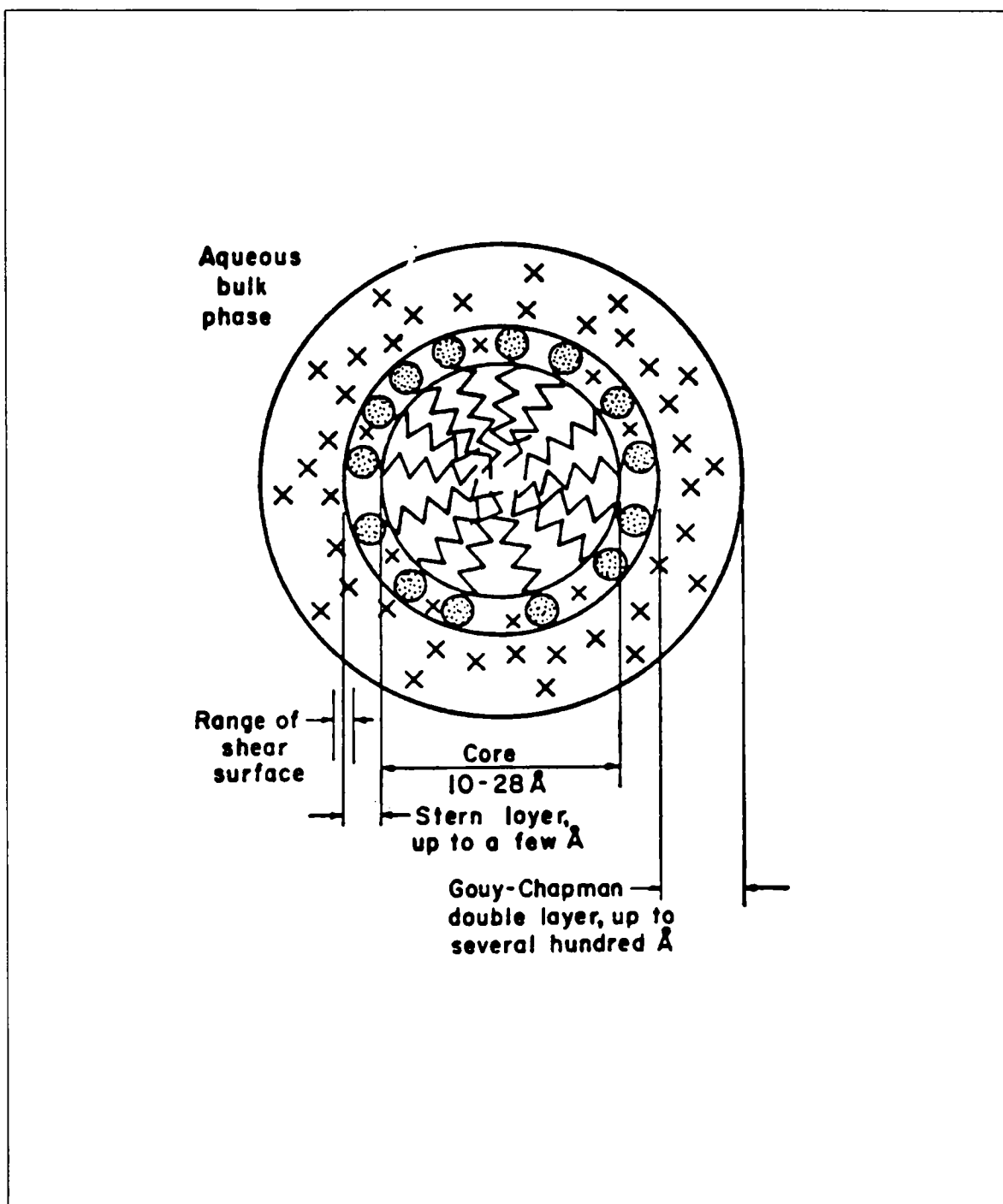
FIGURE 4: An oversimplified two-dimensional representation of a spherical ionic micelle. The counterions (x), the headgroups (O), and the hydrocarbon chains (^) are schematically indicated to denote their relative locations, but not their numbers, distribution, or configuration.

The interfacial region, called Stern layer, contains the ionic or polar headgroups of the surfactant molecules, a fraction of counter ions and water. This stern layer is an extremely anisotropic region and has properties between hydrocarbon and water. Thermal motion creates a diffuse electrical double layer, called Gouy-Chapman layer that extends out into the aqueous phase.[31] For a two-dimensional representation of this, refer to Figure 4.

Surprisingly, this process is driven, not by a decrease in energy, but rather an increase in entropy associated with removing the hydrocarbon chains from water.[30] If a hydrocarbon is dissolved in water, the water molecules surrounding it adopt a netlike structure that is more highly ordered than the structure of pure liquid water. Burying the hydrocarbon tails of the detergent molecules in the center of a micelle frees many water molecules from these nets and increases the overall amount of disorder in the system. Within my study, micellar solutions provide a very convenient way to introduce ionic character and still have a solvent media capable of solubilizing the larger, hydrophobic PAH solutes.

In organized media, changes in the nature of the environment experienced by a given solute on transfer from a bulk aqueous medium to the host aggregate are strongly reflected in the fluorescence emission. Thermodynamically, it is conceivable that the extent of quenching could be altered by changing the electronic nature of the surrounding solvent medium in order to either stabilize or destabilize the charge (or partial charge) that is temporarily formed on the polycyclic aromatic hydrocarbon and/or on the quenching agent.

Within this study, nitromethane selective quenching would be examined in mixed surfactant systems with different physiochemical properties. The micellar systems that are investigated comprise of surfactant monomers with different charged polar headgroups, different counterions, and varying hydrocarbon chain length. Greater detail into these systems is described in Chapter Three—Fluorescence Studies.

Mixed micellar solutions of anionic + nonionic will be utilized to investigate the behavior of nitromethane quenching towards alternant versus nonalternant polycyclic aromatic hydrocarbons. Finally, the need for having more efficient selective quenchers is addressed using alkylpyridinium cations as surfactant quenchers which act to minimize the inner-filtering corrections.

Chapter Bibliography

1. Wetzel, S.C.; Banks, M.K.; Schwab, A.P. *Proceedings of the 10th Annual Conference on Hazardous Waste Research* (1995).

2. Blumer, M *Scientific American*, **1978**, *234*, 3, 35.

3. Hurst, C.J.; Sims, R.C.; Sims, J.L.; Sorensen, D.L.; McLean, J.E.; Huling, S. *Proceedings of the 10th Annual Conference on Hazardous Waste Research* (1995).

4. McGinnes, P.R.; Snoeyink, V.L, *WRC Res. Rept.*, **1974**, *80*, UILU-WRC-74-0080, PB-232, 168.

5. Dobbins, D.C.; Aelion C.M; Pfaender F. *Crit. Rev. Environ. Control*, **1992**, *22* (1/2) 67.

6. Reiley, K.A.; Banks, M.K.; Schwab, A.P. *J. Environ. Quality*, **1996**, *25*, 212.

7. McGinnis, G.D., U.S. EPA, Washington D.C., EPA 600/S2-88/055, **1998**.

8. Madsen, T.; Kristensen, P. *Environmental Toxicology and Chemistry* , **1996**, *16*, 4, 631.

9. Tabak, HH; Fovind, R.; Gao, C.; Fu, C *Journal of Environmental Science and Health Part A, Toxic/Hazardous Substances and Environmental Engineering*, **1998**, *33*, 8, 1533.

10. Sims, R.C.; Overcash, M.R *Residue Reviews*, **1983**, *88*, 1.

11. Atlas, R.M. *Microbiological Reviews*, **1981**, *45* 180.

12. Kobayaski, H.; Rittman, B.E. *Environmental Science and Technology*, **1982**, *16* 170A.

13. Mahmook, S.K.; Rao, P.R. *Bulletin of Environmental Contamination and Toxicology*, **1997**, *50*, 4, 486.

14. Mahro, B.; Eschenbach, A; Schaefer, G; Kaestner, M. *DECHEMA Monographien*, 133, 509.

15. Saim, N., Dean, J., Abdullah, M.P.; Zakaria, Z. *J. Chrom. A*, **1997**, *791*, 361.

16. Skoog, D.; Holler, F.J.; Nieman, T.A. <u>Principles of Instrumental Analysis</u>, 5th Ed., Saunders College Publishing, New York, 1998.

17. Wehry, E.L. <u>In Fluorescence: Theory, Instrumentation, and Practice</u>, Guilbault, G.G. (Ed.). Marcel Dekker, Inc. New York, 1967, pp. 37.

18. Pandey, S. Dissertation, University of North Texas (1998).

19. Acree, Jr., W.E.; Zvangzne, A.I. *Fluid Phase Equilibria*, **1994**, *99*, 167.

20. Acree, Jr., W.E.; Powell, J.R.; McHale, M.E.R.; Pandey, S.; Borders, T.L.; Campbell, S.W. *Research Trends in Physical Chemistry*, **1997**, *6*, 197.

21. Huyskens, P.L. *J. Mol. Struct.* **1993**, 297.

22. Ruelle, P.; Buchmann, M.; Kesselring, U.W. *J. Pharm Sci*, **1994**, *83*, 396.

23. Acree, Jr., W.E.; Zvaigzne, A.I.; Tucker, S.A. *Fluid Phase Equilibria*, **1994**, *92*, 233.

24. McHale, M.E.R.; Coym, K.S.; Roy, L.E.; Hernandez, C.E.; Acree, Jr., W.E. *Can. J. Chem.*, **1997**, *75*, 1403.

25. Pringsheim, P. <u>Fluorescence and Phosphorescence</u>, Interscience, New York, 1949.

26. Acree, Jr., W.E. *Environ. Sci. Technol.*, **1993**, *27*, 757.

27. Breymann, U.; Preeskamp, H.; Koch, E; Zander, M *Chem. Phys. Lett.*, **1978**, *59*, 68.

28. McBain, J.W. *Trans Faraday Soc.* **1913**, *9*, 99.

29. Fendler, J.H. *Pure and Appl. Chem.*, **1982**, *54*, 1809.

30. Zubay, G.L <u>Biochemistry</u>, Wm. C. Brown Publishers, Dubuque, 1998, pg. 448.

31. Fendler, J.H. <u>Membrane Mimetic Chemistry</u>, Wiley-Interscience: New York, 1982.

Chapter 2

Materials and Methods

Solubility Studies

The PAHs used in Table I were recrystallized several times with the appropriate

solvent. All solvents from Tables II-V were stored over molecular sieves and distilled

shortly before use. Gas chromatographic analysis showed solvent purities to be 99.7

mole percent or better.

Alkoxyalcohol + alkane binary solvent mixtures and alcohol + alkane binary

solvent mixtures were prepared by mass so that compositions could be calculated to

0.0001 mole fraction. Excess solute and solvent were placed in amber glass bottles and

allowed to equilibrate in a constant temperature water bath at 25.0 ± 0.1 °C (26.0 ± 0.1

°C in the case of pyrene) with periodic agitation for at least three days (often longer).

Attainment of equilibrium was verified both by repetitive measurements after a minimum

of three additional days and by approaching equilibrium from supersaturation by pre-

equilibrating the solutions at a higher temperature. Aliquots of saturated PAH solutions

were transferred through a coarse filter into a tared volumetric flask to determine the

amount of sample and diluted quantitatively with methanol for spectrophotometric

analysis at the analysis wavelength (see Table I) on a Bausch and Lomb Spectronic 2000.

In the case of hexadecane and decane solvent systems, dilutions were made with ethanol

because of miscibility problems encountered when trying to dilute the saturated solutions

methanol. Concentrations of the dilute solutions were determined from a Beer-Lambert

law absorbance versus concentration working curve derived from measured absorbances

36

of standard solutions of known molar concentrations. Ranges of the molar absorptivity,

ε, and standard molar concentrations are given in Table I.

Apparent molar absorptivities of the nine standard solutions varied systematically

with molar concentration. Identical molar absorptivities were obtained for select PAH

standard solutions that contained up to 5 volume percent of the neat alkane +

alkoxyalcohol, alkane + alcohol, or organic cosolvents. Experimental molar

concentrations were converted to (mass/mass) solubility fractions by multiplying by

molar mass of the solute, volume(s) of volumetric flask(s) used and any dilutions

required to place the measured absorbances on the Beer-Lambert law absorbance versus

concentration working curve, and then dividing by the mass of the saturated solution

analyzed. Mole fraction solubilities were computed from (mass/mass) solubility fractions

using the molar masses of the solutes and solvents.

Experimental anthracene solubilities in the binary solutions are listed in Tables VI

to XII. Experimental pyrene solubilities in the binary solutions are listed in Tables XIII to

XV. Experimental anthracene solubility in 21 different organic solvents studied are listed

in Table XVI. Experimental *trans*-stilbene solubility in 17 different organic solvents

studied are listed in Table XVII. Numerical values represent the average of between four

and eight independent determinations, with the measured values being reproducible to

within ±1.5% to ±2.0%.

TABLE I. Names of polycyclic aromatic hydrocarbons, Source/Supplier, percent purity, recrystallizing solvent, analysis wavelength, molar absorptivity ranges for each PAH, and standard molar concentration ranges.

Name of PAH	Anthracene	Pyrene	trans-Stilbene
Source/Supplier (%Purity)	Gold Label, Aldrich (99.99%+)	Aldrich (99%+)	Aldrich (96%)
Recrystallizing solvent	2-Propanone	Methanol	Methanol
λ_{anal} (nm)	356	372	294
ε ranges (Liter mol^{-1} cm^{-1})	7450 to 7150	234 to 220	28,850
Concentration ranges * 10^5 (mol L^{-1})	6.75 to 22.5	6.75 to 22.5	1.38 to 4.62

TABLE II. Name of alkoxyalcohol solvents, Source/Supplier, and percent purity.[1-5]

Name of Alkoxyalcohol	Source/Supplier (% Purity)
2-Ethoxyethanol	Aldrich (99%)
2-Propoxyethanol	Aldrich (99%)
2-Isopropoxyethanol	Aldrich (99%)
2-Butoxyethanol	Acros (99%)
3-Methoxy-1-butanol	Aldrich (99%)

TABLE III. Name of alcohol solvents, Source/Supplier, and percent purity.[6-8]

Name of Alcohol	Source/Supplier (% Purity)
1-Pentanol	Aldrich (99%)
2-Ethyl-1-hexanol	Aldrich (99%)
1-Butanol	Aldrich (99%)
2-Butanol	Aldrich (99%)
2-Methyl-1-propanol	Aldrich (99%)

TABLE IV. Name of alkane solvents, Source/Supplier, and percent purity.[1-10]

Name of Alkane	Source/Supplier (% Purity)
Hexane	Aldrich (99+%)
Heptane	Aldrich, HPLC
Octane	Aldrich (99%)
Cyclohexane	Aldrich, HPLC
Methylcyclohexane	Aldrich (99+%)
2,2,4-Trimethylpentane	Aldrich, HPLC
tert-Butylcyclohexane	Aldrich (99%)
n-Nonane	TCI (99+%)
n-Decane	TCI (99+%)
n-hexadecane	Aldrich (99+%)

TABLE V. Names of organic nonelectrolyte solvents, Source/Supplier, and percent purity.[9,10]

Name of Solvent	Source/Supplier (% Purity)
Ethylene glycol	Aldrich (99%)
Acetonitrile	Aldrich, HPLC (99.9+%)
Benzene	Aldrich, HPLC (99.9+%)
Toluene	Aldrich (99.8%)
2,2,2-Trifluoroethanol	Aldrich (99+%)
Tetrachloromethane	Aldrich, HPLC, (99+%)
Chlorobenzene	Aldrich, HPLC, (99+%)
m-Xylene	Aldrich (99+%)
p-Xylene	Aldrich (99+%)
o-Xylene	Aldrich, HPLC (99+%)
Ethylbenzene	Aldrich (99.8%)
2-Butanone	Aldrich, HPLC (99.5+%)
1,4-Dioxane	Aldrich, HPLC (99.9%)
Tetrahydrofuran	Aldrich (99.9%)
1-Chlorohexane	Aldrich (99%)
Trichloromethane	Aldrich (99%)
Dichloromethane	HPLC, Aldrich (99.9+%)
Methyl acetoacetate	Aldrich (99%)
Ethyl acetoacetate	Aldrich (99%)

TABLE V. Continued.

Name of Solvent	Source/Supplier (% Purity)
Methanol	Aldrich (99.9+%)
Ethanol	Aaper Alcohol and Chemical Co.
1-Hexanol	Alfa Aesar (99+%)
1-Heptanol	Alfa Aesar (99+%)
Cyclopentanol	Aldrich (99%)
Benzonitrile	Aldrich (99%)
N,N-Dimethylformamide	Aldrich (99.8%)
N,N-Dimethylacetamide	Aldrich (99.8%)

TABLE VI. Experimental Mole Fraction Solubilities of Anthracene (x_A^{sat}) in Binary Alkane (B) + 2-Ethoxyethanol (C) Solvent Mixtures at 25.0 °C.[1]

$x_C^°$	x_A^{sat}
Hexane (B) + 2-Ethoxyethanol (C)	
0.0000	0.001274
0.1278	0.001740
0.2647	0.002157
0.4837	0.002698
0.5851	0.002947
0.6786	0.003106
0.8386	0.003158
0.9340	0.003074
1.0000	0.002921
Heptane (B) + 2-Ethoxyethanol (C)	
0.0000	0.001571
0.1583	0.002085
0.2787	0.002402
0.5044	0.002920
0.6029	0.003109
0.6998	0.003229
0.8573	0.003276
0.9265	0.003152
1.0000	0.002921

TABLE VI. Continued.

x_C°	x_A^{sat}
Octane (B) + 2-Ethoxyethanol (C)	
0.0000	0.001838
0.1779	0.002397
0.2987	0.002703
0.5246	0.003146
0.6224	0.003278
0.7186	0.003376
0.8679	0.003293
0.9315	0.003173
1.0000	0.002921
Cyclohexane (B) + 2-Ethoxyethanol (C)	
0.0000	0.001553
0.1151	0.002076
0.2195	0.002461
0.4346	0.003051
0.5300	0.003238
0.6247	0.003321
0.8151	0.003287
0.9033	0.003142
1.0000	0.002921

TABLE VI. Continued.

x_C^o	x_A^{sat}
Methylcyclohexane (B) + 2-Ethoxyethanol (C)	
0.0000	0.001649
0.1224	0.002196
0.2531	0.002604
0.4700	0.003059
0.5775	0.003224
0.6745	0.003313
0.8452	0.003266
0.9181	0.003134
1.0000	0.002921
2,2,4-Trimethylpentane (B) + 2-Ethoxyethanol (C)	
0.0000	0.001074
0.1778	0.001528
0.3156	0.001885
0.5317	0.002420
0.6207	0.002609
0.7288	0.002859
0.8670	0.003020
0.9376	0.003013
1.0000	0.002921

TABLE VII. Experimental Mole Fraction Solubilities of Anthracene (x_A^{sat}) in Binary Alkane (B) + 2-Propoxyethanol (C) Solvent Mixtures at 25.0 °C.[2]

x_C^o	x_A^{sat}
Hexane (B) + 2-Propoxyethanol (C)	
0.0000	0.001274
0.1249	0.001759
0.2326	0.002146
0.4317	0.002711
0.5320	0.002953
0.6522	0.003132
0.8262	0.003357
0.9002	0.003380
1.0000	0.003343
Heptane (B) + 2-Propoxyethanol (C)	
0.0000	0.001571
0.0978	0.001908
0.2328	0.002308
0.4686	0.002874
0.5579	0.003031
0.6638	0.003165
0.8444	0.003346
0.9301	0.003357
1.0000	0.003343

TABLE VII. Continued.

x_C°	x_A^{sat}
Octane (B) + 2-Propoxyethanol (C)	
0.0000	0.001838
0.1508	0.002338
0.2637	0.002646
0.4798	0.003140
0.5839	0.003302
0.6912	0.003448
0.8465	0.003493
0.9284	0.003435
1.0000	0.003343
Cyclohexane (B) + 2-Propoxyethanol (C)	
0.0000	0.001553
0.0890	0.002003
0.1777	0.002341
0.3903	0.002949
0.4892	0.003127
0.5941	0.003238
0.8009	0.003368
0.8854	0.003377
1.0000	0.003343

TABLE VII. Continued.

x_C°	x_A^{sat}
Methylcyclohexane (B) + 2-Propoxyethanol (C)	
0.0000	0.001649
0.1025	0.002154
0.2075	0.002520
0.4274	0.003039
0.5240	0.003233
0.6156	0.003355
0.8149	0.003416
0.9246	0.003409
1.0000	0.003343
2,2,4-Trimethylpentane (B) + 2-Propoxyethanol (C)	
0.0000	0.001074
0.1322	0.001458
0.2477	0.001764
0.4922	0.002402
0.5876	0.002631
0.6856	0.002872
0.8605	0.003217
0.9286	0.003297
1.0000	0.003343

TABLE VII. Continued.

$x_C{}^o$	$x_A{}^{sat}$
tert-Butylcyclohexane (B) + 2-Propoxyethanol (C)	
0.0000	0.001978
0.1468	0.002545
0.2793	0.002880
0.4952	0.003307
0.6002	0.003457
0.6974	0.003549
0.8544	0.003524
0.9230	0.003442
1.0000	0.003343

TABLE VIII. Experimental Mole Fraction Solubilities of Anthracene $(x_A{}^{sat})$ in Binary Alkane (B) + 2-Isopropoxyethanol (C) Solvent Mixtures at 25.0 °C.[3]

$x_C{}^o$	$x_A{}^{sat}$
Hexane (B) + 2-Isopropoxyethanol (C)	
0.0000	0.001274
0.1110	0.001686
0.2247	0.002073
0.4685	0.002667
0.5285	0.002778
0.6392	0.002950
0.8258	0.003133
0.9068	0.003125
1.0000	0.003093
Heptane (B) + 2-Isopropoxyethanol (C)	
0.0000	0.001571
0.1228	0.001973
0.2487	0.002319
0.4603	0.002760
0.5592	0.002924
0.6717	0.003058
0.8367	0.003120
0.9228	0.003106
1.0000	0.003093

TABLE VIII. Continued.

x_C^o	x_A^{sat}
Octane (B) + 2-Isopropoxyethanol (C)	
0.0000	0.001838
0.1600	0.002351
0.2834	0.002616
0.4881	0.002972
0.5878	0.003103
0.7075	0.003186
0.8531	0.003155
0.9277	0.003125
1.0000	0.003093
Cyclohexane (B) + 2-Isopropoxyethanol (C)	
0.0000	0.001553
0.1006	0.002009
0.1992	0.002367
0.3871	0.002854
0.4818	0.003032
0.5895	0.003121
0.7854	0.003120
0.8929	0.003110
1.0000	0.003093

TABLE VIII. Continued.

x_C°	x_A^{sat}
Methylcyclohexane (B) + 2-Isopropoxyethanol (C)	
0.0000	0.001649
0.1065	0.002147
0.2203	0.002484
0.4270	0.002919
0.5244	0.003084
0.6247	0.003168
0.8137	0.003209
0.9021	0.003147
1.0000	0.003093
2,2,4-Trimethylpentane (B) + 2-Isopropoxyethanol (C)	
0.0000	0.001074
0.1399	0.001447
0.2729	0.001776
0.4915	0.002272
0.5779	0.002436
0.6710	0.002613
0.8537	0.002906
0.9285	0.002996
1.0000	0.003093

TABLE VIII. Continued.

x_C°	x_A^{sat}

tert-Butylcyclohexane (B) + 2-Isopropoxyethanol (C)

x_C°	x_A^{sat}
0.0000	0.001978
0.1477	0.002502
0.2738	0.002803
0.5032	0.003184
0.6050	0.003240
0.6959	0.003307
0.8604	0.003233
0.9305	0.003152
1.0000	0.003093

TABLE IX. Experimental Mole Fraction Solubilities of Anthracene (x_A^{sat}) in Binary Alkane (B) + 2-Butoxyethanol (C) Solvent Mixtures at 25.0 °C.[4]

x_C°	x_A^{sat}
Hexane (B) + 2-Butoxyethanol (C)	
0.0000	0.001274
0.1152	0.001748
0.2026	0.002092
0.3970	0.002726
0.4984	0.002952
0.6013	0.003188
0.7970	0.003526
0.8974	0.003642
1.0000	0.003785
Heptane (B) + 2-Butoxyethanol (C)	
0.0000	0.001571
0.1162	0.002013
0.2221	0.002340
0.4265	0.002916
0.5177	0.003127
0.6334	0.003302
0.8369	0.003608
0.9286	0.003690
1.0000	0.003785

TABLE IX. Continued

$x_C^{\,o}$	$x_A^{\,sat}$

Octane (B) + 2-Butoxyethanol (C)

$x_C^{\,o}$	$x_A^{\,sat}$
0.0000	0.001838
0.1061	0.002225
0.2312	0.002604
0.4565	0.003187
0.5513	0.003333
0.6293	0.003435
0.8453	0.003683
0.9243	0.003733
1.0000	0.003785

Cyclohexane (B) + 2-Butoxyethanol (C)

$x_C^{\,o}$	$x_A^{\,sat}$
0.0000	0.001553
0.0917	0.002026
0.1736	0.002356
0.3516	0.002897
0.4437	0.003092
0.5532	0.003282
0.7600	0.003532
0.8636	0.003655
1.0000	0.003785

TABLE IX. Continued.

$x_C{}^\circ$	$x_A{}^{sat}$
Methylcyclohexane (B) + 2-Butoxyethanol (C)	
0.0000	0.001649
0.1210	0.002254
0.2126	0.002560
0.4039	0.003035
0.5074	0.003248
0.6058	0.003342
0.8149	0.003576
0.9037	0.003679
1.0000	0.003785
2,2,4-Trimethylpentane (B) + 2-Butoxyethanol (C)	
0.0000	0.001074
0.0977	0.001389
0.2275	0.001747
0.4395	0.002348
0.5470	0.002659
0.6370	0.002864
0.8417	0.003376
0.9188	0.003551
1.0000	0.003785

TABLE IX. Continued.

x_C°	x_A^{sat}
tert-Butylcyclohexane (B) + 2-Butoxyethanol (C)	
0.0000	0.001978
0.1313	0.002522
0.2591	0.002896
0.4588	0.003317
0.5696	0.003512
0.6725	0.003662
0.8348	0.003770
0.9273	0.003780
1.0000	0.003785

TABLE X. Experimental Mole Fraction Solubilities of Anthracene (x_A^{sat}) in Binary Alkane (B) + 3-Methoxy-1-butanol (C) Solvent Mixtures at 25.0 °C.[5]

$x_C°$	x_A^{sat}
Hexane (B) + 3-Methoxy-1-butanol (C)	
0.0000	0.001274
0.1175	0.001696
0.2440	0.002079
0.4481	0.002576
0.5596	0.002785
0.6554	0.002893
0.8271	0.002889
0.9141	0.002803
1.0000	0.002702
Heptane (B) + 3-Methoxy-1-butanol (C)	
0.0000	0.001571
0.1216	0.002009
0.2596	0.002337
0.4640	0.002705
0.5653	0.002878
0.6659	0.002964
0.8421	0.002933
0.9125	0.002863
1.0000	0.002702

TABLE X. Continued.

x_C°	x_A^{sat}
Octane (B) + 3-Methoxy-1-butanol (C)	
0.0000	0.001838
0.1406	0.002288
0.2681	0.002542
0.4926	0.002921
0.5954	0.003045
0.6860	0.003079
0.8435	0.003040
0.9102	0.002936
0.9287	0.002905
1.0000	0.002702
Cyclohexane (B) + 3-Methoxy-1-butanol (C)	
0.0000	0.001553
0.0919	0.001991
0.2033	0.002407
0.3865	0.002817
0.4914	0.002978
0.5915	0.003021
0.7926	0.002969
0.8827	0.002870
1.0000	0.002702

TABLE X. Continued.

x_C°	x_A^{sat}
Methylcyclohexane (B) + 3-Methoxy-1-butanol (C)	
0.0000	0.001649
0.1251	0.002234
0.2244	0.002522
0.4239	0.002911
0.5353	0.003104
0.6258	0.003156
0.8104	0.003112
0.9039	0.002950
1.0000	0.002702
2,2,4-Trimethylpentane (B) + 3-Methoxy-1-butanol (C)	
0.0000	0.001074
0.1346	0.001465
0.2734	0.001780
0.4997	0.002238
0.5963	0.002414
0.6901	0.002578
0.8541	0.002741
0.9268	0.002739
1.0000	0.002702

TABLE X. Continued.

x_C°	x_A^{sat}
tert-Butylcyclohexane (B) + 3-Methoxy-1-butanol (C)	
0.0000	0.001978
0.1745	0.002564
0.2876	0.002808
0.5072	0.003116
0.6071	0.003179
0.7027	0.003200
0.8581	0.003039
0.9262	0.002899
1.0000	0.002702

TABLE XI. Experimental Mole Fraction Solubilities of Anthracene (x_A^{sat}) in Binary Alkane (B) + 1-Pentanol (C) Solvent Mixtures at 25.0 °C.[6]

x_C^o	x_A^{sat}
Octane (B) + 1-Pentanol (C)	
0.0000	0.001838
0.1484	0.001859
0.2791	0.001816
0.5026	0.001668
0.6018	0.001572
0.6974	0.001476
0.8585	0.001256
0.9270	0.001166
1.0000	0.001097
Cyclohexane (B) + 1-Pentanol (C)	
0.0000	0.001553
0.0946	0.001643
0.2023	0.001646
0.4103	0.001578
0.5108	0.001501
0.6088	0.001427
0.7975	0.001248
0.8991	0.001154
1.0000	0.001097

TABLE XI. Continued.

x_C^o	x_A^{sat}
Methylcyclohexane (B) + 1-Pentanol (C)	
0.0000	0.001649
0.1269	0.001778
0.2316	0.001734
0.4458	0.001615
0.5347	0.001542
0.6304	0.001451
0.8161	0.001245
0.9074	0.001157
1.0000	0.001097
2,2,4-Trimethylpentane (B) + 1-Pentanol (C)	
0.0000	0.001074
0.1428	0.001182
0.2960	0.001224
0.5244	0.001235
0.6141	0.001214
0.7171	0.001196
0.8640	0.001143
0.9318	0.001115
1.0000	0.001097

TABLE XII. Experimental Mole Fraction Solubilities of Anthracene (x_A^{sat}) in Binary Alkane (B) + 2-Ethyl-1-hexanol (C) Solvent Mixtures at 25.0 °C.[6]

x_C°	x_A^{sat}

Hexane (B) + 2-Ethyl-1-hexanol (C)

x_C°	x_A^{sat}
0.0000	0.001274
0.0983	0.001422
0.1794	0.001469
0.3597	0.001516
0.4565	0.001525
0.5590	0.001529
0.7647	0.001504
0.8718	0.001451
1.0000	0.001397

Heptane (B) + 2-Ethyl-1-hexanol (C)

x_C°	x_A^{sat}
0.0000	0.001571
0.1116	0.001647
0.1972	0.001669
0.3931	0.001656
0.4806	0.001639
0.5718	0.001615
0.7850	0.001517
0.8865	0.001464
1.0000	0.001397

TABLE XII. Continued.

x_C°	x_A^{sat}
Octane (B) + 2-Ethyl-1-hexanol (C)	
0.0000	0.001838
0.1190	0.001907
0.2139	0.001898
0.4149	0.001835
0.5098	0.001785
0.6148	0.001712
0.8102	0.001606
0.8932	0.001527
1.0000	0.001397
Cyclohexane (B) + 2-Ethyl-1-hexanol (C)	
0.0000	0.001553
0.0590	0.001658
0.1441	0.001689
0.3159	0.001659
0.4036	0.001632
0.5098	0.001596
0.7412	0.001535
0.8616	0.001492
1.0000	0.001397

TABLE XII. Continued.

x_C^o	x_A^{sat}
Methylcyclohexane (B) + 2-Ethyl-1-hexanol (C)	
0.0000	0.001649
0.0890	0.001830
0.1771	0.001819
0.3610	0.001726
0.4509	0.001685
0.5499	0.001633
0.7667	0.001563
0.8751	0.001498
1.0000	0.001397
2,2,4-Trimethylpentane (B) + 2-Ethyl-1-hexanol (C)	
0.0000	0.001074
0.1144	0.001184
0.2135	0.001232
0.4193	0.001325
0.5143	0.001357
0.6103	0.001387
0.7935	0.001415
0.8027	0.001419
0.8974	0.001414
1.0000	0.001397

TABLE XIII. Experimental Mole Fraction Solubilities of Pyrene (x_A^{sat}) in Binary Alkane (B) + 1-Butanol (C) Solvent Mixtures at 299.15K.[8]

x_C°	x_A^{sat}
Hexane (B) + 1-Butanol (C)	
0.0000	0.00857
0.1567	0.00972
0.2639	0.00969
0.4865	0.00910
0.5882	0.00876
0.6833	0.00836
0.8509	0.00735
0.9170	0.00689
1.0000	0.00622
Heptane (B) + 1-Butanol (C)	
0.0000	0.01102
0.1641	0.01210
0.2924	0.01205
0.5148	0.01073
0.6140	0.00990
0.7066	0.00920
0.8570	0.00775
0.9358	0.00694
1.0000	0.00622

TABLE XIII. Continued.

x_C°	x_A^{sat}
Octane (B) + 1-Butanol (C)	
0.0000	0.01372
0.1797	0.01462
0.3107	0.01397
0.5445	0.01206
0.6422	0.01105
0.7321	0.01007
0.8807	0.00798
0.9396	0.00712
1.0000	0.00622
Cyclohexane (B) + 1-Butanol (C)	
0.0000	0.01100
0.1344	0.01229
0.2319	0.01213
0.4311	0.01112
0.5380	0.01030
0.6433	0.00940
0.8226	0.00776
0.9045	0.00712
1.0000	0.00622

TABLE XIII. Continued.

x_C°	x_A^{sat}
Methylcyclohexane (B) + 1-Butanol (C)	
0.0000	0.01292
0.1542	0.01434
0.2634	0.01389
0.4752	0.01219
0.5829	0.01106
0.6717	0.01011
0.8451	0.00813
0.9194	0.00726
1.0000	0.00622

TABLE XIV. Experimental Mole Fraction Solubilities of Pyrene (x_A^{sat}) in Binary Alkane (B) + 2-Butanol (C) Solvent Mixtures at 299.15K.[7]

x_C^o	x_A^{sat}
Hexane (B) + 2-Butanol (C)	
0.0000	0.00857
0.1521	0.00926
0.2621	0.00917
0.4836	0.00866
0.5879	0.00807
0.6827	0.00741
0.8564	0.00581
0.9242	0.00517
1.0000	0.00439
Heptane (B) + 2-Butanol (C)	
0.0000	0.01102
0.1581	0.01182
0.2941	0.01155
0.5030	0.01040
0.6129	0.00927
0.7066	0.00828
0.8666	0.00618
0.9289	0.00539
1.0000	0.00439

TABLE XIV. Continued.

x_C°	x_A^{sat}
Octane (B) + 2-Butanol (C)	
0.0000	0.01372
0.1847	0.01427
0.3137	0.01333
0.5238	0.01138
0.6383	0.01011
0.7295	0.00902
0.8739	0.00658
0.9304	0.00565
1.0000	0.00439
Cyclohexane (B) + 2-Butanol (C)	
0.0000	0.01100
0.1319	0.01192
0.2322	0.01166
0.4374	0.01047
0.5375	0.00962
0.6457	0.00851
0.8213	0.00649
0.9100	0.00547
1.0000	0.00439

TABLE XIV. Continued.

$x_C{}^\circ$	$x_A{}^{sat}$
Methylcyclohexane (B) + 2-Butanol (C)	
0.0000	0.01292
0.1522	0.01382
0.2648	0.01318
0.4810	0.01128
0.5809	0.01010
0.6842	0.00879
0.8456	0.00659
0.9171	0.00563
1.0000	0.00439
2,2,4-Trimethylpentane (B) + 2-Butanol (C)	
0.0000	0.00720
0.1802	0.00783
0.3285	0.00791
0.5401	0.00743
0.6430	0.00697
0.7299	0.00658
0.8800	0.00553
0.9388	0.00504
1.0000	0.00439

TABLE XV. Experimental Mole Fraction Solubilities of Pyrene (x_A^{sat}) in Binary Alkane (B) + 2-Methyl-1-propanol (C) Solvent Mixtures at 299.15K.[8]

x_C°	x_A^{sat}
Hexane (B) + 2-Methyl-1-propanol (C)	
0.0000	0.00857
0.1458	0.00907
0.2706	0.00878
0.4827	0.00764
0.5899	0.00682
0.6823	0.00603
0.8488	0.00455
0.9270	0.00387
1.0000	0.00326
Heptane (B) + 2-Methyl-1-propanol (C)	
0.0000	0.01102
0.1679	0.01146
0.2885	0.01078
0.5141	0.00886
0.6110	0.00781
0.7071	0.00666
0.8500	0.00502
0.9221	0.00418
1.0000	0.00326

TABLE XV. Continued.

x_C°	x_A^{sat}
Octane (B) + 2-Methyl-1-propanol (C)	
0.0000	0.01372
0.1796	0.01373
0.3174	0.01244
0.5436	0.00984
0.6357	0.00858
0.7122	0.00758
0.8774	0.00501
0.9473	0.00397
1.0000	0.00326
Cyclohexane (B) + 2-Methyl-1-propanol (C)	
0.0000	0.01100
0.1365	0.01149
0.2315	0.01092
0.4339	0.00904
0.5428	0.00783
0.6534	0.00660
0.8253	0.00476
0.9057	0.00400
1.0000	0.00326

TABLE XV. Continued.

$x_C{}^o$	$x_A{}^{sat}$
Methylcyclohexane (B) + 2-Methyl-1-propanol (C)	
0.0000	0.01292
0.1423	0.01365
0.2639	0.01272
0.4723	0.01016
0.5618	0.00892
0.6799	0.00725
0.8433	0.00513
0.9285	0.00410
1.0000	0.00326

TABLE XVI. Experimental Anthracene Mole Fraction Solubilities in Select Organic Solvents at 25.0°C.[9]

Organic Solvent	X_A^{sat}
Nonane	0.002085
Decane	0.002345
o-Xylene	0.008458
m-Xylene	0.007956
1-Chlorohexane	0.007177
Trichloromethane	0.01084
Dichloromethane	0.009387
Chlorobenzene	0.009962
Methyl acetoacetate	0.003191
Ethyl acetoacetate	0.004533
Methanol	0.000243
Ethanol	0.000460
1-Hexanol	0.001483
1-Heptanol	0.001869
Cyclopentanol	0.001330
Ethylene glycol	0.0000715
2,2,2-Trifluoroethanol	0.0000865
Acetonitrile	0.000830
Benzonitrile	0.008426
N,N-Dimethylformamide	0.007839
N,N, Dimethylacetamide	0.01267

TABLE XVII. Experimental *trans*-Stilbene Mole Fraction Solubilities in Select Organic Solvents at 25.0°C.[10]

Organic Solvent	X_A^{sat}
Nonane	0.01383
Decane	0.01511
Hexadecane	0.02178
Benzene	0.06232
Toluene	0.06066
o-Xylene	0.06126
m-Xylene	0.05690
p-Xylene	0.06342
Ethylbenzene	0.05331
Chlorobenzene	0.07363
Tetrachloromethane	0.03970
Ethylene glycol	0.000296
2,2,2-Trifluoroethanol	0.000666
Acetonitrile	0.00995
1,4-Dioxane	0.06615
Tetrahydrofuran	0.1035
2-Butanone	0.06273

Tests for Data Validity

Mathematical representations provide not only a means to screen experimental data sets for possible outliers in need of redetermination, but also facilitate interpolation at solvent compositions falling between measured data points.

Acree and Zvaigzne suggested possible mathematical representations for isothermal solubility data upon either a Combined NIBS/Redlich-Kister model;

$$\ln x_A{}^{sat} = x_B{}^{\circ}\ln(x_A{}^{sat})_B + x_C{}^{\circ}\ln(x_A{}^{sat})_C + x_B{}^{\circ}x_C{}^{\circ}\Sigma S_i (x_B{}^{\circ} - x_C{}^{\circ})^i \qquad 2.1$$

or Modified Wilson equation:

$$\ln[a_A(s)/x_A{}^{sat}] = 1 - x_B{}^{\circ}\{1 - \ln[a_A(s)/(x_A{}^{sat})_B]\}/(x_B{}^{\circ} + x_C{}^{\circ}\Lambda_{BC}{}^{adj})$$

$$- x_C{}^{\circ}\{1 - \ln[a_A(s)/(x_A{}^{sat})_C]\}/(x_B{}^{\circ}\Lambda_{CB}{}^{adj} + x_C{}^{\circ}) \qquad 2.2$$

where the various S_i and ${}^{\circ}\Lambda_{ij}{}^{adj}$ "curve-fit" parameters can be evaluated via least squares analysis.[11] In equations 2.1 and 2.2, $x_B{}^{\circ}$ and $x_C{}^{\circ}$ refer to the initial mole fraction composition of the binary solvent calculated as if solute (A) were not present, $a_A(s)$ is the activity of the solid solute, N is the number of "curve-fit" parameters used and $(x_A{}^{sat})_i$ is the saturated mole fraction solubility of the solute in pure solvent i. The numerical values of $a_A(s)$ used in the Modified Wilson computations were $a_A(s) = 0.00984$ [5] and $a_A(s) = 0.1312$ for anthracene and pyrene, respectively. The activities were calculated using equation 1.15 and enthalpy of fusion data as discussed in Chapter 1.

The ability of equations 2.1 and 2.2 to mathematically represent the experimental solubility of anthracene in several alkane + alkoxyalcohol and alkane + alcohol mixtures and solubility of pyrene in several alkane + 2-butanol are summarized in Tables XVIII to XXV in the form of "curve-fit" parameters and percent deviations in back-calculated solubilities. Each percent deviation is based upon the measured anthracene and pyrene solubility data at the several different binary solvent compositions. Careful examination reveals that both equations provide an accurate mathematical expression for how the solubility of anthracene and pyrene varies with solvent composition.

Tables XVIII-XXII summarize the ability of equations 2.1 and 2.2 to mathematically represent the experimental solubility of anthracene in alkane + alkoxyalcohol solvent systems. Inspection of these tables reveal that the three-parameter from the combined NIBS/Redlich-Kister equation provides the better mathematical description for how the solubility of anthracene varies with solvent composition. Slightly larger deviations are noted in the case of the Modified Wilson equation.

Tables XXIII-XXIV summarize the ability of equations 2.1 and 2.2 to mathematically represent the experimental solubility of anthracene in alkane + alcohol solvent systems. Inspection of these tables reveal that the three-parameter from the combined NIBS/Redlich-Kister equation provides the better mathematical description for how the solubility of anthracene varies with solvent composition. Slightly larger deviations are noted in the case of the Modified Wilson equation.

Tables XXV summarize the ability of equations 2.1 and 2.2 to mathematically represent the experimental solubility of pyrene in several alkane + 2-butanol solvent systems. Inspection of these tables reveal that the three-parameter from the combined

NIBS/Redlich-Kister equation provides the better mathematical description for how the solubility of pyrene varies with solvent composition.

The overall conclusion of the investigation by the NIBS/Redlich-Kister and Modified Wilson equations is that no "outliers" or erroneous data points are present. This leads to the conclusion that all data points are valid and are, therefore ready for investigation and interpretation.

TABLE XVIII. Mathematical Representation of Anthracene Solubilities in Several Binary Alkane (B) + 2-Ethoxyethanol (C) Solvent Mixtures.[1]

Binary Solvent System Component (B) and Component (C)	S_i^a	Eq 2.1 %Dev[b]	$\Lambda_{ij}^{adj,c}$	Eq 2.2 %Dev[b]
Hexane + 2-Ethoxyethanol	1.434 0.126 0.526	0.6	2.960 10.130	1.0
Heptane + 2-Ethoxyethanol	1.220 -0.168 0.594	0.2	2.900 12.970	1.5
Octane + 2-Ethoxyethanol	1.158 -0.205 0.571	0.3	3.230 15.390	1.6
Cyclohexane + 2-Ethoxyethanol	1.606 0.354 0.374	0.5	4.332 12.990	2.8
Methylcyclohexane + 2-Ethoxyethanol	1.410 0.354 0.613	0.6	5.739 9.450	2.3
2,2,4-Trimethylpentane + 2-Ethoxyethanol	1.101 0.289 0.613	0.3	1.990 6.970	0.6
Overall Average Deviation		0.4		1.6

[a] Combined NIBS/Redlich-Kister curve-fit parameters are ordered as S_0, S_1, S_2

[b] Deviation (%) = $(100/N)\Sigma|[(x_A^{sat})^{calc} - (x_A^{sat})^{exp}]/(x_A^{sat})^{exp}|$

[c] Adjustable parameters for the Modified Wilson equations are ordered as Λ_{BC}^{adj} and Λ_{CB}^{adj}

TABLE XIX. Mathematical Representation of Anthracene Solubilities in Several Binary Alkane (B) + 2-Propoxyethanol (C) Solvent Mixtures.[2]

Binary Solvent System Component (B) and Component (C)	S_i^a	Eq 2.1 %Dev[b]	Max. Dev.
Hexane + 2-Propoxyethanol	1.319 0.442 0.361	0.2	0.6
Heptane + 2-Propoxyethanol	0.977 0.290 0.219	0.2	0.4
Octane + 2-Propoxyethanol	0.994 0.091 0.209	0.2	0.4
Cyclohexane + 2-Propoxyethanol	1.260 0.756 0.518	0.5	1.3
Methylcyclohexane + 2-Propoxyethanol	1.214 0.634 0.531	0.8	1.6
2,2,4-Trimethylpentane + 2-Propoxyethanol	0.978 0.234 0.343	0.2	0.6
tert-Butylcyclohexane + 2-Propoxyethanol	1.041 0.246 0.274	0.7	1.3
Overall Average Deviation		0.4	0.9

[a] Combined NIBS/Redlich-Kister curve-fit parameters are ordered as S_0, S_1, S_2

[b] Deviation (%) = $(100/N)\Sigma|[(x_A^{sat})^{calc} - (x_A^{sat})^{exp}]/(x_A^{sat})^{exp}|$

TABLE XX. Mathematical Representation of Anthracene Solubilities in Several Binary Alkane (B) + 2-Isopropoxyethanol (C) Solvent Mixtures.[3]

Binary Solvent System Component (B) and Component (C)	S_i^a	Eq 2.1 %Dev[b]	$\Lambda_{ij}^{adj,c}$	Eq 2.2 %Dev[b]
Hexane + 2-Isopropoxyethanol	1.282 0.462 0.336	0.2	3.140 3.980	0.3
Heptane + 2-Isopropoxyethanol	1.018 0.322 0.103	0.4	2.780 4.580	0.5
Octane + 2-Isopropoxyethanol	0.930 0.291 0.084	0.6	3.110 4.730	0.7
Cyclohexane + 2-Isopropoxyethanol	1.297 0.755 0.216	0.5	4.220 3.050	1.5
Methylcyclohexane + 2-Isopropoxyethanol	1.185 0.650 0.460	1.1	4.340 4.100	0.7
2,2,4-Trimethylpentane + 2-Isopropoxyethanol	0.912 0.364 0.113	0.2	2.159 1.144	0.2
tert-Butylcyclohexane + 2-Isopropoxyethanol	1.016 0.350 0.153	0.6	3.860 5.780	1.0
Overall Average Deviation		0.5		0.7

[a] Combined NIBS/Redlich-Kister curve-fit parameters are ordered as S_0, S_1, S_2
[b] Deviation (%) = $(100/7)\Sigma|[(x_A^{sat})^{calc} - (x_A^{sat})^{exp}]/(x_A^{sat})^{exp}|$
[c] Adjustable parameters for the Modified Wilson equations are ordered as Λ_{BC}^{adj} and Λ_{CB}^{adj}

TABLE XXI. Mathematical Representation of Anthracene Solubilities in Several Binary Alkane (B) + 2-Butoxyethanol (C) Solvent Mixtures.[4]

Binary Solvent System Component (B) and Component (C)	S_i[a]	Eq 2.1 %Dev[b]	Λ_{ij}[adj,c]	Eq 2.2 %Dev[b]
Hexane + 2-Butoxyethanol	1.217 0.679 0.224	0.3	3.400 0.303	0.7
Heptane + 2-Butoxyethanol	0.928 0.488 0.123	0.5	3.160 0.332	0.7
Octane + 2-Butoxyethanol	0.832 0.366 0.105	0.3	3.790 0.274	1.1
Cyclohexane + 2-Butoxyethanol	1.081 0.863 0.565	0.4	3.970 0.100	0.5
Methylcyclohexane + 2-Butoxyethanol	0.992 0.868 0.489	0.7	4.730 2.971	0.3
2,2,4-Trimethylpentane + 2-Butoxyethanol	0.883 0.548 0.198	0.8	2.260 2.971	0.6
tert-Butylcyclohexane + 2-Butoxyethanol	0.883 0.427 0.275	0.6	4.080 0.245	1.7
Overall Average Deviation		0.5		0.8

[a] Combined NIBS/Redlich-Kister curve-fit parameters are ordered as S_0, S_1, S_2
[b] Deviation (%) = $(100/N)\Sigma|[(x_A{}^{sat})^{calc} - (x_A{}^{sat})^{exp}]/(x_A{}^{sat})^{exp}|$
[c] Adjustable parameters for the Modified Wilson equations are ordered as $\Lambda_{BC}{}^{adj}$ and $\Lambda_{CB}{}^{adj}$

TABLE XXII. Mathematical Representation of Anthracene Solubilities in Several Binary Alkane (B) + 3-Methoxy-1-butanol (C) Solvent Mixtures.[5]

Binary Solvent System Component (B) and Component (C)	$S_i{}^a$	Eq 2.1 %Dev[b]	$\Lambda_{ij}{}^{adj,c}$	Eq 2.2 %Dev[b]
Hexane + 3-Methoxy-1-butanol	1.489 0.344 0.189	0.7	2.960 4.160	1.1
Heptane + 3-Methoxy-1-butanol	1.196 0.217 0.476	0.8	3.170 4.190	0.7
Octane + 3-Methoxy-1-butanol	1.088 -0.032 0.516	0.4	3.070 6.100	0.5
Cyclohexane + 3-Methoxy-1-butanol	1.480 0.670 0.465	0.6	4.623 3.506	1.0
Methylcyclohexane + 3-Methoxy-1-butanol	1.459 0.377 0.692	1.0	4.550 6.470	0.9
2,2,4-Trimethylpentane + 3-Methoxy-1-butanol	1.108 0.265 0.487	0.5	2.101 2.970	0.9
tert-Butylcyclohexane + 3-Methoxy-1-butanol	1.199 0.084 0.353	0.3	3.890 5.870	1.0
Overall Average Deviation		0.6		0.9

[a] Combined NIBS/Redlich-Kister curve-fit parameters are ordered as S_0, S_1, S_2

[b] Deviation (%) = $(100/N)\Sigma|[(x_A{}^{sat})^{calc} - (x_A{}^{sat})^{exp}]/(x_A{}^{sat})^{exp}|$

[c] Adjustable parameters for the Modified Wilson equations are ordered as $\Lambda_{BC}{}^{adj}$ and $\Lambda_{CB}{}^{adj}$

TABLE XXIII. Mathematical Representation of Anthracene Solubilities in Several Binary Alkane (B) + 1-Pentanol (C) Solvent Mixtures.[6]

Binary Solvent System Component (B) and Component (C)	S_i^a	Eq 2.1 %Dev[b]	$\Lambda_{ij}^{adj,c}$	Eq 2.2 %Dev[b]
Octane + 1-Pentanol	0.688 0.130 -0.241	0.7	1.695 1.289	0.6
Cyclohexane + 1-Pentanol	0.591 0.472 0.010	0.7	2.681 0.854	0.7
Methylcyclohexane + 1-Pentanol	0.622 0.524 0.058	0.9	2.884 0.883	1.0
2,2,4-Trimethylpentane + 1-Pentanol	0.530 0.242 -0.011	0.5	2.043 0.767	0.3
Overall Average Deviation		0.7		0.7

[a] Combined NIBS/Redlich-Kister curve-fit parameters are ordered as S_0, S_1, S_2

[b] Deviation (%) = $(100/N)\Sigma|[(x_A^{sat})^{calc} - (x_A^{sat})^{exp}]/(x_A^{sat})^{exp}|$

[c] Adjustable parameters for the Modified Wilson equations are ordered as Λ_{BC}^{adj} and Λ_{CB}^{adj}

TABLE XXIV. Mathematical Representation of Anthracene Solubilities in Several
Binary Alkane (B) + 2-Ethyl-1-hexanol (C) Solvent Mixtures.[6]

Binary Solvent System Component (B) and Component (C)	$S_i{}^a$	Eq 2.1 %Dev^b	$\Lambda_{ij}{}^{adj,c}$	Eq 2.2 %Dev^b
Hexane + 2-Ethyl-1-hexanol	0.527 0.344 0.417	0.8	2.478 0.709	0.9
Heptane + 2-Ethyl-1-hexanol	0.389 0.166 0.131	0.2	1.927 0.883	0.3
Octane + 2-Ethyl-1-hexanol	0.430 0.023 0.356	0.3	1.898 1.028	1.0
Cyclohexane + 2-Ethyl-1-hexanol	0.278 0.323 0.810	0.8	2.884 0.593	1.5
Methylcyclohexane + 2-Ethyl-1-hexanol	0.327 0.458 0.944	1.1	2.913 0.651	2.5
2,2,4-Trimethylpentane + 2-Ethyl-1-hexanol	0.394 0.118 0.233	0.3	1.492 0.941	0.7
Overall Average Deviation		0.6		1.2

^{a} Combined NIBS/Redlich-Kister curve-fit parameters are ordered as S_0, S_1, S_2

^{b} Deviation (%) = $(100/N)\Sigma|[(x_A{}^{sat})^{calc} - (x_A{}^{sat})^{exp}]/(x_A{}^{sat})^{exp}|$

^{c} Adjustable parameters for the Modified Wilson equations are ordered as $\Lambda_{BC}{}^{adj}$ and $\Lambda_{CB}{}^{adj}$

TABLE XXV. Mathematical Representation of Pyrene Solubilities in Several Binary Alkane (B) + 2-Butanol (C) Solvent Mixtures.[7]

Binary Solvent System Component (B) and Component (C)	$S_i{}^a$	Eq 2.1 %Dev[b]	$\Lambda_{ij}{}^{adj,c}$	Eq 2.2 %Dev[b]
Hexane + 2-Butanol	1.344 -0.128 0.216	0.5	1.202 1.550	0.5
Heptane + 2-Butanol	1.583 -0.232 0.392	0.5	1.260 1.724	0.7
Octane + 2-Butanol	1.631 -0.490 0.794	0.5	0.999 2.130	1.5
Cyclohexane + 2-Butanol	1.426 0.064 0.447	0.5	1.579 1.405	1.0
Methylcyclohexane + 2-Butanol	1.512 -0.091 0.670	0.5	1.579 1.521	1.3
2,2,4-Trimethylpentane + 2-Butanol	1.148 -0.274 0.558	0.7	1.086 1.579	1.2
Overall Average Deviation		0.5		1.0

[a] Combined NIBS/Redlich-Kister curve-fit parameters are ordered as S_0, S_1, S_2

[b] Deviation (%) = $(100/N)\Sigma|[(x_A{}^{sat})^{calc} - (x_A{}^{sat})^{exp}]/(x_A{}^{sat})^{exp}|$

[c] Adjustable parameters for the Modified Wilson equations are ordered as $\Lambda_{BC}{}^{adj}$ and $\Lambda_{CB}{}^{adj}$

Chapter Bibliography

1. Hernandez, C.E.; Roy, L.E.; Deng, T.; Tuggle, M.B.; Acree, Jr., W.E. *Phys. Chem. Liq.*, in press.

2. Hernandez, C.E.; Roy, L.E.; Reddy, G.D.; Martinez, G.L.; Parker, A.; Jackson, A.; Brown, G.; Acree, Jr., W.E. *J. Chem. Eng. Data*, **1998**, *169*, 137.

3. Hernandez, C.E.; Roy, L.E.; Reddy, G.D.; Martinez, G.L.; Jackson, A.; Brown, G.; Borders, T.L.; Sanders, J.T.; Acree, Jr., W.E. *Phys. Chem. Liq.*, **1998**, *36*, 257.

4. Hernandez, C.E.; Roy, L.E.; Reddy, G.D.; Martinez, G.L.; Parker, A.; Jackson, A.; Brown, G.; Acree, Jr., W.E. *J. Chem. Eng. Data*, **1997**, *42*, 1249.

5. Hernandez, C.E.; Roy, L.E.; Reddy, G.D.; Borders, T.L.; Sanders, J.T.; Acree, Jr., W.E. *Phys. Chem. Liq.*, **1998**, *37*, 31.

6. Roy, L.E.; Hernandez, C.E.; Reddy, G.D.; Sanders, J.T.; Deng, T.; Tuggle, M.B.; Acree, Jr., W.E. *J. Chem. Eng. Data*, **1998**, *43*, 493.

7. Hernandez, C.E.; Coym, K.S.; Roy, L.E.; Powell, J.R.; Acree, Jr., W.E. *J. Chem. Thermodyn.*, **1998**, *30*, 37.

8. Borders, T.L.; McHale, M.E.R.; Powell, J.R.; Coym, K.S.; Hernandez, C.E.; Roy, L.E.; Acree, Jr., W.E.; Williams, C.D.; Campbell, S.W *Fluid Phase Equilibria*, **1998**, *37*, 31.

9. Roy, L.E.; Hernandez, C.E.; Acree, Jr., W.E. *Polycyclic Aromatic Compounds*, **1999**, *13*, 105.

10. Roy, L.E.; Hernandez, C.E.; De Fina, K.M.; Acree, Jr., W.E. *Phys. Chem. Liq.*, in press.

11. Acree, Jr., W.E.; Zvaigzne, A.I. *Thermochim. Acta*, **1991**, *178*, 151.

Chapter 3

Methods and Materials

Fluorescence Studies

Utilization of selective fluorescence quenching agents for detection, identification, and separation of polycyclic aromatic hydrocarbons requires that the experimentally determined spectra must be free of chemical and instrumental interference that might unexpectedly alter emission intensities. Inner-filtering is a major problem associated with obtaining correct fluorescence data, which assumes that the sample is optically dilute at all analytical wavelengths.[1] The inner-filtering effects may decrease the intensity of the excitation at the point of observation, or decrease the observed fluorescence by absorption of this fluorescence. The relative importance of each process depends on the optical densities of the sample at the excitation and emission wavelength.[2] Most commercial instruments use right-angle fluorometry, which reduces stray radiation by placing the emission detector at 90° with respect to the incoming excitation beam. Figure 5 shows an accurate depiction of the fluorescence area.

Within a sample cell, only fluorescence emission originating from the center is actually collected. A reduction of the excitation beam before it reaches the region viewed by the fluorescence detection optics (pre-filtering region) and goes through the interrogation area is denoted as primary inner-filtering. The correction factor, f_{prim} for primary inner-filtering is given by;[3]

$$F_{prim} = F^{corr}/F^{obs} = 2.303 \, A \, (y-x)/[10^{-Ax} - 10^{-Ay}] \qquad 3.1$$
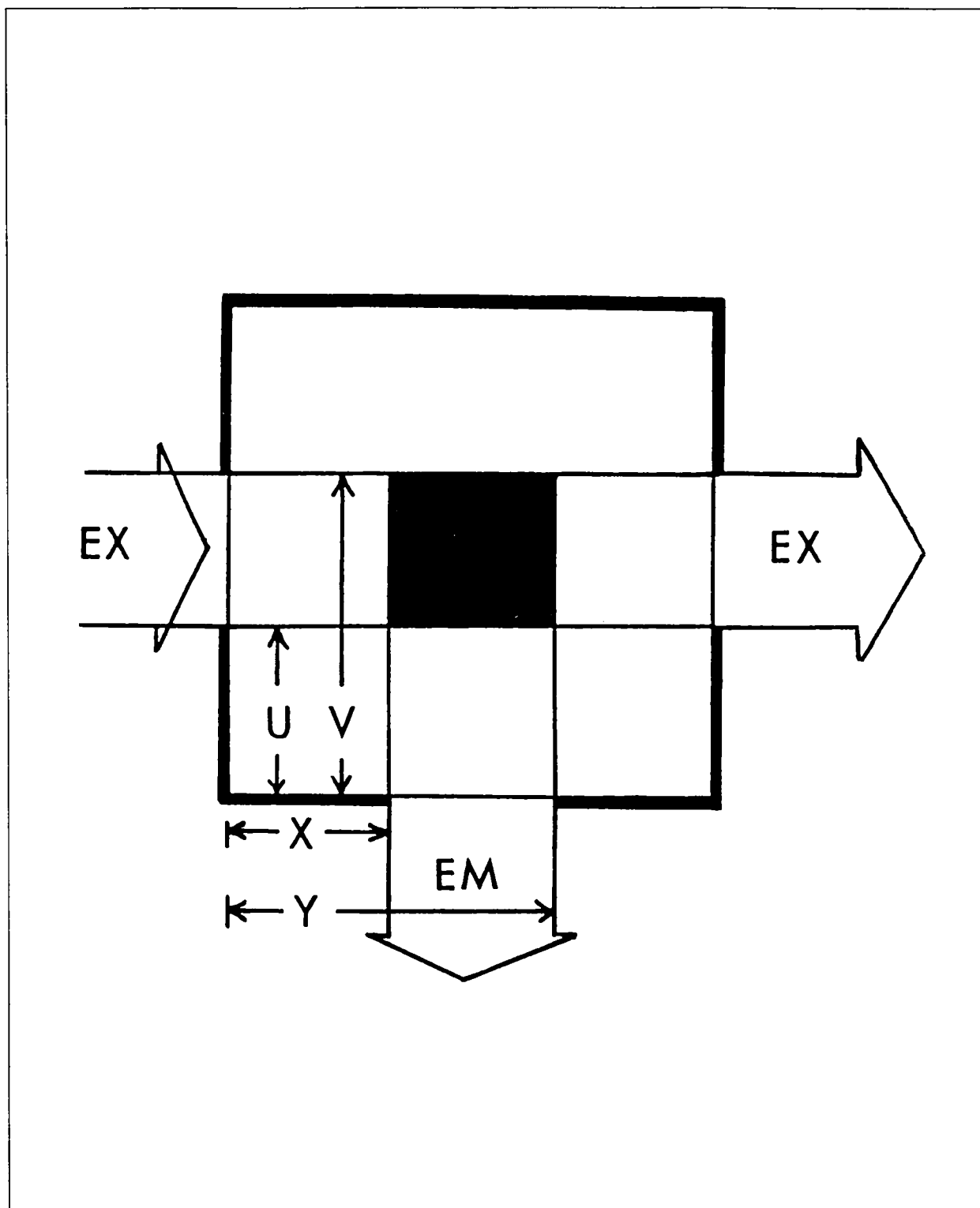
FIGURE 5: Typical cell configuration for right-angle fluorometry. Window parameters (x,y) and (u,v) are determined by masking gaps or some other limiting gap in emission and excitation beam, respectively.

where F^{corr} and F^{obs} refer to the corrected and observed fluorescence emission signal, A is the absorbance per centimeter of the pathlength at the excitation wavelength, and x and y denote distance from the boundaries of the interrogation zone to the excitation as shown in Figure 5. Equation 3.1 strictly applies to monochromatic light.

In experiments requiring determination of intensity ratios, primary inner-filtering can be ignored as the excitation wavelength remains constant. Emission intensities of both bands are thus affected by the same relative amount. In selective quenching, the absorption of the excitation beam by the quenching agent would reduce emission intensities of every fluorophore having the given excitation wavelength. With nitromethane, inner-filtering would reduce emission intensities of both alternant and nonalternant PAH by the same relative amount. For determination of whether selective quenching occurred, observed emission intensities, F^{obs}, must be multiplied by the primary inner-filtering correction factor, f_{prim}, in order to eliminate the undesired effects from this chemical interference. Failure to correct the observed intensities may lead to erroneous conclusions concerning PAH identification (alternant versus nonalternant), particularly if the excitation wavelengths are 300-320 nm.

Secondary inner-filtering results from absorption of large quantities of emitted fluorescence, and the correction factor, f_{sec}, contains;

$$f_{sec} = F^{corr}/F^{obs} = [(v - u)(1/b) \ln T]/[T_{at\ v/b} - T_{at\ u/b}] \qquad 3.2$$

the sample transmittance (T) across the entire cell pathlength (b) at the emission wavelength. Transmittance at the two interrogation zone boundaries, $T_{at\ v/b}$ and $T_{at\ u/b}$, are calculated from the measured absorbance at the emission wavelength via the Beer-Lambert law. Selective

quenching experiments involving nitromethane are not generally affected by secondary inner-filtering artifacts as much as by primary inner-filtering. PAH emission bands appear in the 370-500 nm spectral region, where nitromethane's absorbances are greatly diminished.

The corrected fluorescence emission intensity is given by:

$$F^{corr} = f_{prim}f_{sec}F^{obs} \qquad\qquad 3.3$$

Assuming that primary and secondary inner-filtering are independent processes. In such instances, the correction factors can be computed using an approximate expression;

$$\log(f_{prim}f_{sec}) = 0.5 \ (A_{at\ \lambda ex} + A_{at\ \lambda em}) \qquad\qquad 3.4$$

that requires only measured absorbances at the excitation and emission wavelengths.

Another interference that can have a significant effect on the measured and calculated emission intensities and thus the extent of quenching, is solvent blank correction. Mixed-micellar solutions display significant background emission in some instances. These fluorescence emission signals could be attributed to the trace impurities present in the commercially purchased surfactants. If one does not subtract the undesired blank emission signals from the solute containing emission signals, it is possible to end up with erroneous conclusions regarding extent of quenching for the particular probe as well as quenching selectivity determinations. In some instances, it is necessary to subtract the blank solvent + quencher emission spectrum from the solvent and solute + quencher emission spectrum covering the same wavelength range. Throughout these studies, an internal software program

in the spectrofluorophotometer is used to subtract the solvent blank and obtain the desired

fluorescence emission spectrum free of undesired solvent and quencher emission spectrum.[4]

Temperature as a variable can have a significant effect on measured fluorescence

emission intensities. It is well documented in the literature that nonradiative deactivation

from the excited states increase with an increase in temperature at the expense of the rate of

radiative deactivation.[5] Most of the physiochemical properties of molecularly organized

media have been shown to be strongly temperature dependent.[6] Critical micelle concentration

(CMC), aggregation number (N), size and molar volume, solubilization properties, entry and

exit rate of monomer surfactants, and a hose of other properties change in different fashion

with a change in temperature. In the present studies, best efforts were made to maintain a

constant temperature with minimum variation.

Materials and Methods

Molecular structures of the various polycyclic aromatic hydrocarbons (PAHs)

examined are depicted in Figures 6 and 7. For the purpose of simplicity, all of the PAH

solutes are assigned a code used throughout the thesis. Tables XXVI and XXVII list all the

different classes of PAH solutes used. All PAH solutes were obtained from either commercial

sources or various researchers throughout the world. PAHs purchased from commercial

suppliers were recrystallized several times from methanol. Synthetic reference and/or

commercial suppliers for the PAH solutes contained in Tables XXVI-XXX.

Solutions of all PAH solutes were prepared by dissolving the solutes in

dichloromethane, and were stored in closed amber glass bottles in the dark to retard any

photochemical reactions between the PAH solute and dichloromethane solvent. Small

aliquots (5 to 200 µL) of each stock solutions were transferred by Eppendorf pipette into test tubes, allowed to evaporate, and dilute with 10 mL (graduated cylinder) of the micellar solvent media of interest. Solute concentrations were sufficiently dilute (10^{-6}M) so as to prevent excimer formation. All solutions were ultrasonicated, vortexed and allowed to equilibrate for a minimum of 24 hours before any spectrofluorometric measurements were made. Final solute concentrations were sufficiently dilute to minimize any inner-filtering artifacts.

Commercial sources of surfactants used are listed in Table XXXI. In Table XXXI, chemical formulas and abbreviations used for these surfactants are also listed. Table XXXII lists critical micelle concentration (CMC) of each surfactant. In order to form micellar aggregates in solution, the concentration of the surfactant in the solution was so as to exceed the critical micelle concentration. The different aqueous micellar mixed surfactant solvent media were prepared by dissolving the commercial surfactants in double deionized water in appropriate volumetric flask, mixed thoroughly and then heated for complete solublization of surfactant.

External quenching agents (nitromethane) were added to the known volume of micellar solutions using an Eppendorf pipette and microtip of appropriate size. Names, commercial sources, and purity of quenching agents are listed in Table XXXIII.

Absorption spectra were recorded on a Bausch and Lomb Spectronic 2000, Milton Roy Spectronic 1001 Plus, and/or a Hewlett-Packard 8450 A photodiode array spectrophotometer in the usual manner using a 1 cm^2 quartz cuvette. The fluorescence measurements were performed on a Shimadzu RF-5000U spectrofluorophotometer with the detector set at high sensitivity. Excitation and emission slit width setters were set at 15 and 3

nm, respectively. Fluorescence data were accumulated in a 1 cm^2 quartz cuvette at ambient

room-temperature. Solutions containing specific PAH solutes were excited at the

wavelengths listed in Tables XXVI and XXVII. The information regarding approximate

excitation and emission wavelength was obtained from various resources. Inner-filtering

corrections were performed utilizing equations 3.3 and 3.4, whenever nitromethane was used.

Solution absorbed at A cm^{-1} ≤ 0.95 (f_{prim} ≤ 3.0), where inner-filtering equation is valid.

Secondary inner-filtering was taken into consideration whenever the emission wavelength was

below 400 nm.

TABLE XXVI. Names of alternant polycyclic aromatic hydrocarbons PAH6 series and the excitation wavelengths (λ_{ex}). Corresponding code will be used in subsequent tables.

Chemical Name	λ_{ex}(nm)	Code
Coronene	334	A1
Pyrene	338	A2
Perylene	406	A3
Benzo(a)pyrene	350	A4
Benzo(e)pyrene	335	A5
Dibenzo(a,e)pyrene	360	A6
Anthracene	340	A7
Naphtho(2,3g)chrysene	350	A8
Benzo[ghi]perylene	380	A9
Benzo[rst]pentaphene	307	A10
Naphtho[1,2,3,4ghi]perylene	316	A11
Chrysene	320	A12
Benzo[g]chrysene	320	A13

TABLE XXVII. Names of nonalternant fluoranthenoids and fluorenoids and the excitation wavelengths (λ_{ex}). Corresponding code will be used in subsequent tables.

Chemical Name	λ_{ex} (nm)	Code
Benz(def)indeno(1,2,3hi)chrysene	406	N1
Benz(def)indeno(1,2,3qr)chrysene	408	N2
Dibenzo(a,e)fluoranthene	390	N3
Naphtho(1,2b)fluoranthene	350	N4
Benzo(b)fluoranthene	346	N5
Benzo(ghi)fluoranthene	340	N6
Naphtho(2,1a)fluoranthene	400	N7
Benzo(a)fluoranthene	406	N8
Naphtho[2,1k]benzo[ghi]fluoranthene	368	N9
Naphtho[1,2k]benzo[ghi]fluoranthene	366	N10
Benzo[j]fluoranthene	315	N11
Dibenzo[ghi,mno]fluoranthene	290	N12

TABLE XXVIII. Summary of chemical suppliers and/or synthetic references for alternant polycyclic aromatic hydrocarbons PAH6 series.

Code	Chemical Supplier	Synthetic Reference
A1	John C. Fetzer, Ph.D. Aldrich Chemical Co.	(33,34)
A2	Aldrich Chemical Co.	
A3	Aldrich Chemical Co.	
A4	Aldrich Chemical Co.	
A5	John C. Fetzer, Ph.D. Aldrich Chemical Co.	(33,34)
A6	AccuStandard	
A7	Aldrich Chemical Co.	
A8	Ronald G. Harvey, Ph.D.	(40)
A9	Aldrich Chemical Co.	
A10	John C. Fetzer, Ph.D.	(33,34)
A11	John C. Fetzer, Ph.D.	(33,34)
A12	Aldrich Chemical Co.	
A13	Ronald G. Harvey, Ph.D.	(40)

TABLE XXIX. Summary of chemical suppliers and/or synthetic references for nonalternant fluoranthenoids and fluorenoids.

Code	Chemical Supplier	Synthetic Reference
N1	Ronald G. Harvey, Ph.D.	(51)
N2	Ronald G. Harvey, Ph.D.	(51)
N3	Ronald G. Harvey, Ph.D.	(51)
N4	Ronald G. Harvey, Ph.D.	(51)
N5	Ronald G. Harvey, Ph.D. Community Bureau of Reference	(51)
N6	Community Bureau of Reference	
N7	Ronald G. Harvey, Ph.D.	(51)
N8	Ronald G. Harvey, Ph.D.	(51)
N9	Bongsup P. Cho, Ph.D.	(53-55)
N10	Bongsup P. Cho, Ph.D.	(53-55)
N11	Community Bureau Reference	
N12	Lawrence T. Scott, Ph.D.	(52)

TABLE XXX. Address of PAH suppliers.

Chemical Supplier	Address
AccuStandard	25 Science Park, Suite 687 New Haven, CT 06511, USA
Aldrich Chemical Co.	1001 West Saint Paul Avenue Milwaukee, WI 53233, USA
Bongsup P. Cho, Ph.D.	Department of Medicinal Chemistry University of Rhode Island Kingston, RI 02881, USA
Community Bureau of Reference	Directorate General XII Commission of the European Communities 200 Rue de la Loi 1049 Brussels, Belgium
John C. Fetzer, Ph.D.	Chevron Research and Technology Center Richmond, CA 94802, USA
Ronald G. Harvey, Ph.D.	Ben May Institute University of Chicago Chicago, IL 60637, USA
Lawrence T. Scott, Ph.D.	Chemistry Department Boston College Chestnut Hill, MA 02167, USA

TABLE XXXI. Name and chemical formula of the surfactants used. Abbreviation provided for each surfactant would be used in subsequent tables.

Name of the Surfactant	Chemical Formula	Abbr.
Anionic Surfactants:		
Sodium Dodecyl Sulfate	$CH_3(CH_2)_{11}OSO_3^-Na^+$	SDS
Sodium Dodecyl Benzene Sulfonate	$p\text{-}CH_3(CH_2)_{11}C_6H_4SO_3^-Na^+$	SDBS
Cationic Surfactant:		
Hexadecyltrimethylammonium chloride	$CH_3(CH_2)_{15}N^+(CH_3)_3Cl^-$	CTAC
Nonionic Surfactants:		
Triton X-100	$(CH_3)_3CCH_2C(CH_3)C_6H_4(OCH_2CH_2)_9OH$	TX-100
Zwitterionic Surfactants:		
N-Hexadecyl-N,N-dimethyl-3-ammonio-1-propanesulfonate	$CH_3(CH_2)_{11}(CH_3)_2N^+(CH_2)_3SO_3^-$	SB-16

TABLE XXXII Source/Supplier and percent purity of the surfactants used. Critical micelle concentration (CMC) of each surfactant is also provided.[7]

Surfactant	Source/Supplier (% purity)	CMC (mM)
Anionic Surfactants:		
SDS	Aldrich (98%)	8.1
SDBS	Aldrich	1.6
Cationic Surfactants:		
CTAC	Aldrich (25 wt% in water)	1.3
Nonionic Surfactants:		
TX-100	Aldrich	0.2
Zwitterionic Surfactants:		
SB-16	Sigma	0.1-0.3

TABLE XXXIII. Name, chemical formula, source/supplier and percent purity of the quenching agent/surfactant quenchers used. Abbreviations provided will be used in subsequent tables.

Quenching Agent/ Surfactant Quencher	Chemical Formula	Source/supplier (% purity)
Quenching Agent:		
Nitromethane	CH_3NO_2	Aldrich (99%)
Surfactant Quencher:		
Dodecylpyridinium Chloride	$CH_3(CH_2)_{11}N^+C_5H_5Cl^-$	Aldrich (98%)
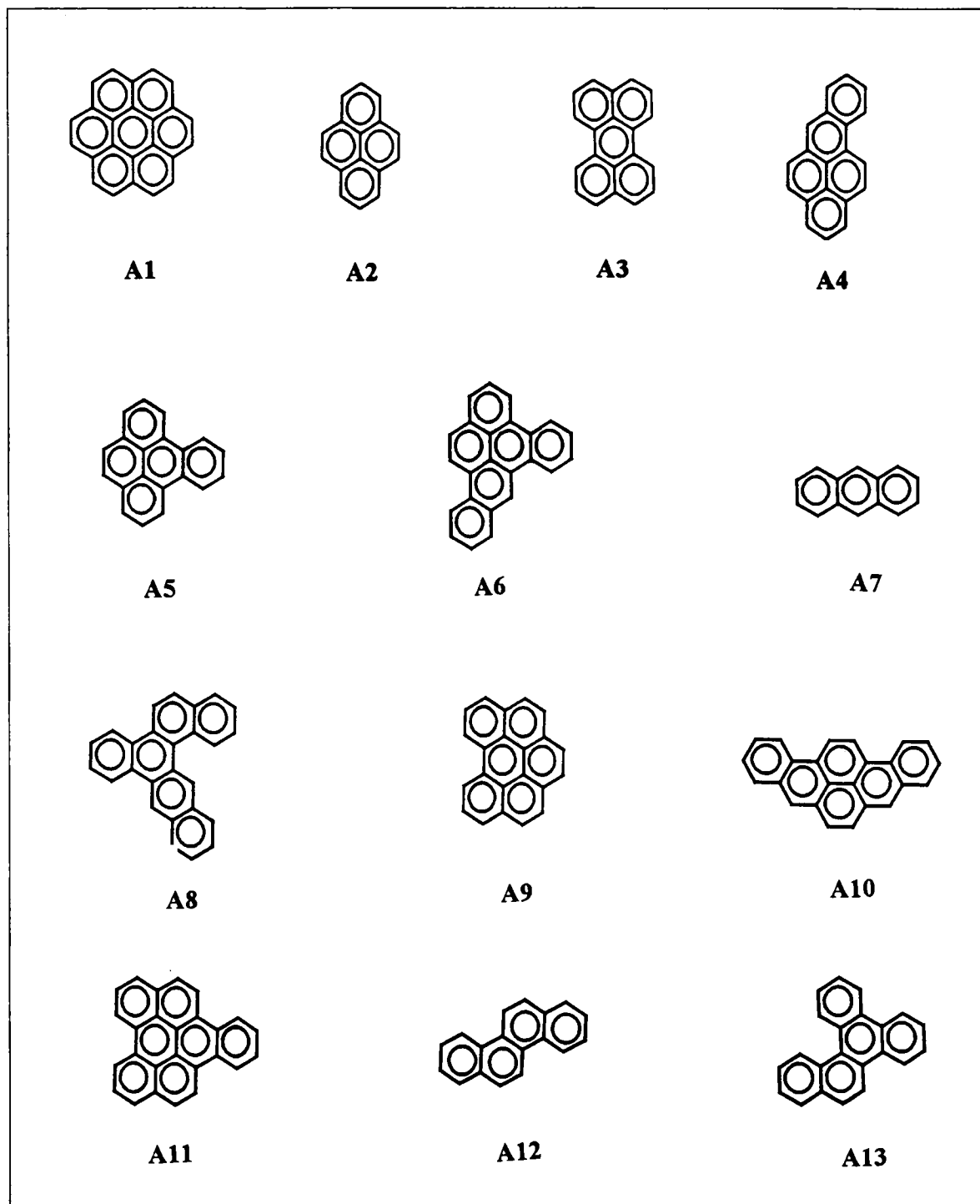
FIGURE 6: Molecular structures of alternant PAH6 benzenoids: Coronene (A1), Pyrene (A2), Perylene (A3), Benzo(a)pyrene (A4), Benzo(e)pyrene (A5), Dibenzo(a,e)pyrene (A6), Anthracene (A7), Naphtho(2,3g)chrysene (A8), Benzo[ghi]perylene (A9), Benzo[rst]pentaphene (A10), Naphtho[1,2,3,4ghi]perylene (A11), Chrysene (A12), Benzo[g]chrysene (A13).
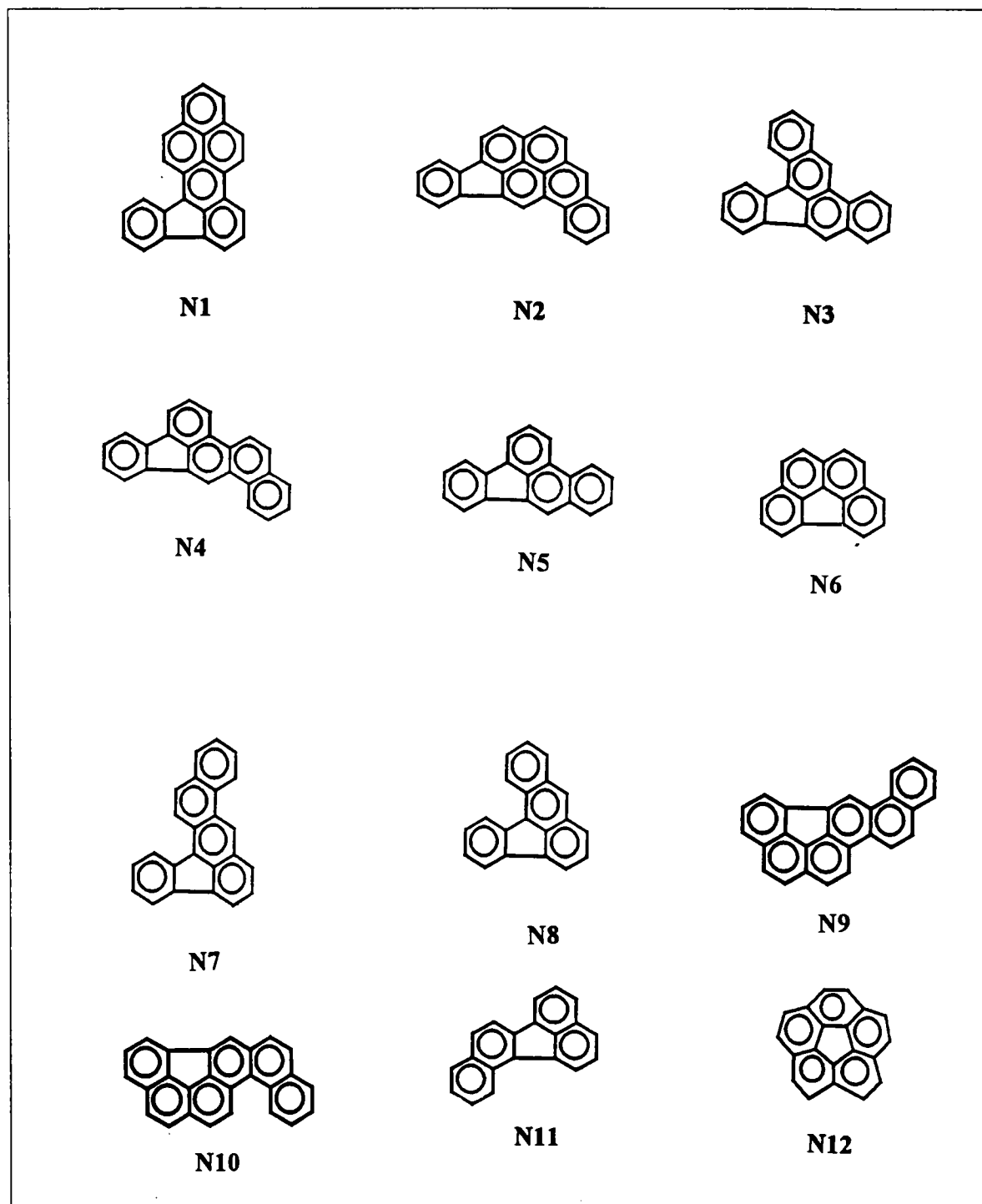
FIGURE 7: Molecular structures of nonalternant fluoranthenoids and fluorenoids: Benz(def)indeno(1,2,3hi)chrysene (N1), Benz(def)indeno(1,2,3qr)chrysene (N2), Dibenzo(a,e)fluoranthene (N3), Naphtho(1,2b)fluoranthene (N4), Benzo(b)fluoranthene (N5), Benzo(ghi)fluoranthene (N6), Naphtho(2,1a)fluoranthene (N7), Benzo(a)fluoranthene (N8), Naphtho[2,1k]benzo[ghi]fluoranthene (N9), Naphtho[1,2k]benzo[ghi]fluoranthene (N10), Benzo[j]fluoranthene (N11), Dibenzo[ghi,mno]fluoranthene (N12).

Chapter Bibliography

1. Tucker, S.A.; Amszi, V.L.; Acree, Jr., W.E. *J. Chem. Ed.*, **1992**, *69*, A8.

2. Lakowicz, J.R. Principles of Fluorescence Spectroscopy; Plenum: New York, 1983, 44.

3. Holland, J.F; Teets, R.E.; Kelly, P.M.; Timnick, A. *Anal. Chem.*, **1977**, *49*, 706.

4. Pandey, S. Dissertation, University of North Texas (1998).

5. Guilbault, G.G. Practical Fluorescence: Theory, Methods, and Techniques; Marcel Dekker: New York, 1973.

6. Swarbrick, J.; Darawala, J. *J. Phys. Chem.*, **1969**, *73*, 2627.

7. Murkerjee, P.; Mysels, K. Critical Micelle Concentration of Aqueous Surfactant Systems. National Standards Reference Data Series, Vol. 36, National Bureau of Standards, Washington, DC, 1971.

Chapter 4

Results and Discussion of Mobile Order Theory:

Huyskens, Ruelle, and coworkers have presented a very impressive set of comparisons between experimental and predicted values of PAHs in a wide range of both noncomplexing and complexing solvents to document the predictive ability of Mobile Order theory.[1-4] Acree, Zvaigzne, McHale, Powell and coworkers assessed the applications and limitations of Mobile Order theory for predicting anthracene solubilities in alkane + alcohol, alcohol + alcohol, alcohol + ether, and alcohol + alkoxyalcohol solvent mixtures.[5-9] The preliminary computations revealed that both expressions provide a very accurate estimate for how the solubility varies as a function of binary solvent composition. The purpose of this thesis is to improve Mobile Order theory's predictability in nonelectrolyte solutions and alkane + alcohol solvent mixtures, and develop an expression to accurately describe the solubility behavior of anthracene in alkane + alkoxyalcohol solvent mixtures.

Recalling discussion from Chapter 1, in the case of an inert crystalline solute dissolved in a self-associating solvent, Mobile Order theory expresses the volume fraction saturation solubility, ϕ_A^{sat}, as;

$$\ln \phi_A^{sat} = \ln a_A^{solid} - 0.5\,(1 - V_A/V_{solv})\phi_{solv} + 0.5 \ln [\phi_A^{sat} + \phi_{solv}\,(V_A/V_{solv})]$$

$$- \phi_{solv}^2 V_A(\delta_A{}' - \delta_{solv}{}')^2\,(RT)^{-1} - r_{solv}(V_A/V_{solv})\phi_{solv} \qquad 4.1$$

where $\phi_{solvent}$ is the volume fraction of the solvent [i.e. $\phi_{solvent} = 1 - \phi_A^{sat}$], and the $r_{solvent}$

$(V_A/V_{solvent})$ $\phi_{solvent}$ term represents the contributions resulting from hydrogen bond

formation between the solvent molecules. For most of the published applications, $r_{solvent}$

was assumed to be unity for strongly associated solvents with single hydrogen bonded

chains such as monofunctional alcohol, to be two for water or diols, and to equal zero for

non-associated solvents such as saturated hydrocarbons. A more exact value for

monofunctional alcoholic solvents can be calculated by;

$$r_{solv} = (K_{solv}\ \phi_{solv}/V_{solv})\ /(1 + K_{solv}\ \phi_{solv}/V_{solv}) \qquad 4.2$$

with a numerical value of $K_{solvent} = 5{,}000\ cm^3\ mol^{-1}$ assumed for all monofunctional

alcohols. Regressing spectroscopic and vapor pressure data determined this numerical

value.

If complexation does occur between the crystalline solute and solvent;

$$\ln \phi_A^{sat} = \ln a_A^{solid} - 0.5\ (1 - V_A/V_{solv})\phi_{solv} + 0.5 \ln [\phi_A^{sat} + \phi_{solv}\ (V_A/V_{solv})]$$

$$- \phi_{solv}^2 V_A(\delta_A{}' - \delta_{solv}{}')^2\ (RT)^{-1} - \ln[1 + \phi_{solvent}(K_{Asolvent}/V_{solvent})] \qquad 4.3$$

then an additional term involving the solute-solvent equilibrium constant, $K_{Asolvent}$, must

be introduced to describe the solubility enhancement that arises as a result of specific

interactions. A slightly more complex expression applies in the case of solute

complexation with a self-associating solvent. The symbols $\delta_A{}'$ and $\delta_{solvent}{}'$ denote the

modified solubility parameters of the solute and solvent, V_i is the molar volume, and

$a_A{}^{solid}$ is the activity of the solid solute. This latter quantity is defined as the ratio of the

fugacity of the solid to the fugacity of the pure hypothetical supercooled liquid. The

numerical value of $a_A{}^{solid}$ can be computed from;

$$\ln a_A{}^{solid} = -\Delta H_A{}^{fus}(T_{mp} - T)/(RTT_{mp}) \qquad\qquad 4.4$$

the solute's molar enthalpy of fusion, $\Delta H_A{}^{fus}$, at the normal melting point temperature,

T_{mp}. Equation 4.4 assumes that the enthalpy of fusion is independent of temperature, and

that there are no solid phase transitions between the melting point and system

temperature, T. Lack of heat capacity data for anthracene, pyrene, and *trans*-stilbene as a

function of temperature necessitated this assumption. Additional terms must be included

if the solid undergoes a phase transition. Contributions from nonspecific interaction are

incorporated into Mobile Order theory through the $\phi_{solv}{}^2 V_A(\delta_A{}' - \delta_{solv}{}')^2 (RT)^{-1}$ term.

Organic Nonelectrolyte Solvents

Predictive application of equations 4.1 and 4.3 is relatively straight forward.

First, average numerical values of $\delta_{anth}{}' = 20.32$ MPa$^{1/2}$ and $\delta_{stilbene}{}' = 19.69$ MPa$^{1/2}$ are

computed by requiring that each equation (with $r_{solvent} = 0$ and/or $K_{Asolvent} = 0$) perfectly

describes anthracene and *trans*-stilbene mole fraction solubility data in hexane, heptane,

and octane. For anthracene, the numerical value of $a_A{}^{solid} = 0.01049$ is calculated using

equation 4.4 with $\Delta H_A{}^{fus} = 28,860$ J mol^{-1} and $T_{mp} = 490.0$ K.[10] For *trans*-stilbene, the

numerical value of $a_A{}^{solid} = 0.06227$ is calculated using equation 4.4 with $\Delta H_A{}^{fus} = 27,400$

J mol^{-1} and T$_{mp}$ = 398.15 K.[11] Numerical values of V$_{anth}$ = 150.0 cm^3 mol^{-1} and V$_{stilbene}$ =

177.0 cm^3 mol^{-1} were used for the molar volumes of the hypothetical subcooled liquid

solute. Calculation of the solute's modified solubility parameter in this fashion

eliminated any computational errors/uncertainties that might occur as a result of

solubility enhancement from either specific solute-solvent interactions or formation of

solute-solvent association complexes. Saturated hydrocarbons are incapable of molar

complexation.

Table XXXIV summarizes the predictive ability of Mobile Order theory for the

44 different organic solvents for which both anthracene solubility data and modified

solubility parameters could be found. Similarly, Table XXXV summarizes the predictive

ability of Mobile Order theory for *trans*-stilbene dissolved in 35 organic nonelectrolyte

solvents. Predicted vales were computed using an iterative method in which all $\phi_{solvent}$

values in equation 4.1 were initially set equal to unity. The computed volume fraction

solubility was used to calculate a better estimate for $\phi_{solvent}$, which was then substituted

into equation 4.1 for the second iteration. The calculations converged after three or four

iterations. Solvent molar volumes and modified solubility parameters are listed in Table

XXXVI. Solvent molar volumes were calculated as the molar mass of the solvent

divided by the liquid density at 298.15 K. The modified solubility parameters account for

only nonspecific interactions, and in the case of the alcoholic solvents the hydrogen

bonding contributions have been removed.

Numerical values of $\delta_{solvent}'$ were obtained from published computations and were

either deduced by regressing actual solubility data of solid n-alkanes in organic solvents

in accordance with the configurational entropic model of Huyskens and Haulait-Pirson or

estimated using known values for similar organic solvents.[3,12-14,15] The predicted values

do depend on the numerical values assumed for the various input parameters.

Computations using slightly different numerical values for the solubility parameters

(± 0.10 MPa$^{1/2}$) and molar volumes ($\pm$ 1 cm^3 mol^{-1}) indicate that the predicted value can

vary 5-10% as a result of small changes in these two input parameters. This would be

true of any predictive model that uses solubility parameters, functional group contribution

energies, or other similar input parameters.

Examination of the entries in Table XXXIV and XXXV reveal that Mobile Order

theory does provide fairly reasonable (though by no means perfect) estimates of the

solubility behavior of anthracene and *trans*-stilbene in a wide range of organic solvents.

Average absolute deviation between predicted and observed values is *circa* 31.0% (for

anthracene) and 20.0% (for *trans*-stilbene), which corresponds to $\Delta \log x_A^{sat} \approx \pm 0.12$ when

expressed as the difference in logarithmic mole fraction solubilities. Acetonitrile was

excluded from the average absolute deviation in the case of anthracene.

In evaluating the applicability of Mobile Order theory, one must realize that many

of these particular systems are highly non-ideal and that the experimental solubility data

covers over a 140-fold (in anthracene) and 340-fold (in *trans*-stilbene) range in mole

fraction. Had an ideal solution been assumed, then the predicted anthracene mole

fraction solubility would be $X_A^{sat} = a_A^{sat} = 0.01049$ in each solvent. This corresponds to

an overall average absolute deviation of 910% between predicted and observed values.

For *trans*-stilbene, the predicted ideal mole fraction solubility is $X_A^{sat} = a_A^{sat} = 0.06227$,

which corresponds to an absolute deviation of 1,175% between predicted and observed

values.

TABLE XXXIV. Comparison Between Experimental Anthracene Mole Fraction
Solubilities and Predicted Values Based on Mobile Order Theory

Organic Solvent	$(X_A^{sat})^{exp}$	[Data ref.]	$(X_A^{sat})^{calc}$	% Dev [a]
Hexane	0.001290	[16]	0.001424	10.4
Heptane	0.001571	[16]	0.001519	-3.3
Octane	0.001850	[16]	0.001729	-6.5
Nonane	0.002085	[17]	0.002005	-3.8
Decane	0.002345	[16]	0.002113	-9.9
Hexadecane	0.00380	[16]	0.003015	-20.7
Cyclohexane	0.001574	[16]	0.001746	10.9
Methylcyclohexane	0.00165	[16]	0.001919	16.3
2,2,4-Trimethylpentane	0.001087	[16]	0.001179	8.5
Cyclooctane	0.002258	[16]	0.002451	8.5
tert-Butylcyclohexane	0.001978	[16]	0.002601	31.5
Squalane	0.00472	[16]	0.005047	6.9
Dibutyl ether	0.00354	[16]	0.006433	81.7
1,4-Dioxane	0.008381	[16]	0.01128	34.6
Benzene	0.007418	[16]	0.01016	37.0
Toluene	0.00736	[16]	0.008090	9.9
m-Xylene	0.007956	[17]	0.005930	-25.5

TABLE XXXIV. Continued

Organic Solvent	$(X_A^{sat})^{exp}$	[Data ref.]	$(X_A^{sat})^{calc}$	% Dev [a]
p-Xylene	0.00733	[16]	0.006149	-16.1
Ethyl acetate	0.00484	[16]	0.01088	124.8
Butyl acetate	0.00661	[16]	0.01026	55.2
Diethyl adipate	0.01033	[16]	0.008118	-21.4
Trichloromethane	0.01084	[17]	0.01024	-5.5
Tetrachloromethane	0.00464	[16]	0.005843	25.9
1-Chlorobutane	0.00586	[16]	0.005910	0.9
1-Chlorohexane	0.007177	[17]	0.007628	6.3
1-Chlorooctane	0.007780	[18]	0.007638	-1.8
Chlorocyclohexane	0.006353	[18]	0.008713	37.1
Chlorobenzene	0.009962	[17]	0.01049	5.3
Dichloromethane	0.009387	[17]	0.01316	40.2
1,4-Dichlorobutane	0.01053	[16]	0.01055	0.2
Methanol	0.000243	[17]	0.000492	102.5
Ethanol	0.000460	[17]	0.000762	65.7
1-Propanol	0.000591	[16]	0.000957	61.9
2-Propanol	0.000411	[16]	0.001104	168.6
1-Butanol	0.000801	[16]	0.001212	51.3

TABLE XXXIV. Continued

Organic Solvent	$(X_A{}^{sat})^{exp}$	[Data ref.]	$(X_A{}^{sat})^{calc}$	% Dev [a]
2-Butanol	0.000585	[16]	0.000965	65.0
2-Methyl-1-propanol	0.000470	[16]	0.000778	65.5
1-Pentanol	0.001097	[19]	0.001316	20.0
1-Hexanol	0.001483	[17]	0.001266	-14.6
1-Heptanol	0.001869	[17]	0.001439	-23.0
1-Octanol	0.002160	[16]	0.001598	-26.0
Ethylene glycol	0.0000715	[17]	0.0000693	-3.1
Acetonitrile	0.000830	[17]	0.00820	888.1
N,N-Dimethylformamide	0.007839	[17]	0.009891	26.2

[a] Deviations (%) = 100 $[(X_A{}^{sat})^{calc} - (X_A{}^{sat})^{exp}]/(X_A{}^{sat})^{exp}$

TABLE XXXV. Comparison Between Experimental *trans*-Stilbene Mole Fraction Solubilities and Predicted Values Based on Mobile Order Theory

Organic Solvent	$(X_A{}^{sat})^{exp}$	[Data ref.]	$(X_A{}^{sat})^{calc}$	% Dev [a]
Hexane	0.00960	[20]	0.01025	6.8
Heptane	0.01085	[20]	0.01080	-0.4
Octane	0.01241	[20]	0.01224	-1.4
Nonane	0.01383	[21]	0.01416	2.4
Decane	0.01511	[21]	0.01482	-1.9
Hexadecane	0.02178	[21]	0.02062	-5.3
Cyclohexane	0.01374	[20]	0.01316	-4.3
Methylcyclohexane	0.01413	[20]	0.01414	0.1
2,2,4-Trimethylpentane	0.00803	[20]	0.00812	1.1
Cyclooctane	0.02080	[20]	0.01814	-12.8
tert-Butylcyclohexane	0.01570	[20]	0.01864	18.7
Benzene	0.06232	[21]	0.06809	9.3
Toluene	0.06066	[21]	0.05724	-5.6
m-Xylene	0.05690	[21]	0.04361	-23.4
p-Xylene	0.06342	[21]	0.04496	-29.1
Ethylbenzene	0.05331	[21]	0.05429	1.8
Chlorobenzene	0.07363	[21]	0.06699	-9.0
Dibutyl ether	0.02783	[20]	0.04498	61.6
1,4-Dioxane	0.06615	[21]	0.06597	-0.3

TABLE XXXV. Continued.

Organic Solvent	$(X_A^{sat})^{exp}$	[Data ref.]	$(X_A^{sat})^{calc}$	% Dev [a]
Tetrahydrofuran	0.1035	[21]	0.07213	-30.3
Tetrachloromethane	0.03970	[21]	0.04486	13.0
Methanol	0.00196	[20]	0.00209	6.5
Ethanol	0.00321	[20]	0.00387	20.5
1-Propanol	0.00403	[20]	0.00519	28.8
2-Propanol	0.00279	[20]	0.00597	114.0
1-Butanol	0.00533	[20]	0.00682	27.9
2-Butanol	0.00382	[20]	0.00547	43.1
2-Methyl-1-propanol	0.00330	[20]	0.00441	33.7
1-Pentanol	0.00691	[20]	0.00761	10.1
1-Hexanol	0.00841	[20]	0.00746	-11.4
1-Heptanol	0.01092	[20]	0.00858	-21.4
1-Octanol	0.01251	[20]	0.00955	-23.6
Ethylene glycol	0.000296	[21]	0.000186	-37.2
2-Butanone	0.06273	[21]	0.05009	-20.1
Acetonitrile	0.00995	[21]	0.00431	-56.7

[a] Deviations (%) = 100 $[(X_A^{sat})^{calc} - (X_A^{sat})^{exp}]/(X_A^{sat})^{exp}$

TABLE XXXVI. Solvent and Solute Properties used in Mobile Order Theory

Component (i)	$V_i/(\text{cm}^3 \text{ mol}^{-1})$	$\delta'_i/(\text{MPa}^{1/2})^{a}$
Hexane	131.51	14.56
Heptane	147.48	14.66
Octane	163.46	14.85
Nonane	179.87	15.07
Decane	195.88	15.14
Hexadecane	294.12	15.61
Cyclohexane	108.76	14.82
Methylcyclohexane	128.32	15.00
2,2,4-Trimethylpentane	166.09	14.30
Cyclooctane	134.9	15.40
tert-Butylcyclohexane	173.9	15.50
Squalane	525.0	16.25
Dibutyl ether	170.3	17.45
1,4-Dioxane	85.8	20.89
Benzene	89.4	18.95
Toluene	106.84	18.10
m-Xylene	123.2	17.2

TABLE XXXVI. Continued.

Component (i)	$V_i/(\text{cm}^3 \text{ mol}^{-1})$	$\delta'_i/(\text{MPa}^{1/2})^{\text{a}}$
p-Xylene	123.9	17.30
Ethyl acetate	98.5	20.79
Butyl acetate	132.5	19.66
Diethyl adipate	202.2	18.17
Trichloromethane	80.7	18.77
Tetrachloromethane	97.08	17.04
1-Chlorobutane	105.0	17.12
1-Chlorohexane	138.1	18.00
1-Chlorooctane	171.1	18.00
Chlorocyclohexane	120.3	18.45
Chlorobenzene	102.1	19.48
Dichloromethane	64.5	20.53
1,4-Dichlorobutane	112.1	19.78
Methanol	40.7	19.25
Ethanol	58.7	17.81
1-Propanol	75.10	17.29
2-Propanol	76.90	17.60
1-Butanol	92.00	17.16

TABLE XXXVI. Continued.

Component (i)	$V_i/(cm^3\ mol^{-1})$	$\delta'_i/(MPa^{1/2})^a$
2-Butanol	92.4	16.60
2-Methyl-1-propanol	92.8	16.14
1-Pentanol	108.6	16.85
1-Hexanol	125.2	16.40
1-Heptanol	141.9	16.39
1-Octanol	158.30	16.38
Ethylene glycol	56.0	19.90
Acetonitrile	52.9	23.62
N,N-Dimethylformamide	77.0	22.15
Tetrahydrofuran	81.4	16.30
Ethylbenzene	123.1	18.02
2-Butanone	90.2	22.10
2-Ethoxyethanol	97.50	20.30
2-Propoxyethanol	114.92	19.80
2-Isopropoxyethanol	116.20	19.30
2-Butoxyethanol	131.92	19.20
3-Methoxy-1-butanol	115.09	19.80

TABLE XXXVI. Continued.

Component (i)	$V_i/(cm^3 \, mol^{-1})$	$\delta'_i/(MPa^{1/2})^a$
Anthracene [b]	150.0	20.32 [d]
trans-Stilbene [c]	177.0	19.69 [d]
Pyrene	166.5	

[a] Tabulated values are taken from a compilation given in Ruelle *et al.*[3,12-14] Modified solubility parameters for the five alkoxyalcohols were estimated and were calculated by adding an incremental ether group contribution value to the known modified parameters of alcohols of comparable molecular size. The numerical value of the ether group contribution value to δ_i' was computed from differences between the known modified solubility parameters of dialkyl ethers and the corresponding alkane homomorph hydrocarbon, taking into account the length of the alkyl chain.

[b] The numerical value of $a_A^{solid} = 0.01049$ was calculated from the molar enthalpy of fusion, $\Delta H_A^{fus} = 28,860 \, J \, mol^{-1}$, at the normal melting point temperature of the solute, $T_{mp} = 490.0 \, K$.[10]

[c] The numerical value of $a_A^{solid} = 0.06227$ was calculated from the molar enthalpy of fusion, $\Delta H_A^{fus} = 27,400 \, J \, mol^{-1}$, at the normal melting point temperature of the solute, $T_{mp} = 398.15 \, K$.[10]

[d] Numerical value was calculated using the measured anthracene mole fraction solublitiies in n-hexane, n-heptane, and n-octane, in accordance with equations 4.1 and 4.3; with $r_{solvent} = 0$ and/or $K_{Asolvent} = 0$.

Alkane + Alcohol Solvent Mixtures

Optimized values of the Mobile Order theory association constants were obtained by fitting the mobile order model to isothermal vapor-liquid equilibrium data for binary mixtures of alkane (B) + alcohol (C). The criteria for the equilibrium are;

$$\gamma_i x_i P_i^{sat} = F_i y_i P \qquad (i = B,C) \qquad\qquad 4.5$$

where γ_i, x_i, y_i, and P_i^{sat} are the liquid phase activity coefficient, liquid phase mole fraction, vapor phase mole fraction, and pure component vapor pressure, respectively, of species 'i'. The total equilibrium pressure is denoted as P. The correction factors F_i are defined as;

$$F_I = f_i / \{f_i^{sat} exp[(V_i/RT)(P_i - P_i^{sat})]\} \qquad\qquad 4.6$$

where f_i^{sat} and f_i denote the fugacity coefficients for the pure saturated species i at the temperature of the mixtures and for species i in the vapor mixture, respectively, and V_i is the molar saturated liquid volume of pure species i. The two-term virial equation (expansion in pressure) was used to calculate all fugacity coefficients. The Tsonopoulos correction was used in the second virial coefficient calculations.[22]

Mobile order expressions for the liquid phase activity coefficients in mixtures of alkane (B) + alcohol (C) are given by;[7]

$$\ln \gamma_B = 0.5[\ln(\phi_B/X_B) + \phi_C(1 - V_B/V_C)]$$

$$+ (V_B/V_C)K_C'\phi_C{}^2/[1 + K_C'\phi_C] + r_B\phi_C{}^2\beta_{BC}(RT)^{-1} \qquad\qquad 4.7$$

and

$$\ln \gamma_C = 0.5[\ln(\phi_C/X_C) + \phi_B(1 - V_B/V_C)] + \ln(1 + K_C') - \ln(1 + K_C'\phi_C)$$

$$- K_C'\phi_B\phi_C/(1 + K_C'\phi_C) + r_C\phi_{C\setminus B}{}^2\beta_{BC}(RT)^{-1} \qquad\qquad 4.8$$

where $K_C' = K_C/V_C$ and $r = V_i/V_{MeOH}$. The molar volume of methanol used in the

regressional analysis was $V_{MeOH} = 41.0 \text{ cm}^3 \text{ mol}^{-1}$. Earlier applications involving Mobile

Order theory described nonspecific physical interactions in terms of a modified solubility

parameter model. To compute alcohol-specific association constants, the more general

β_{BC}-parameter is used because the binary liquid-vapor equilibrium data that is to be

regressed involves several different temperatures. Published tabulation of modified

solubility parameters pertain to 298.15 K, and no systematic study examines how δ_i'

values vary with temperature.[3,12]

Values for the two parameters K_C' and β_{BC} were obtained from binary total

pressure using Barker's method.[23] For a given set of parameter values, the two equations

denoted by equation 4.5 are solvable by trial and error for the total pressure P and vapor

phase mole fraction γ_B corresponding to each liquid mole fraction x_B of an isothermal set

of total pressure data. The sum of the squares of the differences between the calculated

and measured pressure is evaluated and a new set of parameter values is determined using

the Nelder-Mead flexible polyhedron search method. The optimized values of K_C' and

β_{BC} are those numerical values which produce this minimum. Several binary vapor-

liquid equilibrium data sets involved temperatures other than 298.15 K (or 299.15K). For

these systems, equation 4.8 was used to correct the numerical values of the association

constants to 298.15 K:

$$K_{298}'/K_T' = \exp[-(\Delta H^\circ / R)(1/298.15 - 1/T_K)] \qquad 4.9$$

In the above expression, the molar enthalpy of hydrogen-bond formation is taken to be

$\Delta H^\circ = -25.1$ KJ/mol.

Numerical values of the calculated association constants (corrected to 298.15 K)

are tabulated in table XXXVII, along with the calculated β_{BC}-values and overall root

mean square deviations in the back-calculated total pressures. Careful examination of

Table XXXVII reveals that the 'optimized' association constant for any given alcohol

does vary slightly from one binary alkane + alcohol system to another.

Some variation in the calculated values of the association constant of a given

alcohol is to be expected. First, the hydrogen-bonding treatment assumed in the original

development of the Mobile Order theory is probably much simpler than the actual

situation. Second, values of the association constants will depend on both the

uncertainties in the experimental vapor-liquid equilibrium data and the particular solution

model used to describe nonspecific physical interactions. For practical applications of

Mobile Order theory, eventually a fixed value of the association constant at 298.15 K for

each alcohol will be needed. However, this will lead to some degradation of the Mobile

Order theory to represent multisystem and multiproperty data. Computations reported

show that the association constants of alcohols are significantly smaller than the value of

$K_{alcohol}$ = 5,000 cm^3 mol^{-1} previously assumed for all alcohols. These larger $K_{alcohol}$ =

5,000 cm^3 mol^{-1} values were based either on spectroscopic data or thermodynamic

treatment which failed to properly account for nonspecific interactions. In the latter case,

all solutions nonideality would have been attributed to formation of molecular association

complexes.

For an inert crystalline solute dissolved in a binary alkane (B) + alcohol (C)

solvent mixture, Mobile Order theory expresses the volume fraction saturation solubility,

ϕ_A^{sat}, as;

$$RT\{\ln(a_A^{solid}/\phi_A^{sat}) - 0.5[1 - V_A(X_B°V_B + X_C°V_C)] + 0.5\ln[V_A/(X_B°V_B + X_C°V_C)] -$$

$$(V_A/V_C)(K_C(\phi_C°)^2/V_C)/(1 + K_C\phi_C°/V_C)\} = r_A[\phi_B°\beta_{AB} + \phi_C°\beta_{AC} - \phi_B°\phi_C°\beta_{BC}] \qquad 4.10$$

whenever the saturation solubility is sufficiently low so that $1 - \phi_A^{sat}$ = 1.0. The symbol

β_{ij}(J mol^{-1}) denotes the nonspecific interaction parameter for the binary mixture

containing components i and j, and a_A^{solid} is the activity of the solid solute. This latter

quantity is defied as the ratio of the fugacity of the solid to the fugacity of the pure

hypothetical supercooled liquid at the same temperature and pressure.

Contributions from nonspecific interactions are incorporated into the Mobile

Order theory through the $r_A[\phi_B°\beta_{AB} + \phi_C°\beta_{AC} - \phi_B°\phi_C°\beta_{BC}]$ term. Through suitable

mathematical manipulation, the $r_A\phi_B°\beta_{AB}$ and $r_A\phi_C°\beta_{AC}$ terms were eliminated from the

basic model in favor of measured solubility data in both pure solvents, $(\phi_A^{sat})_B$ and

$(\phi_B^{sat})_C$. The final derived expression;

$$\ln \phi_A{}^{sat} = \phi_B{}^° \ln (\phi_A{}^{sat})_B + \phi_C{}^° \ln (\phi_A{}^{sat})_C - 0.5 \, [\ln x_B{}^°V_B + x_C{}^°V_C) - \phi_B{}^° \ln V_B - \phi_C{}^° \ln V_C]$$

$$- (V_A/V_C)(\phi_C{}^°)^2 \, (K_C/V_C)/[1 + \phi_C{}^°(K_C/V_C)]$$

$$+ (V_A K_C \phi_C{}^°/V_C{}^2)(1 + K_C/V_C)^{-1} + r_A \phi_B{}^°\phi_C{}^°\beta_{BC}(RT)^{-1} \qquad\qquad 4.11$$

does not require a prior knowledge of the solute's enthalpy of fusion and melting point

temperature, which would be needed to calculate the numerical value of $a_A{}^{solid}$ at the

temperature corresponding to the solubility measurements.

The predictive ability of equation 4.11 is summarized in Tables XXXVIII and

XXXIX for the solubilities of anthracene and pyrene in several binary alkane + alcohol

solvent mixtures. Experimental uncertainty associated with each mole fraction solubility

data point in a given solvent set is approximately 1.3-2.0 percent. Systems selected

include both linear and branched alcohols ranging in size from $V_i = 75.10 \text{ cm}^3 \text{ mol}^{-1}$ and

$V_i = 158.30 \text{ cm}^3 \text{ mol}^{-1}$. Solute and solvent molar volumes used in the Mobile Order

theory predictions are listed in Table XXXVI. Careful examination of the % deviation of

$K_{AC} = 0$ in Tables XXXVIII and XXXIX reveals that equation 4.11 underpredicts the

experimental solubilities for most of the binary solvent systems considered.

Consistent underprediction of the observed pyrene solubilities, sometimes by as

much as 10-20%, suggests that both PAH solutes may be interacting specifically with the

alcohol cosolvents. Complication involving the PAH's polarizable π-electron cloud and

the alcohol's OH functional group is not unreasonable. Published data often assumes

PAH-alcohol complexes with theoretical models.

Extension of equation 4.11 to systems containing an AC molecular complex is

relatively straightforward. Two terms are added to the final predictive expression;

$$\ln \phi_A{}^{sat} = \phi_B{}^{\circ} \ln (\phi_A{}^{sat})_B + \phi_C{}^{\circ} \ln (\phi_A{}^{sat})_C - 0.5 [\ln x_B{}^{\circ}V_B + x_C{}^{\circ}V_C) - \phi_B{}^{\circ} \ln V_B - \phi_C{}^{\circ} \ln V_C]$$

$$+ \ln[1 + K_{AC}\phi_C{}^{\circ}/V_C] - \phi_C{}^{\circ}\ln[1 + K_{AC}/V_C]$$

$$- (V_A/V_C)(\phi_C{}^{\circ})^2 (K_C/V_C)/[1 + \phi_C{}^{\circ}(K_C/V_C)]$$

$$+ (V_AK_C\phi_C{}^{\circ}/V_C{}^2)(1 + K_C/V_C)^{-1} + r_A\phi_B{}^{\circ}\phi_C{}^{\circ}\beta_{BC}(RT)^{-1} \qquad 4.12$$

to describe complexation in the binary solvent mixture, the $\ln[1 + K_{AC}\phi_C{}^{\circ}/V_C]$ term, and the pure alcohol cosolvent, the $\phi_C{}^{\circ}\ln[1 + K_{AC}/V_C]$ term. The latter term is introduced whenever the $r_A\phi_C{}^{\circ}\beta_{AC}$ nonspecific interactions are eliminated from the basic model in favor of the measure PAH solute solubility data in the pure alcohol cosolvent.

Predictive application of equation 4.12 requires a prior knowledge of the numerical value for a given PAH-alcohol stability constant. In principle, one could have a different numerical value of each alcohol cosolvent studied. Such approaches would restrict predictions to alcohols already studied, and would represent more of a 'curve-fitting' exercise rather than an outright solubility prediction. To maintain as much generality as possible, the numerical values for a single stability constant of the alcohol cosolvent is defined for each PAH. This assumption seems reasonable since only monofunctional alcohols were studied in the present investigation, and the molecular size of the single OH functional group is approximately the same for linear and branched alcohols. This is not the case however with the acceptor sites on the two PAH solutes. The aromatic fused-ring system of pyrene is larger than that of anthracene. From simple microscopic equilibrium constant considerations, it can be argued that the larger ring system will lead to a larger stability constant. Hence, the K_{AC} stability constants for

anthracene-alcohol and pyrene-alcohol complexes have different numerical values for computation.

The last column in tables XXXVIII and XXXIX compare the predictions of equation 4.12 to experimental pyrene solubility data. Numerical values of $K_{AC} = 175$ cm^3 mol^{-1} were used for the stability constants for the presumed pyrene-alcohol complexes, and $K_{AC} = 125$ cm^3 mol^{-1} for the presumed anthracene-alcohol complexes, respectively. No attempt was made to optimize these values as we wanted the computations to represent outright solubility predictions to the extent possible. Each constant was obtained by regressing experimental solubility data for just two binary solvent systems. Computations for the remaining binary alkane + alcohol systems represent predicted values.

It is possible to significantly improve the solubility predictions of the Mobile Order theory to PAH solutes dissolved in binary alkane + alcohol solvent mixtures by including PAH-alcohol complexation into the basic model. In the case of pyrene, stability constants of $K_{AC} = 175$ cm^3 mol^{-1} led to reasonably accurate solubility predictions. The present investigation differs from earlier ones in that PAH molecules are no longer treated as inert solutes. We suspect that the earlier success of the Mobile Order theory in describing the observed PAH solubility behavior in binary alcohol + alcohol and alcohol + alkoxyalcohol solvent mixtures results from the fact that pyrene forms very similar complexes with both alcohol and/or alkoxyalcohol cosolvents. Here, the added correction terms of;

$$\ln[1 + K_{AB}\phi_B^\circ/V_B + K_{AC}\phi_C^\circ/V_C] - \phi_B^\circ\ln[1 + K_{AB}/V_B] - \phi_C^\circ\ln[1 + K_{AC}/V_C] \qquad 4.13$$

in the derived predictive expression must contribute only slightly to the overall solute

solubility. Sample computations with solvent molar volumes between $V_{alcohol} = 75$ cm^3

mol^{-1} and $V_{alcohol} = 150$ cm^3 mol^{-1}, and assuming PAH-alcohol stability constants ranging

from $K_{AB} = K_{AC} = 200$ cm^3 mol^{-1}, suggest that this is indeed the case.

TABLE XXXVII. Mobile Order Theory Association Constants ($K'_{C,298}$) and Physical Interaction Constants (β_{BC}, J mol^{-1}) Calculated From Binary Alkane (B) + Alcohol (C) Vapor-Liquid Equilibrium Data.

Alcohol/Alkane	# of points	T/K	$K'_{C,298}$	β_{BC}	ΔP (kPa)	Data ref.
1-Propanol						
Octane	37	313.15	43.1	97.7	0.07	[25]
Cyclohexane	32	348.15	35.0	12.5	0.36	[26]
Methylcyclohexane	11	333.15	39.1	186.9	0.07	[1]
1-Butanol						
Hexane	26	333.15	31.3	203.0	0.34	[27]
Methylcyclohexane	12	333.15	32.7	218.4	0.15	[1]
2-Butanol						
Methylcyclohexane	10	333.15	19.5	164.9	0.25	[1]
2-Methyl-1-propanol						
Hexane	24	332.53	22.0	243.4	0.44	[27]
Methylcyclohexane	13	333.15	31.7	159.9	0.12	[1]

TABLE XXXVIII. Comparison Between Experimental Anthracene Solubilities and Predicted Values Based Upon Mobile Order Theory

Component (B) + Component (C)	% Dev.[a]	
	$K_{AC} = 0$	$K_{AC} = 125$
Hexane + 1-pentanol	0.9	+5.1
Heptane + 1-pentanol	-2.7	+2.6
Overall average deviation	*-0.9*	*3.85*
Overall deviation of all data points	*5.8*	*2.9*

[a] Deviation (%) = $(100/N)\Sigma|\ln[(x_A^{sat})^{calc}/(x_A^{sat})^{exp}]|$. An algebraic sign indicated that all deviations were either negative or positive.

TABLE XXXIX. Comparison Between Experimental Pyrene Solubilities and Predicted Values Based Upon Mobile Order Theory

Component (B) + Component (C)	%Dev[a]	
	$K_{AC} = 0$	$K_{AC} = 175$
Hexane + 1-butanol	-7.1	3.4
Heptane + 1-butanol	-7.0	3.2
Octane + 1-butanol	-10.0	1.1
Cyclohexane + 1-butanol	-7.3	3.4
Methylcyclohexane + 1-butanol	-9.2	2.6
Hexane + 2-butanol	-13.1	-3.2
Heptane + 2-butanol	-12.4	-2.5
Cyclohexane + 2-butanol	-13.2	-3.2
Methylcyclohexane + 2-butanol	-14.9	-5.0
Hexane + 2-methyl-1-propanol	-12.6	0.4
Heptane + 2-methyl-1-propanol	-10.5	0.7
Methylcyclohexane + 2-methyl-1-propanol	-16.0	-6.2
Overall average deviation	*11.11*	*-0.44*
Overall deviation of all data points	*10.5*	*3.4*

[a] Deviation (%) = $(100/N)\Sigma|\ln[(x_A^{sat})^{calc}/(x_A^{sat})^{exp}|$. An algebraic sign indicated that all deviations were either negative or positive.

Alkane + Alkoxyalcohol Solvent Mixtures
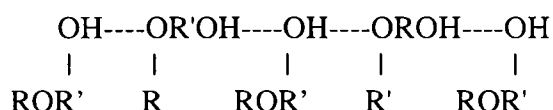
This investigation extends Mobile Order theory to an inert crystalline solute

dissolved in binary alkane + alkoxyalcohol solvent system. These mixtures are

characterized by the presence of long hydrogen bonded chains wherein hydrogen-

bonding occurs both through the hydroxyl group and the ether linkage.

$$OH----OR'OH----OH----OROH----OH$$
$$\quad\ |\qquad\ |\qquad\quad |\qquad\ |\qquad\ |$$
$$ROR' \quad R \quad\ ROR' \quad R' \quad ROR'$$

Both of these scenarios lead to an extension of the hydrogen bonded chain which allows

us to treat alkoxyalcohols as "pseudo" monofunctional alcohol cosolvents. With this in

mind, a slightly modified version of equation 4.11;

$$\ln \phi_A^{sat} = \phi_B^{\circ} \ln (\phi_A^{sat})_B + \phi_C^{\circ} \ln (\phi_A^{sat})_C - 0.5 \, [\ln x_B^{\circ}V_B + x_C^{\circ}V_C) - \phi_B^{\circ} \ln V_B - \phi_C^{\circ} \ln V_C]$$

$$- (V_A/V_C) \, \phi_C^{\circ 2} (K_C/V_C) \, / \, [1+\phi_C^{\circ}K_C/V_C]$$

$$+ \, (V_A K_C \, \phi_C^{\circ}/V_C^2)(1+K_C/V_C)^{-1} + V_A\phi_B^{\circ}\phi_C^{\circ}(\delta_B^{'} - \delta_C^{'})^2 \, (RT)^{-1} \qquad\qquad 4.14$$

must be altered slightly to allow for the additional site for hydrogen bonding caused by

the presence of the ether functional group. To accurately describe the solubility, this

study looks at several different types of alkoxyalcohols and several different alkanes

including linear, branched, and cyclic hydrocarbons.

Comparing anthracene solubilities in simple monofunctional alcohols to

experimental values determined in alkoxyalcohols reveals that anthracene is nearly three

times more soluble in alkoxyalcohol solvents than in the corresponding monofunctional

alcohols of similar size (Table XL compares these published values). This increase in

solubility may arise from either a difference in the hydrogen bonding characteristics of

alkoxyalcohols versus monofunctional alcohols or from a difference in nonspecific

interactions between the dissolved anthracene solute and the two solvent molecules.

As noted, previous studies assumed identical numerical values of $K_{alcohol} \approx 5,000$

cm^3 mol^{-1} for the stability constant of all monofunctional alcohols. There is no reason to

believe that the values for hydrogen bond formation through the OH should be any

different for alcohols and alkoxyalcohols. The numerical value of K_{OH} is set at $K_{OH} =$

$5,000$ cm^3 mol^{-1}. Stability constants for hydrogen bond formation involving alcohols and

ethers are much weaker, ranging from $K_{OC} = 100$ cm^3 mol^{-1} and $K_{OH} = 300$ cm^3 mol^{-1}.

Given the magnitude of the two constants, it is expected that hydrogen bond formation

should occur largely through the OH group. Assuming numerical values of $K_{OH} = 5,000$

cm^3 mol^{-1}, $K_{OC} = 100$ cm^3 mol^{-1}, and $V_C = 100$ cm^3 mol^{-1}, a typical alkoxyalcohol would

be engaged in hydrogen bonding approximately 98% of the time. Similarly, the

corresponding alcohol solvent molecule of comparable molecular size ($K_{alcohol} = 5,000$

cm^3 mol^{-1} and $V_{alcohol} = 100$ cm^3 mol^{-1}) would also be involved in hydrogen bond

formation around 98% of the time. These calculations suggest that the observed

solubility enhancement does not result from differences in hydrogen bonding.

Rather, a more plausible explanation involves a difference in the nonspecific

interactions between the dissolved PAH solute and the two different solvent molecules.

Nonspecific interactions are incorporated into the basic model equation 4.1 through the

$\phi_{solv}{}^2 V_A (\delta_A{}' - \delta_{solv}{}')^2 (RT)^{-1}$ term. The modified solubility parameters $\delta_i{}'$ account for only

nonspecific interactions and hydrogen bonding contributions would have been removed.

To illustrate this point, the calculated solubility parameters of anthracene using equation

4.1 must accurately describe the mole fraction solubility of anthracene in hexane,

heptane, octane, cyclohexane, methylcyclohexane, tert-butylcyclohexane and 2,2,4-

trimethylpentane. For solvents incapable of self-association, K_{solv} equals zero. The

numerical value of $\delta_A{}'$ is found to range from $\delta_A{}' = 20.25$ MPa$^{1/2}$ (in octane) to $\delta_A{}' =$

21.10 MPa$^{1/2}$ (in cyclohexane). Substituting the average of $\delta_A{}' = 20.64$ (± 0.31) MPa$^{1/2}$

into equation 4.1 back-calculates the observed mole fraction solubilities to within $\pm$ 15-

25%. Solvent and solute properties used in the Mobile Order computations are listed in

Table XXXVI.

Examining equation 4.1 reveals that as the saturation solubility increases as

$\delta_{solvent}{}'$ approaches $\delta_A{}'$ with a maximum value being reached whenever $\delta_A{}' = \delta_{solvent}{}'$.

Assuming that alcohols and alkoxyalcohols have similar hydrogen bonding

characteristics, anthracene should exhibit grater solubility in solvents having $\delta_{solvent}{}'$

values closer to $\delta_A{}' = 20.64$ MPa$^{1/2}$. Tabulated modified solubility parameters for

alcohols solvents range from around $\delta_{solvent}{}' = 16.00$ MPa$^{1/2}$ for 3-methyl-

1-butanol to $\delta_{solvent}{}' = 17.29$ MPa$^{1/2}$ for 1-propanol.[3,12,28] Although numerical $\delta_{solvent}{}'$

values for 2-ethoxyethanol, 2-propanoxyethanol, 2-isopropoxyethanol, 2-butoxyethanol,

3-methoxy-1-butanol were not given in the published tabulations, it can be argued that

modified solubility parameters of alkoxyalcohols should exceed the tabulated values of

the corresponding alcohols of comparable molecular size. An alkoxyalcohol possesses an

ether oxygen atom in addition to the alcohol OH functional group. In molecules where

an ether oxygen atom is present, one generally finds a significant increase in the numerical values of the modified solubility parameter relative to that of the n-alkane homolog, i.e., $\delta_{solvent}$' = 17.96 MPa$^{1/2}$ for dipropyl ether vs $\delta_{solvent}$' = 14.56 MPa$^{1/2}$ for hexane. The effect does however level off with increasing alkyl chain length. From these observations, we estimate that the modified solubility parameters of the five alkoxyalcohol solvents studied should lie somewhere in the range of $\delta_{solvent}$' = 19.0 MPa$^{1/2}$ to $\delta_{solvent}$' = 21.0 MPa$^{1/2}$, which is very close to the calculated modified solubility of anthracene of δ_A' = 20.64 ($\pm$0.31) MPa$^{1/2}$. This suggests that the solubility enhancement noted in the alkoxyalcohol solvents results largely from differences in nonspecific interactions, as opposed to differences in the hydrogen bonding characteristics of the two solvent types.

The previous discussion focussed exclusively on the solubility of anthracene in either a neat alcohol and/or neat alkoxyalcohol solvent, where hydrogen bond formation involved self association of the single solvent component. These ideas can be extended to binary alkane (B) + alkoxyalcohol (C) solvent mixtures as the presence of the saturated hydrocarbon merely dilutes the molar concentration of the OH and ether functional groups. The alkoxyalcohol can be treated as a "pseudo" monofunctional alcohol having perhaps a slightly larger hydrogen bond stability constant to reflect the presence a second site for hydrogen bonding. The maximum number of hydrogen bonds that can be formed remains the same, and is determined by the number of OH protons present.

Table XLI provides a summarized comparison between measured anthracene solubilities in 34 different binary alkane + alkoxyalcohol solvent systems and predicted values based on equation 4.14. Each system reports solubility data at seven binary

compositions spanning the solvent's entire more fraction range, plus the measured solute solubilities in both the neat alkane and alkoxyalcohol cosolvents. Each mole fraction solubility represents the average of between four and eight independent experimental determinations, with the measured values being reproducible to $\pm 1.8\%$ (or better). For convenience, we have assumed a numerical value of $K_C = K_{OH} + K_{OC} \approx 5,000 \text{ cm}^3 \text{ mol}^{-1}$ for all five alkoxyalcohols studied. Computations using slightly smaller or larger values of K_C indicated that the predicted more fraction solubility is not too sensitive to the actual numerical value assumed. Stability constants from $K_C = 4,000 \text{ cm}^3 \text{ mol}^{-1}$ to $K_C = 6,000 \text{ cm}^3 \text{ mol}^{-1}$ gave essentially identical predicted values. This is not surprising given the mathematical form of the two chemical contributions in equation 4.14. Any time that K_C/V_C is much larger than unity, the denominators of the fourth and fifth terms simplify to ϕ_C° (K_C/V_C) and K_C/V_C, respectively. This leads to a cancellation of K_C between the numerator and denominator of the two hydrogen bonding terms.

Careful examination of the numerical entries in Table XLI reveals that Mobile Order predicts the observed solubility behavior to within an overall average absolute deviation of $\pm 5\%$. Individual deviations in a given system; however, may be as large as $\pm 15\%$. An algebraic sign in from of the numerical values indicated that equation 4.14 either overpredicted (+ sign) or underpredicted (- sign) the solubility at all seven binary solvent compositions. For 32 of 34 systems investigated deviations were both positive and negative, hence, the absence of an algebraic sign. Part of the large deviations between the predicted and observed values is undoubtedly a result of failure of the Scatchard-Hildebrand solubility parameter equation to accurately describe the nonspecific interactions in these highly nonideal solvent mixtures. Other deviations may

also be caused by errors/uncertainties associated with the estimational scheme used in computing the modified solubility parameters of the alkoxyalcohols. An uncertainty of ± 0.2 MPa$^{1/2}$ in the numerical value of δ_i' can lead to a ± 1-2% difference in the calculated mole fraction solubility of anthracene. This is particularly true in mixtures of solvent components having vastly dissimilar δ_i' values as was the case here.

In evaluating the applicability of Mobile Order theory, one must remember that no solution model is perfect. Often one wishes a reasonable estimate for the saturation solubility in the absence of an experimental value. Earlier studies have documented that equation 4.14 predicted anthracene solubilities in 32 binary alkane + monofunctional alcohol solvent mixtures to within an overall average absolute deviation of $\pm 5.8\%$, which is comparable in magnitude to the deviations noted in the current study. There appears to be no loss in predictive accuracy in extending Mobile Order theory to systems containing an alkoxyalcohol. It may be possible in the future to reduce the deviations by including additional terms to account for specific solute-solvent interactions. At the present time, we feel uncomfortable trying to calculate stability constants for anthracene – alkoxyalcohol complexes that are likely present in solution. There is some error in the $V_A \phi_B^{\circ} \phi_C^{\circ} (\delta_B' - \delta_C')^2 (RT)^{-1}$ term caused by our inability to describe nonspecific interactions in the binary solvent mixtures. When vapor-liquid equilibria data becomes available for alkane + alkoxyalcohol mixtures, the solubility parameters of the alkoxyalcohols will be re-estimated. This should reduce the error in the $V_A \phi_B^{\circ} \phi_C^{\circ} (\delta_B' - \delta_C')^2 (RT)^{-1}$ term and permit a more meaningful computation of the solute-solvent stability constants.

TABLE XL. Experimental Solubilities of Anthracene in Select Alcohol and Alkoxyalcohol Solvents at 25°C.

Solvent	$X_A^{sat, a}$
1-Propanol	0.000591
2-Propanol	0.000411
1-Butanol	0.000801
2-Butanol	0.000585
2-Methyl-1-propanol	0.000470
1-Pentanol	0.001097
2-Pentanol	0.000800
3-Methyl-1-butanol	0.000727
2-Methyl-1-pentanol	0.000966
4-Methyl-2-pentanol	0.000779
1-Octanol	0.002160
2-Ethyl-1-hexanol	0.001397
2-Methoxyethanol	0.002211
2-Ethoxyethanol	0.002921
2-Propoxyethanol	0.003343
2-Isopropoxyethanol	0.003093
2-Butanoxyethanol	0.003785
3-Methoxy-1-butanol	0.002702

[a] Experimental solubility data is taken from references 6-9 and 28-38.

TABLE XLI. Comparison Between Experimental Solubilities and Mobile Order Theory Predictions for Anthracene Dissolved in Binary Alkane (B) + Alkoxyalcohol (C) Solvent Mixtures.

Binary Solvent Systems	% Dev.[a]
Hexane + 2-Ethoxyethanol	6.10
Heptane + 2-Ethoxyethanol	6.84
Octane + 2-Ethoxyethanol	5.93
Cyclohexane + 2-Ethoxyethanol	4.26
Methylcyclohexane + 2-Ethoxyethanol	4.86
2,2,4-Trimethylpentane + 2-Ethoxyethanol	8.75
Hexane + 2-Propoxyethanol	5.62
Heptane + 2-Propoxyethanol	+8.17
Octane + 2-Propoxyethanol	5.62
Cyclohexane + 2-Propoxyethanol	5.94
Methylcyclohexane + 2-Propoxyethanol	4.76
tert-Butylcyclohexane + 2-Propoxyethanol	3.50
2,2,4-Trimethylpentane + 2-Propoxyethanol	8.21
Hexane + 2-Isopropoxyethanol	3.23
Heptane + 2-Isopropoxyethanol	4.47
Octane + 2-Isopropoxyethanol	4.40
Cyclohexane + 2-Isopropoxyethanol	3.46
Methylcyclohexane + 2-Isopropoxyethanol	3.77
tert-Butylcyclohexane + 2-Isopropoxyethanol	5.26

TABLE XLI. Continued.

2,2,4-Trimethylpentane + 2-Isopropoxyethanol	6.39
Hexane + 2-Butoxyethanol	4.35
Heptane + 2-Butoxyethanol	5.23
Octane + 2-Butoxyethanol	4.51
Cyclohexane + 2-Butoxyethanol	4.98
Methylcyclohexane + 2-Butoxyethanol	4.98
tert-Butylcyclohexane + 2-Butoxyethanol	4.18
2,2,4-Trimethylpentane + 2-Butoxyethanol	6.71
Hexane + 3-Methoxy-1-butanol	3.70
Heptane + 3-Methoxy-1-butanol	5.50
Octane + 3-Methoxy-1-butanol	4.59
Cyclohexane + 3-Methoxy-1-butanol	3.20
Methylcyclohexane + 3-Methoxy-1-butanol	-3.17
tert-Butylcyclohexane + 3-Methoxy-1-butanol	3.97
2,2,4-Trimethylpentane + 3-Methoxy-1-butanol	7.72
Overall Average Absolute Deviation	*5.04*

Chapter Bibliography

1. Huyskens, P.L.; Siegel, G.G. *Bull. Soc. Chim. Belg.*, **1988**, *97*, 821.

2. Siegel, G.G.; Huyskens, P.L.; Van der Heyden, G. *Ber. Bunsenges. Phys. Chem.*, **1990**, *94*, 549.

3. Ruelle, P.; Buchmann, M.; Nan-Tran. H.; Kesselring, U.W. *Int. J. Pharm.*, **1992**, *87*, 47.

4. Ruelle, P.; Buchmann, M.; Kesselring, U.W. *J. Pharm. Sci.*, **1994**, *83*, 396.

5. Powell, J.R.; Acree, Jr., W.E.; Huyskens, P.L. *Phys. Chem. Liq.*, in press.

6. McHale, M.E.R.; Powell, J.R.; Kauppila, A-S. M.; Acree, Jr., W.E.; Huyskens, P.L. *J. Solution Chem.*, **1996**, *25*, 1089.

7. Powell, J.R.; McHale, M.E.R.; Kauppila, A-S. M.; Acree, Jr., W.E.; Flanders, P.H., Varanasi, V.G.; Campbell, S.W. *Fluid Phase Equil.*, **1997**, *134*, 185.

8. Acree, Jr., W.E.; Zvaigzne, A.I. *Fluid Phase Equil.*, **1994**, *99*, 167.

9. McHale, M.E.R.; Coym, K.S.; Roy, L.E.; Hernandez, C.E.; Acree, Jr., W.E. *Can. J. Chem.*, **1997**, *75*, 1403.

10. Weast, R.C (1993) Ed., <u>CRC Handbook of Chemistry and Physics</u>, 64th Edition, CRC Press, Boca Raton, FL.

11. Acree, W.E. *Thermochim. Acta*, **1991**, *189*, 37.

12. Ruelle, P.; Rey-Mermet, C.; Buchmann, M.; Nam-Tran, H.; Kesselring, U.W.; Huyskens, P.L. *Pharm. Res.*, **1991**, *8*, 840.

13. Ruelle, P.; Sarraf, E.; Kesselring, U.W. *Int. J. Pharm.*, **1994**, *104*, 125.

14. Ruelle, P.; Sarrat, E.; Van den Berge, L.; Seghers, K.; Buchmann, M.; Kesselring, U.W. *Pharm Acta Helv.*, **1993**, *68*, 49.

15. Huyskens, P.L.; Haulait-Pirson, M.C. *J. Mol. Liq.*, **1985**, *31*, 135.

16. Acree, Jr., W.E. (1995). Polycyclic Aromatic Hydrocarbons: Binary Nonaqueous Systems: Part I (Solutes A – E): IUPAC Solubility Data Series. Oxford University Press, Oxford, United Kingdom, Vol. 58.

17. Roy, L.E.; Hernandez, C.E.; Acree, Jr., W.E. *Polycyclic Aromatic Compounds*, **1999**, *13*, 105.

18. Hernandez, C.E.; Coym, K.S.; Roy, L.E.; Powell, J.R.; McHale, M.E.R.; Acree, Jr., W.E. *J. Chem. Eng. Data*, **1997**, *42*, 954.

19. Powell, J.R.; McHale, M.E.R.; Kauppila, A-S. M.; Acree, Jr., W.E.; Campbell, S.W. *J. Solution Chem.*, **1996**, *25*, 1001.

20. Fletcher, K.A.; McHale, M.E.R.; Coym, K.S.; Acree, Jr., W.E. *Can. J. Chem.*, **1997**, *75*, 258.

21. Roy, L.E.; Hernandez, C.E.; De Fina, K.M.; Acree, Jr., W.E. *Phys. Chem. Liq.* (in press).

22. Tsonopoulos, C. *AIChE J.*, **1974**, *20*, 263.

23. Barker, J.A. *Aust, J. Chem.*, **1953**, *6*, 207.

24. Acree, Jr., W.E., Zvaigzne, A.I.; Tucker, S.A. *Fluid Phase Equil.*, **1994**, *92*, 233.

25. Zielkiewicz, J. *J. Chem. Thermodyn.*, **1994**, *24*, 445.

26. Nagata, I. *Thermochim. Acta*, **1989**, *144*, 95.

27. Berr, C.; Rogalski, M.; Peneloux, A. *J. Chem. Eng. Data*, **1982**, *27*, 352.

28. Zvaigzne, A.I.; Powell, J.R.; Acree, Jr., W.E.; ;Campbell, S.W. *Fluid Phase Equil.*, **1996**, *121*, 1.

29. Borders, T.L.; McHale, M.E.R.; Powell, J.R.; Coym, K.S., Hernandez, C.E.; Roy, L.E.; Acree, Jr., W.E.; Williams, D.C.; Campbell, S.W. *Fluid Phase Equil.*, **1998**, *37*, 31.

30. Powell, J.R.; McHale, M.E.R.; Kauppila, A-S.M.; Acree, Jr., W.E.; Campbell, S.W. *J. Solution Chem.*, **1996**, *25*, 1001.

31. Powell, J.R.; Fletcher, K.A.; Coym, K.S.; Acree, Jr., W.E.; Varanasi, V.G.; Campbell, S.W. *Int. J. Thermophys.*, **1997**, *18*, 1495.

32. McHale, M.E.R.; Zvaigzne, A.I.; Powell, J.R.; Kauppila, A.-S.M.; Acree, Jr., W.E.; Campbell, S.W. *Phys. Chem. Liq.*, **1996**, *34*, 103.

33. McHale, M.E.R.; Fletcher, K.A.; Coym, K.S.; Acree, Jr., W.E.; Varanasi, V.G.; Campbell, S.W. *Phys. Chem. Liq.*, **1997**, *34*, 103.

34. Hernandez, C.E.; Roy, L.E.; Reddy, G.D.; Martinez, G.L.; Parker, A.; Jackson, A.; Brown, G.; Acree, Jr., W.E. *J. Chem. Eng. Data*, **1997**, *42*, 1249.

35. Hernandez, C.E.; Roy, L.E.; Reddy, G.D.; Borders, T.L.; Sanders, J.T.; Acree, Jr., W.E. *Phys. Chem. Liq.*, **1998**, *37*, 31.

36. Hernandez, C.E.; Roy, L.E.; Reddy, G.D.; Martinez, G.L.; Jackson, A.; Brown, G.; Borders, T.L.; Sanders, J.T.; Acree, Jr., W.E. *Phys. Chem. Liq*, **1998**, *36*, 257.

37. Hernandez, C.E.; Roy, L.E.; Reddy, G.D.; Martinez, G.L.; Jackson, A.; Brown, G.; Acree, Jr., W.E. *Chem. Eng. Commun.*, **1998**, *169*, 137..

38. Hernandez, C.E.; Roy, L.E.; Deng, T.; Tuggle, M.B.; Acree, Jr., W.E. *Phys. Chem. Liq.*, (in press).

Chapter 5

Results and Discussion of Selective Quenching Agents

Nitromethane Quenching in Mixed Surfactant Solutions

Surfactants used in practical applications are often mixtures of surface-active compounds. Properly designed mixtures of dissimilar surfactants can have peculiar properties, sometimes superior to those of the pure surfactant.[1] As mentioned in earlier chapters, micellar solutions provide a very convenient means to introduce ionic character, and still have a solvent medium capable of solubilizing the larger, hydrophobic PAH solutes. Mixed surfactant solutions form a wide range of microstructures depending on the polar headgroup, alkyl-chain lengths and structures, concentrations of individual surfactants, and the mole fraction ratios within the mixtures. This study of micellar systems comprises of surfactant monomers with different charged polar headgroups, different counterions, and varying hydrocarbon chain length.

Many spectroscopic techniques have been applied to mixed surfactant systems in order to better understand some of the complex phenomena surrounding the mixing of two or more surfactants.[2-5] In this section, fluorescent behavior of select alternant and nonalternant polycyclic aromatic hydrocarbons in mixed micellar solutions of anionic + zwitterionic and anionic + nonionic micelles was established in both the presence and absence of nitromethane. The largest structural micellar changes are expected for systems which display strong intra-micellar interactions, specifically anionic + zwitterionic and to a lesser extent, anionic + nonionic mixed surfactant systems.

Tables XLII-XLV summarize fluorescence quenching measurements of various

alternant and nonalternant polycyclic aromatic hydrocarbons with nitromethane

corresponding to mixed micellar solvent media of SDS + SB-16 and SDBS + TX-100.

Experimental results are reported as the percent reduced in the fluorescence emission

intensity;

$$(F_0 - F)/F_0 * 100\% \qquad\qquad 5.1$$

observed after the addition of nitromethane. The values of equation 5.1 reported in

Tables XLII-XLV can be algebraically manipulated to provide the product of

$\tau_{fluor}k_{fluor}$[Quencher] in the Stern-Volmer equation;

$$(F_0/F) - 1 = \tau_{fluor}k_{fluor}[\text{Quencher}] \qquad\qquad 5.2$$

where F_0 and F refer to the observed emission intensities in the absence and presence of

nitromethane, τ_{fluor} is the fluorescence lifetime, k_{fluor} is the quenching rate constant, and

[Quencher] is the molar concentration of nitromethane around the solubilized PAH

fluorophore. All emission intensities used in the computations were corrected for

primary and secondary inner-filtering and solute self-absorption as discussed in chapter 3.

Careful examination of Tables XLII and XLIV reveals that nitromethane

effectively quenched the fluorescence emission of all the alternant PAHs, according to

the nitromethane selective quenching rule. Past research has shown that the percent

reduction in the emission signal is greater in the anionic + anionic surfactant systems than

in either the anionic + nonionic and anionic + zwitterionic surfactant systems. Within the

anionic + anionic system, the mixed micelles formed would have only negatively charged

headgroups, which would help stabilize the developing positive charge on the excited

PAH fluorophore as the electron/charge is transferred to nitromethane. In the case of

anionic + nonionic and anionic + zwitterionic mixed surfactant systems, there would be

fewer negatively charged headgroups on the surface per unit area. Moreover, it is known

that the largest micellar structural changes occur in systems that display strong intra-

micellar coulombic attractions. In the case of anionic and zwitterionic and to a lesser

extent in anionic + nonionic mixed surfactant systems, coulombic interactions lead to an

increase in the micelle size.

The overall fluorescence quenching behavior of alternant PAH solutes towards

nitromethane show that nitromethane quenches in all types of mixed surfactant systems.

The difference in the headgroup charge and the chain length of the surfactant has no

effect on quenching of alternant PAH emission intensities by nitromethane. However,

the extent of quenching varies from micelle to micelle.

Examining Tables XLIII and XLV, nitromethane quenching selectivity is

reestablished in nonalternant fluoranthenoid and fluorenoid PAH fluorophores by

addition of a relatively small amount of nonionic or zwitterionic surfactant to the anionic

surfactant. It would be expected that nonionic and zwitterionic headgroups should have

no effect on the electron/charge transfer. However, there is a large decrease in the extent

of quenching of nonalternant PAHs dissolved in the mixed anionic + nonionic and

anionic + zwitterionic micellar solutions. The solubilized PAH molecule resides in the

interior micellar region in the close proximity to the negatively charged exterior surface

of the anionic surfactant micelles. Ionic interactions involving the negatively charged micellar surface then stabilized the positively charged on the PAH as it develops. Such stabilization would facilitate electron/charge transfer for both alternant and nonalternant PAHs, perhaps to the point where quenching selectivity is lost in the case of anionic micellar solution. Nonionic and to an extent, zwitterionic headgroups should have no effect on the electron/charge transfer.

The unexpected decrease in the extent of quenching of nonalternant PAH fluorophores in mixed anionic + nonionic and anionic + zwitterionic micellar solutions shows that by adding non-anionic surfactants to anionic surfactants significantly alters the anionic micellar surface so that it is no longer able to stabilize the developing positive charge on nonalternant PAHs. The difference in the composition of mixed micelles and considerable changes in the size of the mixed micelles give retention of nitromethane's selectivity towards quenching of alternant versus nonalternant PAH fluorophores.

TABLE XLII. Summary of Nitromethane Quenching Results for Alternant Polycyclic Aromatic Hydrocarbons Dissolved in Aqueous Micellar SDBS + TX-100 Solvent Media.

Alternant PAH	Sol I[a]	Sol II[b]	Sol III[c]	Sol IV[d]	Sol V[e]
Perylene	22%	29%	32%	33%	34%
Benzo(a)pyrene	56%	62%	64%	68%	56%
Naphtho(2,3g)chrysene	50%	44%	43%	33%	11%
Anthracene	38%	38%	42%	41%	59%
Pyrene	96%	96%	97%	97%	95%
Coronene	31%	41%	54%	57%	51%
Benzo(e)pyrene	59%	71%	73%	75%	68%
Dibenzo(a,e)pyrene	73%	78%	77%	79%	69%

[a] Solvent media was circa 0.004 M TX-100.
[b] Solvent media was circa 0.002 M TX-100 + 0.002 M SDBS.
[c] Solvent media was circa 0.001 M TX-100 + 0.003 M SDBS.
[d] Solvent media was circa 0.0005 M TX-100 + 0.0035 M SDBS.
[e] Solvent media was circa 0.004 M SDBS.

TABLE XLIII. Summary of Nitromethane Quenching Results for Nonalternant Polycyclic Aromatic Hydrocarbons Dissolved in Aqueous Micellar SDBS + TX-100 Solvent Media.

Nonalternant PAH	Sol I[a]	Sol II[b]	Sol III[c]	Sol IV[d]	Sol V[e]
Benz(def)indeno(1,2,3hi)chrysene	0%	0%	0%	8%	38%
Benz(def)indeno(1,2,3qr)chrysene	0%	0%	0%	0%	0%
Naphtho(2,1a)fluoranthene	0%	0%	0%	0%	5%
Benzo(a)fluoranthene	0%	3%	5%	9%	24%
Benzo(b)fluoranthene	2%	31%	36%	48%	42%
Naphtho(1,2b)fluoranthene	10%	17%	25%	32%	29%
Benzo(ghi)fluoranthene	0%	0%	0%	0%	36%
Dibenzo(a,e)fluoranthene	0%	0%	0%	0%	8%

[a] Solvent media was circa 0.004 M TX-100.
[b] Solvent media was circa 0.002 M TX-100 + 0.002 M SDBS.
[c] Solvent media was circa 0.001 M TX-100 + 0.003 M SDBS.
[d] Solvent media was circa 0.0005 M TX-100 + 0.0035 M SDBS.
[e] Solvent media was circa 0.004 M SDBS.

TABLE XLIV. Summary of Nitromethane Quenching Results for Alternant Polycyclic Aromatic Hydrocarbons Dissolved in Aqueous Micellar SDS + SB-16 Solvent Media.

Alternant PAH	Sol I[a]	Sol II[b]	Sol III[c]	Sol IV[d]
Perylene	91%	81%	66%	53%
Benzo(a)pyrene	95%	90%	79%	68%
Naphtho(2,3g)chrysene	51%	44%	23%	34%
Anthracene	71%	54%	30%	20%
Pyrene	99%	98%	96%	95%
Coronene	90%	79%	52%	31%
Benzo(e)pyrene	96%	89%	86%	76%
Dibenzo(a,e)pyrene	94%	88%	73%	58%

[a] Solvent media was circa 2×10^{-2} M SDS.
[b] Solvent media was circa 1.8×10^{-2} M SDS + 0.2×10^{-2} M SB-16.
[c] Solvent media was circa 1.6×10^{-2} M SDS + 0.4×10^{-2} M SB-16.
[d] Solvent media was circa 1.4×10^{-2} M SDS + 0.6×10^{-2} M SB-16.

TABLE XLV. Summary of Nitromethane Quenching Results for Nonalternant Polycyclic Aromatic Hydrocarbons Dissolved in Aqueous Micellar SDS + SB-16 Solvent Media.

Nonalternant PAH	Sol I[a]	Sol II[b]	Sol III[c]	Sol IV[d]
Benz(def)indeno(1,2,3hi)chrysene	57%	29%	5%	2%
Benz(def)indeno(1,2,3qr)chrysene	24%	11%	3%	0%
Naphtho(2,1a)fluoranthene	51%	21%	4%	4%
Benzo(a)fluoranthene	37%	18%	5%	3%
Benzo(b)fluoranthene	89%	75%	49%	24%
Naphtho(1,2b)fluoranthene	82%	60%	31%	13%

[a] Solvent media was circa 2×10^{-2} M SDS.
[b] Solvent media was circa 1.8×10^{-2} M SDS + 0.2×10^{-2} M SB-16.
[c] Solvent media was circa 1.6×10^{-2} M SDS + 0.4×10^{-2} M SB-16.
[d] Solvent media was circa 1.4×10^{-2} M SDS + 0.6×10^{-2} M SB-16.

Alkylpyridinium Surfactant Cation as

Selective Quenching Agent

This section focuses on the fluorescence quenching results of polycyclic aromatic hydrocarbons dissolved in different micellar solutions in the absence and presence of alkylpyridinium surfactants. Alkylpyridinium halides have been used as a fluorescence quenching agent for PAH fluorescence emission numerous times to probe micellar aggregates.[6-9] The alkylpyridinium cation $(AlkPy^+)$ is known to be a good electron acceptor.[6] Studies concerning dissociation of fluorescence quenching surfactant ions, called quencher surfactants, from various ionic host micelles were performed using alkylpyridinium ions as the quencher surfactants.

An investigation of quenching behavior of dodecylpyridinium surfactant cation is carried out via studying the photophysical properties of various PAH solutes dissolved in different surfactant solutions. Tables XLVI-XLIX summarize the relative fluorescence emission intensities of selected alternant and nonalternant PAHs solubilized in aqueous micellar CTAC + DDPC and SDS + DDPC mixed surfactant media. Various different DDPC concentrations were studied for each mixed surfactant system.

Careful examination of numerical entries reveals that addition of varying amount of DDPC surfactants led to a significant decrease in the emission signals of all the alternant PAH solutes considered. Alkylpyridinium surfactant cations act as quenching agents towards alternant PAH fluorophores. Emission intensities of nonalternant PAH solutes show unusual behavior in some of the mixed surfactant systems.

For nearly ideal mixed surfactant systems of CTAC + DPC (cation + cation), behavior of relative emission intensities is depicted in Tables XLVI and XLVII. In this

mixed micellar system, emission intensities of nonalternant PAHs, with the exception of naphtho(2,3b)fluoranthene, benzo(k)fluoranthene, naphtho(1,2b)fluoranthene, and to a lesser extent benzo(b)fluoranthene, were for the most part not affected by the addition of DDPC. No special significance is given to the slight variations in emission intensities, which in all likelihood partly result from the fact that the solutions were prepared using a graduated cylinder. The four nonalternant PAHs who emission intensities were quenched by dodecylpyridinium cations are either known exceptions to the nitromethane selectivity rule or borderline cases.[9] Observed similarities in the PAH fluorescence behavior in solutions containing nitromethane and alkylpyridinium chloride surfactants is rationalized in terms of the known quenching mechanisms as mentioned in chapter 1.

The second category of the mixed surfactant systems containing alkylpyridinium surfactant constitutes anionic + DDPC; more specifically, SDS + DDPC. Examination of Tables XLVIII and XLIX reveals that alkylpyridinium cation's quenching selectivity is not affected by the headgroup charge on the cosurfactant. It was expected that quenching selectivity would be lost in the case of the anionic SDS cosurfactant. From simple coulombic considerations, the negatively charged SDS headgroup was expected to stabilize the developing positive charge on the PAH ring system, thereby facilitating electron/charge transfer from the excited PAH fluorophore to DDPy$^+$, which acts as an electron/charge acceptor. The inability of the negatively charged SDS anionic headgroup to facilitate electron/charge transfer in case of nonalternant PAHs is perhaps best explained in terms of the properties of mixed surfactant solutions and the effective micellar surface charge density. Mixed surfactant solutions do form a wide range of microstructures depending on the surfactant headgroup charges and sizes, alkyl-chain

lengths, concentrations and mole fraction ratios. The largest structural micellar changes are expected for the systems which display strong intra-micellar interactions and considerable deviations from ideality in mixed solutions.

In the case of SDS + DDPC solvent media, both surfactants would have to be in fairly close proximity to the dissolved PAH molecule in order to affect its fluorescence behavior. This would also place the oppositely charged surfactants in close proximity to each other. Attractive interactions between oppositely charged headgroups would reduce the negative electron surface density in the vicinity of the solubilized PAH molecule, to the point where the SDS headgroup is no longer able to stabilize any developing charge on the PAH ring system.

In a mixture of SDS + DDPC, even towards the SDS-rich region, the concentration of SDS is approximately same as that of DDPC. The expected effect of SDS is not observed because a majority of it is neutralized by the oppositely charged DDPC.

Discovery of alkylpyridinium surfactant cations as selective fluorescence quenching agents is important from a chemical analysis standpoint in that its solutions are optically transparent in the excitation spectral region of many other PAHs. Primary inner-filtering corrections are minimized, and in many cases eliminated. Inner-filtering corrections are much larger for nitromethane solutions as a few drops of quenching agent results in appreciable absorbances at excitation wavelengths of 350 nm and less. Therefore, accurate quantification of PAH concentrations using nitromethane requires both absorbance and fluorescence emission measurements.

TABLE XLVI. Relative Emission Intensities of Alternant Polycyclic Aromatic Hydrocarbons Dissolved in Aqueous Micellar (CTAC + DDPC) Solvent Media.

Alternant PAHs	Sol I[a]	Sol II[b]	Sol III[c]	Sol IV[d]
Benzo[ghi]perylene	840	760	290	16
Benzo[e]pyrene	610	500	230	11
Pyrene	860	680	150	8.3
Naphtho[2,3g]chrysene	560	560	290	45
Chrysene	900	810	380	24
Benzo[g]chrysene	400	330	180	16
Perylene	720	270	120	46
Benzo[rst]pentaphene	280	190	80	2.5
Naphtho[1,2,3,4ghi]perylene	390	250	130	31
Anthracene	330	210	130	38
Coronene	840	750	430	120
Benzo[a]pyrene	530	480	230	8.5
Dibenzo[a,e]pyrene	940	520	180	22

[a] Solvent media was circa 3.78×10^{-2} M in CTAC.
[b] Solvent media was circa 3.78×10^{-2} M in CTAC + 2.0×10^{-4} M in DDPC.
[c] Solvent media was circa 3.78×10^{-2} M in CTAC + 2.0×10^{-3} M in DDPC.
[d] Solvent media was circa 3.78×10^{-2} M in CTAC + 2.0×10^{-2} M in DDPC.

TABLE XLVII. Relative Emission Intensities of Nonalternant Polycyclic Aromatic Hydrocarbons Dissolved in Aqueous Micellar (CTAC + DDPC) Solvent Media.

Nonalternant PAHs	Sol I[a]	Sol II[b]	Sol III[c]	Sol IV[d]
Naphtho[1,2b]fluoranthene	630	360	240	290
Benzo[ghi]fluoranthene	960	940	940	890
Benz[def]indeno[1,2,3hi]chrysene	570	560	500	490
Benzo[a]fluoranthene	540	530	530	490
Naphtho[2,1k]benzo[ghi]fluoranthene	180	160	180	180
Naphtho[1,2k]benzo[ghi]fluoranthene	390	350	330	350
Benz[def]indeno[1,2,3qr]chrysene	170	190	150	150
Dibenzo[a,e]fluoranthene	500	490	530	490
Benzo[j]fluoranthene	400	350	340	360
Dibenzo[ghi,mno]fluoranthene	460	470	450	430
Naphtho[2,1a]fluoranthene	560	560	490	470
Benzo[b]fluoranthene	490	460	460	330

[a] Solvent media was circa 3.78 x 10^{-2} M in CTAC.
[b] Solvent media was circa 3.78 x 10^{-2} M in CTAC + 2.0 x 10^{-4} M in DDPC.
[c] Solvent media was circa 3.78 x 10^{-2} M in CTAC + 2.0 x 10^{-3} M in DDPC.
[d] Solvent media was circa 3.78 x 10^{-2} M in CTAC + 2.0 x 10^{-2} M in DDPC.

TABLE XLVIII. Relative Emission Intensity of Alternant Polycyclic Aromatic Hydrocarbons Dissolved in Aqueous Micellar (SDS + DDPC) Solvent Media.

Alternant PAHs	Sol I[a]	Sol II[b]	Sol III[c]	Sol IV[d]
Benzo[ghi]perylene	740	480	40	13
Benzo[e]pyrene	910	610	67	12
Pyrene	850	480	23	20
Naphtho[2,3g]chrysene	280	150	35	12
Chrysene	810	530	69	8.0
Benzo[g]chrysene	360	290	47	7.1
Perylene	840	680	210	44
Benzo[rst]pentaphene	140	66	8.3	4.6
Naphtho[1,2,3,4ghi]perylene	170	56	19	11
Anthracene	790	650	250	35
Coronene	230	140	29	12
Benzo[a]pyrene	530	340	50	14
Dibenzo[a,e]pyrene	370	230	24	8.9

[a] Solvent media was circa 3.71×10^{-2} M in SDS.
[b] Solvent media was circa 3.71×10^{-2} M in SDS + 2.0×10^{-4} M in DDPC.
[c] Solvent media was circa 3.71×10^{-2} M in SDS + 2.0×10^{-3} M in DDPC.
[d] Solvent media was circa 3.71×10^{-2} M in SDS + 2.0×10^{-2} M in DDPC.

TABLE XLIX. Relative Emission Intensity of Nonalternant Polycyclic Aromatic Hydrocarbons Dissolved in Aqueous Micellar (SDS + DDPC) Solvent Media.

Nonalternant PAHs	Sol I[a]	Sol II[b]	Sol III[c]	Sol IV[d]
Naphtho[1,2b]fluoranthene	370	330	320	360
Benzo[ghi]fluoranthene	880	890	900	910
Benz[def]indeno[1,2,3hi]chrysene	340	280	270	320
Benzo[a]fluoranthene	230	230	250	260
Naphtho[2,1k]benzo[ghi]fluoranthene	90	99	120	140
Naphtho[1,2k]benzo[ghi]fluoranthene	210	200	180	180
Benz[def]indeno[1,2,3qr]chrysene	130	130	140	180
Dibenzo[a,e]fluoranthene	320	380	340	390
Benzo[j]fluoranthene	400	370	410	380
Dibenzo[ghi,mno]fluoranthene	460	440	430	470
Naphtho[2,1a]fluoranthene	410	420	390	410
Benzo[b]fluoranthene	440	380	370	400

[a] Solvent media was circa 3.71 x 10^{-2} M in SDS.
[b] Solvent media was circa 3.71 x 10^{-2} M in SDS + 2.0 x 10^{-4} M in DDPC.
[c] Solvent media was circa 3.71 x 10^{-2} M in SDS + 2.0 x 10^{-3} M in DDPC.
[d] Solvent media was circa 3.71 x 10^{-2} M in SDS + 2.0 x 10^{-2} M in DDPC.

Chapter Bibliography

1. Pandey, S. Dissertation, University of North Texas (1998).

2. Penfold, J.; Staples, E.; Tucker, I. *Adv. Colloid Interface Sci.*, **1996**, *68*, 31.

3. Khan, M.N. *J. Colloid Interface Sci.*, **1996**, *182*, 602.

4. Shimizu, K.; Iwatsuru, M. *Chem. Pharm. Bull.*, **1990**, *38*, 744.

5. Huang, J.B.; Zhao, G-X. *Colloid Polym. Sci.*, **1996**, *274*, 747.

6. Hashimoto, S.; Thomas, J.K. *J. Am. Chem. Soc.*, **1983**, *105*, 5230.

7. Lang, J. *J. Phys. Chem.*, **1990**, *46*, 3734.

8. Velazquez, M.M.; Costa, S.M.B. *J. Chem. Soc. Faraday Trans.*, **1990**, *86*, 4043.

9. Tucker, S.A.; Bates, H.C.; Acree, Jr., W.E.; Fetzer, J.C. *Appl. Spectrosc.*, **1993**, *47*, 1775.

Bibliography

Acree, Jr., W.E. (1995). Polycyclic Aromatic Hydrocarbons: Binary Nonaqueous Systems: Part I (Solutes A – E): IUPAC Solubility Data Series. Oxford University Press, Oxford, United Kingdom, Vol. 58.

Acree, Jr., W.E. *Environ. Sci. Technol.*, **1993**, *27*, 757.

Acree, Jr., W.E.; Powell, J.R.; McHale, M.E.R.; Pandey, S.; Borders, T.L.; Campbell, S.W. *Research Trends in Physical Chemistry*, **1997**, *6*, 197.

Acree, Jr., W.E.; Zvaigzne, A.I. *Fluid Phase Equil.*, **1994**, *99*, 167.

Acree, Jr., W.E.; Zvaigzne, A.I. *Thermochim. Acta*, **1991**, *178*, 151.

Acree, Jr., W.E.; Zvaigzne, A.I.; Tucker, S.A. *Fluid Phase Equil.*, **1994**, *92*, 233.

Acree, W.E. *Thermochim. Acta*, **1991**, *189*, 37.

Atlas, R.M. *Microbiological Reviews*, **1981**, *45* 180.

Barker, J.A. *Aust, J. Chem.*, **1953**, *6*, 207.

Berr, C.; Rogalski, M.; Peneloux, A. *J. Chem. Eng. Data*, **1982**, *27*, 352.

Blumer, M *Scientific American*, **1978**, *234*, 3, 35.

Borders, T.L.; McHale, M.E.R.; Powell, J.R.; Coym, K.S., Hernandez, C.E.; Roy, L.E.; Acree, Jr., W.E.; Williams, D.C.; Campbell, S.W. *Fluid Phase Equil.*, **1998**, *37*, 31.

Breymann, U.; Preeskamp, H.; Koch, E; Zander, M *Chem. Phys. Lett.*, **1978**, *59*, 68.

Dobbins, D.C.; Aelion C.M; Pfaender F. *Crit. Rev. Environ. Control*, **1992**, *22* (1/2) 67.

Fendler, J.H. Membrane Mimetic Chemistry, Wiley-Interscience: New York, 1982.

Fendler, J.H. *Pure and Appl. Chem.*, **1982**, *54*, 1809.

Fletcher, K.A.; McHale, M.E.R.; Coym, K.S.; Acree, Jr., W.E. *Can. J. Chem.*, **1997**, *75*, 258.

Guilbault, G.G. Practical Fluorescence: Theory, Methods, and Techniques; Marcel Dekker: New York, 1973.

Hashimoto, S.; Thomas, J.K. *J. Am. Chem. Soc.*, **1983**, *105*, 5230.

Hernandez, C.E.; Coym, K.S.; Roy, L.E.; Powell, J.R.; Acree, Jr., W.E. *J. Chem. Thermodyn.*, **1998**, *30*, 37.

Hernandez, C.E.; Coym, K.S.; Roy, L.E.; Powell, J.R.; McHale, M.E.R.; Acree, Jr., W.E. *J. Chem. Eng. Data*, **1997**, *42*, 954.

Hernandez, C.E.; Roy, L.E.; Deng, T.; Tuggle, M.B.; Acree, Jr., W.E. *Phys. Chem. Liq.*, in press.

Hernandez, C.E.; Roy, L.E.; Reddy, G.D.; Borders, T.L.; Sanders, J.T.; Acree, Jr., W.E. *Phys. Chem. Liq.*, **1998**, *37*, 31.

Hernandez, C.E.; Roy, L.E.; Reddy, G.D.; Martinez, G.L.; Jackson, A.; Brown, G.; Borders, T.L.; Sanders, J.T.; Acree, Jr., W.E. *Phys. Chem. Liq.*, **1998**, *36*, 257.

Hernandez, C.E.; Roy, L.E.; Reddy, G.D.; Martinez, G.L.; Parker, A.; Jackson, A.; Brown, G.; Acree, Jr., W.E. *J. Chem. Eng. Data*, **1998**, *169*, 137.

Hernandez, C.E.; Roy, L.E.; Reddy, G.D.; Martinez, G.L.; Parker, A.; Jackson, A.; Brown, G.; Acree, Jr., W.E. *J. Chem. Eng. Data*, **1997**, *42*, 1249.

Holland, J.F; Teets, R.E.; Kelly, P.M.; Timnick, A. *Anal. Chem.*, **1977**, *49*, 706.

Huang, J.B.; Zhao, G-X. *Colloid Polym. Sci.*, **1996**, *274*, 747.

Hurst, C.J.; Sims, R.C.; Sims, J.L.; Sorensen, D.L.; McLean, J.E.; Huling, S. *Proceedings of the 10th Annual Conference on Hazardous Waste Research* (1995).

Huyskens, P.L. *J. Mol. Struct.* **1993**, 297.

Huyskens, P.L.; Haulait-Pirson, M.C. *J. Mol. Liq.*, **1985**, *31*, 135.

Huyskens, P.L.; Siegel, G.G. *Bull. Soc. Chim. Belg.*, **1988**, *97*, 821.

Khan, M.N. *J. Colloid Interface Sci.*, **1996**, *182*, 602.

Kobayaski, H.; Rittman, B.E. *Environmental Science and Technology*, **1982**, *16* 170A.
Lakowicz, J.R. Principles of Fluorescence Spectroscopy; Plenum: New York, 1983, 44.

Lang, J. *J. Phys. Chem.*, **1990**, *46*, 3734.

Madsen, T.; Kristensen, P. *Environmental Toxicology and Chemistry* , **1996**, *16*, 4, 631.

Mahmook, S.K.; Rao, P.R. *Bulletin of Environmental Contamination and Toxicology*, **1997**, *50*, 4, 486.

Mahro, B.; Eschenbach, A; Schaefer, G; Kaestner, M. *DECHEMA Monographien*, 133, 509.

McBain, J.W. *Trans Faraday Soc.* **1913**, *9*, 99.

McGinnes, P.R.; Snoeyink, V.L, *WRC Res. Rept.*, **1974**, *80*, UILU-WRC-74-0080, PB-232, 168.

McGinnis, G.D., U.S. EPA, Washington D.C., EPA 600/S2-88/055, **1998**.

McHale, M.E.R.; Coym, K.S.; Roy, L.E.; Hernandez, C.E.; Acree, Jr., W.E. *Can. J. Chem.*, **1997**, *75*, 1403.

McHale, M.E.R.; Fletcher, K.A.; Coym, K.S.; Acree, Jr., W.E.; Varanasi, V.G.; Campbell, S.W. *Phys. Chem. Liq.*, **1997**, *34*, 103.

McHale, M.E.R.; Powell, J.R.; Kauppila, A-S. M.; Acree, Jr., W.E.; Huyskens, P.L. *J. Solution Chem.*, **1996**, *25*, 1089.

McHale, M.E.R.; Zvaigzne, A.I.; Powell, J.R.; Kauppila, A.-S.M.; Acree, Jr., W.E.; Campbell, S.W. *Phys. Chem. Liq.*, **1996**, *34*, 103.

Murkerjee, P.; Mysels, K. Critical Micelle Concentration of Aqueous Surfactant Systems. National Standards Reference Data Series, Vol. 36, National Bureau of Standards, Washington, DC, 1971.

Nagata, I. *Thermochim. Acta*, **1989**, *144*, 95.

Pandey, S. Dissertation, University of North Texas (1998).

Penfold, J.; Staples, E.; Tucker, I. *Adv. Colloid Interface Sci.*, **1996**, *68*, 31.

Powell, J.R.; Acree, Jr., W.E.; Huyskens, P.L. *Phys. Chem. Liq.*, in press.

Powell, J.R.; Fletcher, K.A.; Coym, K.S.; Acree, Jr., W.E.; Varanasi, V.G.; Campbell, S.W. *Int. J. Thermophys.*, **1997**, *18*, 1495.

Powell, J.R.; McHale, M.E.R.; Kauppila, A-S. M.; Acree, Jr., W.E.; Flanders, P.H., Varanasi, V.G.; Campbell, S.W. *Fluid Phase Equil.*, **1997**, *134*, 185.

Powell, J.R.; McHale, M.E.R.; Kauppila, A-S.M.; Acree, Jr., W.E.; Campbell, S.W. *J. Solution Chem.*, **1996**, *25*, 1001.

Pringsheim, P. Fluorescence and Phosphorescence, Interscience, New York, 1949.

Reiley, K.A.; Banks, M.K.; Schwab, A.P. *J. Environ. Quality*, **1996**, *25*, 212.

Roy, L.E.; Hernandez, C.E.; Acree, Jr., W.E. *Polycyclic Aromatic Compounds*, **1999**, *13*, 105.

Roy, L.E.; Hernandez, C.E.; De Fina, K.M.; Acree, Jr., W.E. *Phys. Chem. Liq.* (in press).

Roy, L.E.; Hernandez, C.E.; Reddy, G.D.; Sanders, J.T.; Deng, T.; Tuggle, M.B.; Acree, Jr., W.E. *J. Chem. Eng. Data*, **1998**, *43*, 493.

Ruelle, P.; Buchmann, M.; Kesselring, U.W. *J. Pharm. Sci.*, **1994**, *83*, 396.

Ruelle, P.; Buchmann, M.; Nan-Tran. H.; Kesselring, U.W. *Int. J. Pharm.*, **1992**, *87*, 47.

Ruelle, P.; Rey-Mermet, C.; Buchmann, M.; Nam-Tran, H.; Kesselring, U.W.; Huyskens, P.L. *Pharm. Res.*, **1991**, *8*, 840.

Ruelle, P.; Sarraf, E.; Kesselring, U.W. *Int. J. Pharm.*, **1994**, *104*, 125.

Ruelle, P.; Sarrat, E.; Van den Berge, L.; Seghers, K.; Buchmann, M.; Kesselring, U.W. *Pharm Acta Helv.*, **1993**, *68*, 49.

Saim, N., Dean, J., Abdullah, M.P.; Zakaria, Z. *J. Chrom. A*, **1997**, *791*, 361.

Shimizu, K.; Iwatsuru, M. *Chem. Pharm. Bull.*, **1990**, *38*, 744.

Siegel, G.G.; Huyskens, P.L.; Van der Heyden, G. *Ber. Bunsenges. Phys. Chem.*, **1990**, *94*, 549.

Sims, R.C.; Overcash, M.R *Residue Reviews*, **1983**, *88*, 1.

Skoog, D.; Holler, F.J.; Nieman, T.A. Principles of Instrumental Analysis, 5th Ed., Saunders College Publishing, New York, 1998.
Swarbrick, J.; Darawala, J. *J. Phys. Chem.*, **1969**, *73*, 2627.

Tabak, HH; Fovind, R.; Gao, C.; Fu, C *Journal of Environmental Science and Health Part A, Toxic/Hazardous Substances and Environmental Engineering*, **1998**, *33*, 8, 1533.

Tsonopoulos, C. *AIChE J.*, **1974**, *20*, 263.

Tucker, S.A.; Amszi, V.L.; Acree, Jr., W.E. *J. Chem. Ed.*, **1992**, *69*, A8.

Tucker, S.A.; Bates, H.C.; Acree, Jr., W.E.; Fetzer, J.C. *Appl. Spectrosc.*, **1993**, *47*, 1775.

Velazquez, M.M.; Costa, S.M.B. *J. Chem. Soc. Faraday Trans.*, **1990**, *86*, 4043.

Weast, R.C (1993) Ed., <u>CRC Handbook of Chemistry and Physics</u>, 64th Edition, CRC Press, Boca Raton, FL.

Wehry, E.L. <u>In Fluorescence: Theory, Instrumentation, and Practice</u>, Guilbault, G.G. (Ed.). Marcel Dekker, Inc. New York, 1967, pp. 37.

Wetzel, S.C.; Banks, M.K.; Schwab, A.P. *Proceedings of the 10th Annual Conference on Hazardous Waste Research* (1995).

Zielkiewicz, J. *J. Chem. Thermodyn.*, **1994**, *24*, 445.

Zubay, G.L <u>Biochemistry</u>, Wm. C. Brown Publishers, Dubuque, 1998, pg. 448.

Zvaigzne, A.I.; Powell, J.R.; Acree, Jr., W.E.; Campbell, S.W. *Fluid Phase Equil.*, **1996**, *121*, 1.